Russian Original Vol. 35, No. 1, July, 1973

January, 1974

SATEAZ 35(1) 613-704 (1973)

SOVIET ATOMIC ENERGY

АТОМНАЯ ЭНЕРГИЯ
(ATOMNAYA ÉNERGIYA)

TRANSLATED FROM RUSSIAN

CONSULTANTS BUREAU, NEW YORK

SOVIET ATOMIC ENERGY

Soviet Atomic Energy is a cover-to-cover translation of *Atomnaya Énergiya*, a publication of the Academy of Sciences of the USSR.

An arrangement with Mezhdunarodnaya Kniga, the Soviet book export agency, makes available both advance copies of the Russian journal and original glossy photographs and artwork. This serves to decrease the necessary time lag between publication of the original and publication of the translation and helps to improve the quality of the latter. The translation began with the first issue of the Russian journal.

Consultants Bureau journals appear about six months after the publication of the original Russian issue. For bibliographic accuracy, the English issue published by Consultants Bureau carries the same number and date as the original Russian from which it was translated. For example, a Russian issue published in December will appear in a Consultants Bureau English translation about the following June, but the translation issue will carry the December date. When ordering any volume or particular issue of a Consultants Bureau journal, please specify the date and, where applicable, the volume and issue numbers of the original Russian. The material you will receive will be a translation of that Russian volume or issue.

Subscription
$80 per volume (6 Issues)
2 volumes per year
(Add $5 for orders outside the United States and Canada.)

Single Issue: $30
Single Article: $15

CONSULTANTS BUREAU, NEW YORK AND LONDON

227 West 17th Street
New York, New York 10011

Davis House
8 Scrubs Lane
Harlesden, NW10 6SE
England

Published monthly. Second-class postage paid at Jamaica, New York 11431.

Soviet Atomic Energy is abstracted or indexed in *Applied Mechanics Reviews, Chemical Abstracts, Engineering Index, INSPEC—Physics Abstracts and Electrical and Electronics Abstracts, Current Contents,* and *Nuclear Science Abstracts.*

SOVIET ATOMIC ENERGY

A translation of *Atomnaya Énergiya*
January, 1974

Volume 35, Number 1 July, 1973

CONTENTS

CONTENTS

(continued)

The Russian press date (podpisano k pechati) of this issue was 6/27/1973. Publication therefore did not occur prior to this date, but must be assumed to have taken place reasonably soon thereafter.

OBITUARY

NIKITA ALEKSANDROVICH KOLOKOL'TSOV

The editorial board and editor of the journal Atomnaya Énergiya has suffered still another severe loss. Doctor of Technical Sciences Professor Nikita Aleksandrovich Kolokol'tsov, deputy chief editor of the journal, deputy department director of the Moscow Engineering Physics Institute, laureate of the USSR State Prizes, died on June 14, 1973 after a prolonged illness.

A modest and warmhearted person, a talented Soviet scientist and pedagogue, who devoted his entire life to the service of science and to the education of youth, has passed away.

N. A. Kolokol'tsov was born on August 1, 1914 in Leningrad. Having graduated in 1937 from the M. I. Kalinin Leningrad Polytechnical Institute, he was assigned to the job of scientific co-worker in the laboratory of hydraulic machines of this institute. During the Second World War N. A. Kolokol'tsov worked on the construction of the defence structures of Leningrad. Continuing to be engaged in scientific research under the extremely difficult war conditions, he defended his candidate's dissertation in 1943.

Between 1950 and 1967, N. A. Kolokol'tsov worked at the I. V. Kurchatov Institute of Atomic Energy. Here, together with Academician M. D. Millionshchikov and other scientists, he gave his knowledge and experience to the solution of the problem of the use of atomic energy. In 1952 he was awarded the degree of doctor of technical sciences.

N. A. Kolokol'tsov was the author of more than 60 scientific papers on mechanics, hydraulics, and isotope separation. His scientific activities were highly valued by the Soviet government. He was twice awarded the title of laureate of the USSR State Prize and was conferred with two Orders of the Red Banner of Labor, Badge of Honor, and medals.

For more than 25 years N. A. Kolokol'tsov combined research with teaching in institutions of higher learning in Leningrad and Moscow. In recent years he worked as deputy department director at the Moscow Engineering Physics Institute, where his talents as a pedagogue were revealed completely.

Translated from Atomnaya Énergiya, Vol. 35, No. 1, p. 2, July, 1973.

From April 1961 to his last days N. A. Kolokol'tsov performed great public work, being a member of the editorial board and deputy chief editor of the journal Atomnaya Énergiya. In this position he always combined high scientific exactitude and adherence to principle with a cordial and friendly attitude toward people.

The editorial board and editor of the journal Atomnaya Énergiya deeply mourn the premature death of Nikita Aleksandrovich Kolokol'tsov and offer sincere condolences to the family, friends, and students of the deceased.

The bright memory of a remarkable person, talented scientist, and educator of youth will be retained eternally in the hearts of those who knew, respected, and loved him.

ARTICLE

SOME CHARACTERISTIC FEATURES OF THE BEHAVIOR OF URANIUM IN THE FORMATION OF URANIUM – MOLYBDENUM DEPOSITS

I. V. Mel'nikov and I. G. Berzina

UDC 553.495:553.21.24
:553.3/4.065-(571.5)

Recent years have seen the publication of a large number of papers devoted to the mineralogical, structural–geological, and (to a certain extent) geochemical characteristics of the formation of uranium – molybdenum deposits [1, 2, 3]. However, there is as yet insufficient information regarding the behavior of uranium during the whole course of deposit formation. In this paper we shall present some material which will in some measure fill the gap.

The deposits considered in the investigation are characteristic representatives of uranium–molybdenum formations. They are situated within a collapsed caldera filled with a bedded sedimentary–effusive stratum, in which the most widespread features are beds of trachydacites, trachyandesites, trachybasalts, and felsites. The ore materials in these are confined to systems of joints of north-west and submeridional trend. The results of detailed mineralogical investigations (to be published in another article) lead to the conclusion that the deposits are formed in the course of a single hydrothermal stage, within which six stages of mineral formation may be distinguished: 1) albitization of the surrounding rocks; 2) quartz–albite alteration of the rocks; 3) quartz–carbonate–hydromicaceous (argillization); 4) quartz–carbonate–sulfide; 5) molybdenite–pitchblende; 6) quartz–fluorite–calcite.

Processes taking place in the first three stages are the most fully developed. The earliest stage (albitization) appeared in almost all the rocks studied. During the next three stages, veiny formations were created, accompanied by a thin halo of alterations around the veins.

In order to study the characteristic behavior of uranium, we use the method of f-radiography [4] based on the revelation of tracks arising from stimulated uranium fission fragments. This method enables us to determine the spatial distribution and the concentration of the uranium in the minerals and mineral formations developing over the whole mineralization sequence. The composition of uranium-containing minerals was determined on the basis of their physical properties and refined by laser spectral analysis and in the Cameca x-ray microanalyzer.

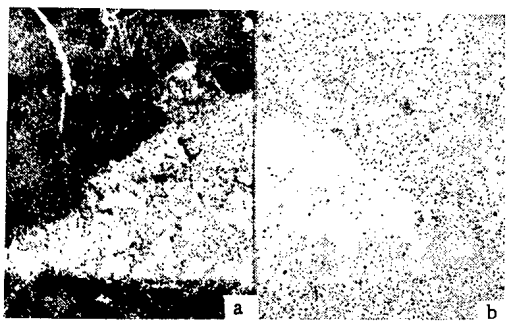

Fig. 1. Uranium distribution in albitized trachydacite: a) transparent microsection; b) detector (mirror image).

Within the collapse caldera there were hardly any rocks which were not affected to one extent or another by alterations. Among the weakest of these alterations, which in a number of cases may be regarded as "background" features, is the hematitization of the rocks associated with their oxidation in the upper and lower regions of the beds, giving the rocks a cherry or lilac color. All the uranium distribution characteristics representative of the nonhematized effusives are still preserved. The uranium occurs mostly in the main bulk of the rock, where it is quite uniformly distributed. The uranium content in

Translated from Atomnaya Énergiya, Vol. 35, No. 1, pp. 3-9, July, 1973. Original article submitted October 20, 1972.

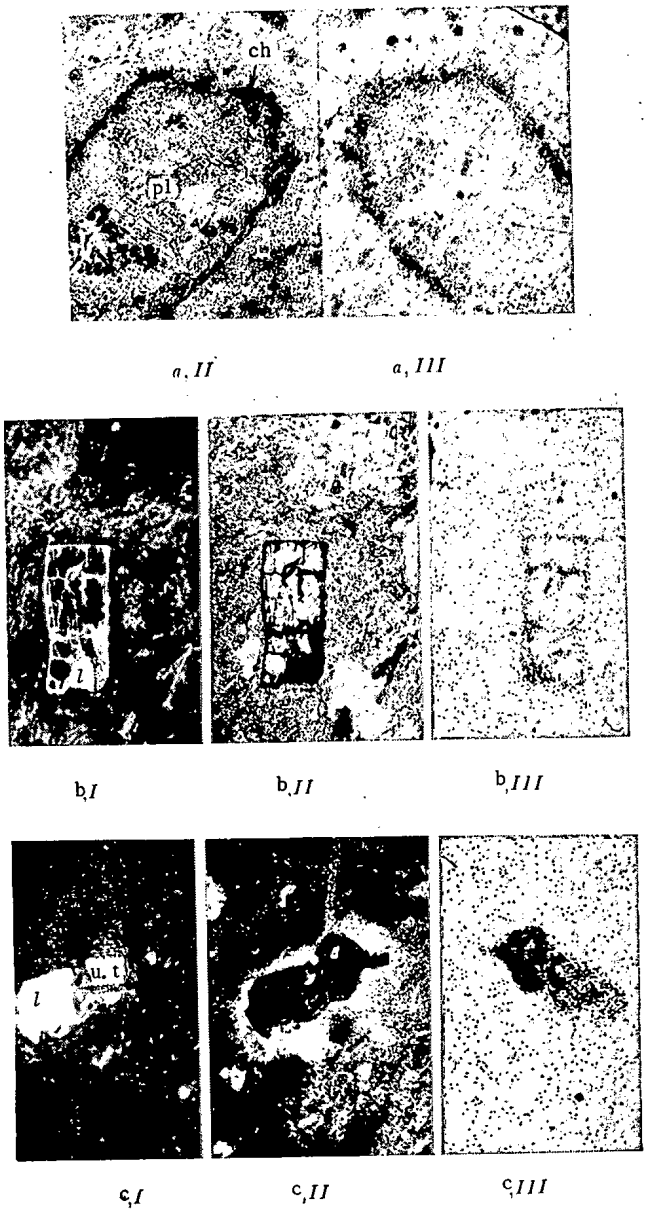

a, II a, III

b, I b, II b, III

c, I c, II c, III

Fig. 2. Uranium distribution in trachydacite during the development of the quartz–carbonate–hydromicaceous alteration. Uranium confined to the following minerals: a) chlorite (ch) developing through an impregnation of plagioclase (pl); b) leucoxenized (*l*) parts of hornblende; c) pseudomorphoses of leucoxene (*l*) and uranium titanates (u.t.) through the ilmenorutile; I) transparent microsection with oblique illumination; II) in transmitted light; III) detector with tracks from stimulated uranium fission fragments (mirror image).

impregnations of rock-forming minerals (quartz, potash feldspar, plagioclase, dark-colored minerals) is $n \cdot 10^{-7}$ wt.%. The total uranium content in the rock fluctuates over the range $(1-2) \cdot 10^{-4}$% for trachyandesites and $(4-6) \cdot 10^{-4}$% for trachydacites.

In the albitization stage, which is the most widely developed, the rocks are altered relatively slightly. Impregnations of feldspars are subject to alterations. Microcline is partly replaced by checkered albite, and plagioclase by hyaline untwinned albite. The main bulk of the deposit and the dark-colored minerals are not altered. The character of the uranium distribution and the uranium content of the albitized rock

TABLE 1. Mean Uranium Concentration in Samples of Altered Rocks

Unaltered rock	Zones of metasomatic columns	Density of tracks in field of view	Neutron flux $\cdot 10^{-13}$ neutrons /cm²	Uranium concentration C $\cdot 10^{13}$, wt%
Trachydacite	Original rock (hematitized and albitized trachydacite)	34	9,4	6,15
	Hydrobiotite–dolomite	40	9,4	6,42
	Dolomite–chlorite	43	9,4	7,73
	Quartz–ankerite–hydromicaceous	65	9,4	11,86
	Quartz–hydromicaceous	95	9,4	17,17
Trachydacite	Original rock (hematitized and albitized trachydacite)	11	3,6	4,49
	Hematitized hydrobiotite–dolomite	13	3,6	5,99
	Dolomite–chlorite	12	3,6	5,19
	Quartz–ankerite–hydromicaceous	8	2,3	5,07
Lava breccia of trachydacite with fragments of trachyandesitobasalt	Quartz–hydromicaceous	36	2,3	25,26
	Quartz–hydromicaceous	7	2,3	5,11
Trachydacite	Original rock (dolomite–chlorite)	12	3,2	5,41
	Relicts of hematitized rock in dolomite–chlorite zone	16	3,2	7,06
	Quartz–ankerite–hydromicaceous	14	3,2	6,22
	Quartz–ankerite–hydromicaceous	23	3,2	11,57
	Quartz–hydromicaceous	68	3,2	34,38
Trachyandesito-basalt	Original rock (albitized trachyandesitobasalt)	20	32,3	1,02
	Dolomite	4	3,6	1,64
		31	32,3	1,59
	Ankerite–hydromicaceous	7	3,6	3,09
	Quartz–ankerite–hydromicaceous	5	3,6	2,53
Trachyandesito-basalt	Original rock (andesitobasalt)	2	3,6	1,05
	Dolomite	20	32,3	1,11
		3	3,6	1,3
		23	32,3	1,24
	Ankerite–hydromicaceous	5	3,6	2,23

are preserved as in the unaltered rock (Fig. 1). There is a preference of the uranium toward the main bulk of the rock and a lower uranium content in impregnations of partially albitized plagioclase.

The uranium distribution in rocks subjected to the quartz–albite alteration could not be studied in view of their partial coincidence with the uranium scattering halos around the uranium ore materials. At this stage of mineral formation, together with the development of a quartz–albite aggregate, impregnations of ilmenorutile, zircon, apatite, sphene, and ilmenite were formed. At the end of the stage, vein formations consisting of quartz and apatite and containing impregnations of zircon and titanium minerals were created in individual places.

During the next stage (quartz–carbonate–hydromicaceous), large volumes of rocks passing far beyond the limits of the uranium scattering halos around the ore materials were subjected to alteration. The uranium distribution in these rocks was studied in particular detail. We only studied those samples which had been collected well beyond the limits of the uranium scattering halos and contained no microscopic segregations of any minerals which had accompanied the deposition of pitchblende in the ore stage of mineral formation. It should be noted that, when these minerals appear (even for low uranium contents of the rock as a whole), the character of the uranium distribution in the rock changes completely.

The most favorable regions for selecting samples were the contacts between rocks altered in the third stage and cherry and lilac rocks hematitized and albitized in the second stage.

Rocks subjected to the quartz–carbonate–hydromicaceous alteration are characterized by a zonal distribution of the metasomatic minerals in space. The zonal structure is clearly expressed around individual joints but becomes indistinguishable (as a result of the merging of the halos) wherever more intensive jointing occurs.

In the outer zone of the altered trachyandesite–basalts, impregnations of plagioclase (in part previously albitized), pyroxene, and biotite are intensively replaced by dolomite. Pyrite also develops in

TABLE 2. Content of Certain Elements in Accessory Minerals and New Formations

Mineral	Method of analysis	Content of elements, wt. % (partial analysis)
Ilmenite	X-ray (Cameca microanalyzer)	Fe—36,3; Ti—31,5; O—31,9; ThandU not observed
Rutile	X-ray (Cameca microanalyzer)	Ti—58,6; Fe—0,6; Si—0,1; O—40.1; Th, U, Zr not observed
Leucoxene in ilmenite	X-ray (Cameca microanalyzer)	Fe—0,7; U—0,1; Ti—35,8; Si—0,1; Zn—0,6; Th $<$ 0,1; Pb—0,1; O—11,4; Sc, Y—0,05; V, As not observed
Zirkelite in rutile and ilmenite	Laser spectral	Ti $>$ 10; Zn $>$ 10; Mn—0,*n*; Si—0,1; Fe—0,*n*; Ca—0,*n*; Y—weak lines
	X-ray (Cameca microanalyzer)	Ca—0,53; Mg—0,1; Pb—0,2; Fe—2,7; Al—0,16; Ce—0,15; Y—2,3; Si—3,3; Ti—18,5; Zr—17,6; Sc—0,3; Th—1,6; U—0,4; As—0,1; O—42,4
Uranium silicates	X-ray (Cameca microanalyzer)	U, Si, O—10*n*; Ti—*n*; Ca—0,*n*; Pb—*n*; Th—0,*n*

accordance with biotite. The main bulk of the rock retains the ophitic structure and a dark green color. In the whole rock a slightly mottled coloring appears (as a result of the clarification of the impregnations).

In the second zone (ankerite–hydromicaceous), the coloring of the rock changes to greenish gray. Both the impregnations and the laths (in the main bulk of the rock) of plagioclase are completely replaced by an aggregate of ankerite and fibrous hydromica. The ankerite also forms segregations in the main bulk of the rock. The dark-colored minerals are replaced by ankerite, leucoxene, and pyrite, the magnetite impregnations by pyrite, and the titanium minerals by leucoxene.

The inner zone of the halo (quartz–ankerite–hydromicaceous) is characterized by an intensive replacement of the main bulk of the rock and the impregnations with an aggregate of quartz, ankerite, and hydromica containing impregnations of pyrite. The leucoxene earlier developing among the titanium minerals is preserved. The rock acquires a white color and finally loses its structure.

The quartz–carbonate–hydromicaceous alteration of the trachydacites leads to the formation of a metasomatic column consisting of four zones.

In the outer zone (hydrobiotite–dolomite) the rock retains its original order. Relicts of the albitized plagioclase are here selectively replaced by dolomite, and the biotite by hydrobiotite. The earlier-formed albite is here retained without any alterations. The main bulk of the rock, including the frequently present hematite and also impregnations of apatite, sphene, ilmenite, and magnetite, are not altered.

In the second zone, the alterations (dolomite–chlorite) of the rock are characterized by a greenish or rosé hue. Chlorite and dolomite are developed among the impregnations of microcline and plagioclase. The earlier-formed albite is replaced by chlorite, and the hydrobiotite by chlorite with minute grains of pyrite and leucoxene. The titanium minerals (sphene, ilmenite, and ilmenorutile) are leucoxenized. Around the grains of ilmenite and magnetite, pyrite fringes develop, severely eroding the grains. Apatite is not altered in this zone.

In the third zone (quartz–ankerite–hydromicaceous) the rock has a light gray or cream color. The main bulk is completely altered and converted into an aggregate of cryptocrystalline quartz and thin flakes of hydromica not containing any hematite. The relicts of the plagioclase impregnations, the albite grains, and the microcline are completely replaced by quartz and hydromica. The earlier-formed chlorite and dolomite are replaced by ankerite. The titanium minerals are completely leucoxenized. There is a certain impregnation of pyrite, which develops in conformity with the ilmenite. The apatite is replaced by quartz and hydromica.

The inner zone of the alteration (quartz–hydromicaceous) only develops in regions of maximum jointing and in the most severe zones of granulation. The rocks acquire a white color and their structure is completely altered. The whole rock is replaced by an aggregate of cryptocrystalline quartz and finely fibrous hydromica. In the quartz–hydromica aggregate there are individual relicts of ankerite pockets, severely eroded by quartz. The impregnations of ilmenorutile and sphene are completely leucoxenized.

During the quartz–carbonate–hydromicaceous alteration of the trachydacites, uranium was introduced; this concentrated in the newly formed minerals in all zones except the outer one. Within the dolomite–chlorite zone uranium is present in the chlorite replacing the plagioclase and potash feldspar, in the leucoxene developing through the biotite and hornblende, and also in the leucoxene and uranium titanates

replacing the sphene, ilmenorutile, and ilmenite (Fig. 2a-c). In the quartz–ankerite–hydromicaceous and quartz–hydromicaceous zones of alteration, the uranium also occurs in extremely fine impregnations (2-4 μ) of uranium silicates scattered in the hydromicadized mass and also in individual impregnations of a mineral of the zirkelite type.

The uranium content in the rocks most severely altered in the quartz–carbonate–hydromicaceous stage is increased by a factor of three, and in individual regions by a factor of five compared with the Clark quantity in weakly altered rocks (Table 1). In the crystal lattice of newly formed minerals, the main components accompanying uranium include thorium, the rare earths, zirconium, and titanium (Table 2). That these elements may be found in the crystal lattice is attested by their uniform distribution in the minerals, as established by laser spectral analysis and in the x-ray microanalyzer. Since the majority of these components (thorium, the rare earths, zirconium) are absent from earlier-formed titanium minerals (Table 2) and only appear in newly formed minerals (leucoxene and zirkelite) replacing the former (rutile, ilmenite, sphene), there is no doubt that these components are introduced by the solutions, while the titanium is redistributed in situ.

In the quartz–carbonate–sulfide stage of mineral formation, quartz, pyrite, arsenopyrite, siderite, hydromica, ankerite, and dolomite were deposited. Quite often the quartz, replaced successively by hydromica and siderite with pyrite, forms veiny deposits intersected by veins of ankerite and dolomite. The uranium content in the quartz, dolomite, and hydromica established by the method of f-radiography varies over the range $n \cdot 10^{-6}$–$n \cdot 10^{-7}$ wt.%.

In the ore-forming molybdenite–pitchblende stage, two paragenetic associations of quartz with pitchblende were formed successively: the paragenesis of molybdenite with pyrite and a trace of pitchblende, and the most productive paragenesis of pitchblende with hydromica and chlorite. At the conclusion of this stage, quartz, hydromica, and a small quantity of hematite were deposited. The veins are accompanied by impregnations of the same minerals in the rock (Fig. 3). At this stage the deposition of most of the uranium from solutions took place. In the impregnated ores the uranium is chiefly found in the main bulk of the rock. Bands of fluidal structure folded by the quartz frequently constitute microscreens (Fig. 3) causing a nonuniform uranium distribution (on the microscale) in the rocks. Pitchblende borders are also formed around eroded pyrite grains.

Spectral analysis shows that in the impregnated uranium ores the concentrations of lead, molybdenum, antimony, beryllium, and arsenic increase substantially. Thorium and the rare earths are absent in any appreciable quantities. Chemical and x-ray–chemical analyses of pitchblendes of various generations of the veins show that these contain the same impurities. In the quartz–fluorite–calcite stage of mineral formation the following paragenetic associations of minerals and individual minerals were successively formed: siderite + ankerite; quartz + ankerite; quartz + adular; chamosite; dark-violet fluorite + pyrite + marcasite + redeposited pitchblende; green fluorite + pyrite + marcasite; brown fluorite + pyrite; porcelain-like fluorite + quartz + iron hydroxides + hydromica; copper-yellow spherulitic fluorite with

I *II* *III*

Fig. 3. Uranium distribution for an impregnated type of mineralization formed in the molybdenite–pitchblende stage of mineral formation. Note the microscreening of the uranium by a quartz band of fluidal structure (qu) in the trachydacites: I) transparent microsection with oblique illumination; II) in transmitted light; III) tracks in Dacron (mirror image).

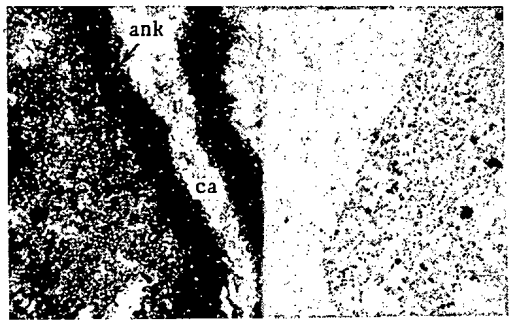

Fig. 4

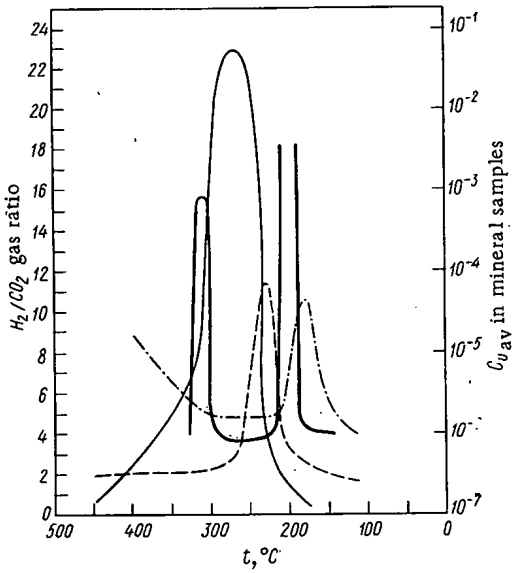

Fig. 5

Fig. 4. Uranium distribution in an ankerite streak (ank) of calcite (ca) composition. There are no tracks in the detector in the part corresponding to the streak: I) transparent microsection in transmitted light; II) tracks in Dacron (mirror image).

Fig. 5. Change in the uranium concentration of hydrothermal formations and values of the H_2/CO_2 ratio in the gas phase of the gas–liquid inclusions of minerals, according to [6, 7]. The horizontal axis gives the homogenization temperatures of the gas–liquid inclusions. ——) change in H_2/CO_2 in a polymetallic deposit; ----) change in H_2O/CO_2 in a molybdenum–tungsten deposit; ———) change in uranium content in hydrothermal formations of a uranium–molybdenum deposit; - - - - - -) change in uranium content in fluorite formations of a fluorite polymetallic deposit.

redeposited pitchblende; marcasite; pyrite + bravoite; chalcopyrite; bornite + fahlerz; galenite + chalcosine among chalcopyrite; calcite + cinnabar + pyrite; quartz + barite; lamellar calcite + marcasite + pyrite; wavellite.

A study of the uranium distribution in aggregates of quartz, ankerite, chlorite, and calcite grains showed that in this stage neither the grains themselves nor the intergranular space were enriched with uranium (Fig. 4). However, when the ore deposits were intersected by streaks and veins folded by the minerals in question, their uranium content frequently increased. Between the grains and along the growth faces of individual crystals, borders and individual spherulites of redeposited pitchblende and molybdenite are formed. In addition to this, in the fluorite of the veins intersecting the ore material (both at the points of intersection and also on moving upward along the rise of the veins), the uranium in the crystal lattice of the mineral amounts to $(1.4\text{-}3.8)\cdot 10^{-5}\%$, independently of the coloring of the mineral [5].

The factual material here presented enables us to visualize the behavior of uranium during the formation of deposits in the following manner. In the period of the early transformations of the rocks (in the stage of albitization), uranium was not carried into the solutions. In the stage of the quartz–carbonate–hydromica alteration, the uranium was introduced in small quantities, together with thorium, rare earths, and zirconium; uranium was introduced for a second time, together with molybdenum, antimony, lead, arsenic, and beryllium, in the main productive molybdenum–pitchblende stage of mineral formation. Between these two stages (in the stage of the quartz–carbonate–sulfide process) no marked transfer of uranium took place. In the post-ore quartz–fluorite–calcite stage, also, no uranium transfer occurred; however, there was a certain redeposition of uranium, the latter becoming fixed in the fluorite lattice and in the form of independent new formations of pitchblende. Thus during a single hydrothermal process uranium was transferred twice.

The characteristic behavior of uranium during the formation of the deposits may clearly be explained in a number of different ways. The authors propose the following explanation. As indicated by determinations of gas composition in the gas–liquid inclusions characterizing the minerals of various types of deposits, the main gases contained in these inclusions are CO_2, H_2, N_2, and more rarely CH_4 and O_2 [6, 7].

Existing information only indicates the relative concentrations of the gases. In order to analyze the behavior of the uranium in hydrothermal solutions, the factor of greatest interest is the H_2/CO_2 ratio, the values of which, referred to the homogenization temperatures of the gas–liquid inclusions, are given in Fig. 5. We see from Fig. 5 that the two maxima of the uranium concentration in the mineral aggregates and individual minerals of the uranium–molybdenum and fluorite polymetallic deposits are separated by a maximum of the curve characterizing the H_2/CO_2 ratio. Since the increase in this ratio is mainly due to a change in the hydrogen concentration [6, 7], it is natural to suppose that it is precisely the increase in hydrogen content which interfered with the transfer of uranium into the solutions. This assumption agrees with the generally accepted views according to which the transfer of uranium by hydrothermal solutions takes place chiefly in the form of readily soluble uranyl complex compounds. It should also be emphasized that, in the formation of polymetallic deposits, it is precisely the stage of mineral formation with a homogenization temperature of the gas–liquid inclusions equal to 220-300°C which is usually the main productive stage.

Thus the results here presented reveal the following characteristic features in the behavior of uranium during the formation of uranium–molybdenum deposits: 1) the uranium-bearing stages of the hydrothermal process are separated by a uranium-free stage, which indicates an interruption in the transfer of uranium; 2) there are sharp differences in the geochemical associations of the elements transferred and deposited together with uranium in different uranium-bearing stages; 3) in the later (productive) stage, incomparably more uranium was deposited than in the earlier uranium-bearing stage, this evidently being due to the different concentration of uranium in solution. These characteristics of the behavior of uranium suggest the existence of different sources effecting its passage into solution during a single hydrothermal process.

LITERATURE CITED

1. Yu. M. Dymkov, in: Questions of Applied Radiogeology [in Russian], No. 2, Atomizdat, Moscow (1967), p. 5.
2. Yu. M. Dymkov et al., in: Uranium Deposits, Zonality, and Paragenesis [in Russian], Atomizdat, Moscow (1970), p. 274.
3. G. B. Naumov and O. F. Mironova, in: Geochemistry of Hydrothermal Ore Formation [in Russian], Nauka, Moscow (1971), p. 61.
4. I. G. Berzina et al., At. Énerg., 23, No. 6, 520 (1967).
5. I. G. Berzina, I. V. Mel'nikov, and D. P. Popenko, At. Énerg., 32, No. 3, 211 (1972).
6. M. M. Elinson and V. S. Polykovskii, Izv. VUZ. Geologiya i Razvedka, No. 11, 31 (1961).
7. M. M. Elinson and V. D. Sazonov, Izv. VUZ. Geologiya i Razvedka, No. 4, 48 (1966).

BOOK REVIEW

T. G. Ratner and A. V. Bibergal'

FORMATION OF DOSE FIELDS IN TELEGAMMA THERAPY*

Reviewed by V. S. Yuzgin

In recent years γ-therapeutic methods have been introduced widely into clinical practice. The success in this area has excited the interest of medical men in tissue dosimetry, methods of creating the necessary dose fields at the foci of malignant neoplasms, problems of the design of devices for radiation therapy of tumors, etc.

Information on methods of forming the dose fields when irradiating patients have been collected and generalized and the regularities of the change of these fields on varying the characteristics of irradiation are examined in the book of T. G. Ratner and A. V. Bibergal'. Domestic γ-therapeutic apparatuses and the characteristics of their use are described.

The book has nine chapters. The first two chapters are essentially introductory. They discuss the characteristics of γ-active isotopes (Co^{60} and Cs^{137}) usually employed in radiation therapy and analyze the design features and advantages of isotope γ-apparatuses of four types: static long-distance (LUCh, GUT-Co-1200), rotational (RAD-1, AGAT-R), convergent (VOL'FRAM, ROKUS), and short-distance (RITS). The book touches briefly upon problems of protecting the personnel and patients against radiation and formulates the tasks of the further development of radiation, among which we need single out the further increase of the efficacy of irradiation by improving the apparatus and methods of irradiation, directed at obtaining optimal distribution of absorbed doses in the irradiated body. Practical methods of checking γ-apparatuses (the mechanical and electrical parts of the apparatuses and also the radiation parameters) are presented.

The following chapters (chapters three to eight) are devoted to different methods of irradiation. The dose distributions in a static beam of radiation in the air and in a tissue-equivalent medium are described. The methods of determining the percentage depth dose for various sizes of the irradiation field at a fixed distance from the source to the irradiated surface are shown. The data given in these chapters for domestic apparatuses are considered from the viewpoint of the recommendations of the International Atomic Energy Agency. Discussing the dose distribution in the case of static single-field irradiation, the authors give great attention to the character of the change of the dose beyond the boundaries of the direct beam of radiation and near the body surface. As a conclusion to this section rules for reducing the dose on the body surface are proposed. Problems of creating shaped irradiation fields occupy a large place in the book. In this connection, methods of using lattice and wedge filters, and also the role of the angle of incidence of the radiation beam to the body surface, are considered. Examples of the practical calculation of the absorbed dose in a malignant focus in the case of single-field irradiation are given. Static multiple-field irradiation is elucidated in the fourth chapter. The central issue of this chapter is the planning of multiple-field irradiation, or calculation of the dose field when irradiating a specific patient. Here two methods of calculating the dose fields are given. The virtues and shortcomings of so-called plateau diagrams in the case of two-, three-, four-, and multichannel irradiation are analyzed.

The characteristics of rotational single-zone (fifth chapter) and multiple-zone sector (sixth) irradiation are considered with reference to domestic γ-therapeutic apparatuses. The effect of the dynamic qualities of the apparatus on the dose distribution in the body is considered and recommendations for the determination of the parameters of eccentric irradiation and the calculation of the focal dose are given. Convergent irradiation by means of the new USSR-produced VOL'FRAM and ROKUS apparatus, which are

*Nauka, Moscow, 1972.

Translated from Atomnaya Énergiya, Vol. 35, No. 1, p. 10, July, 1973.

charged with a Co^{60} source, is elucidated in the seventh and eighth chapters. This method is a further development of the multiple-field and rotational methods of irradiation. It allows the use of the properties both of the multiple-field method (bypassing the critical organs by selecting the direction of the axis of the field) and of the rotational method (decreasing the dose in the surface layers and obtaining a maximum dose at great depth), whilst ensuring, in comparison with them, a maximum absorbed dose at the focus for comparable dimensions of the axial field and angle of oscillation. The effect of inhomogeneity of the body on the dose distribution is shown in the last chapter. The method proposed by A. Dutre for introducing corrections in the case of inhomogeneity is discussed. In addition, the principle of measurement of the so-called transit dose, corresponding to radiation that has passed through the patient's body, and the use of this principle when calculating corrections for inhomogeneity are considered.

The book is concisely written and contains many illustrations (135 figures) which can be used in clinical practice. It answers a number of the topical questions of medical radiology. All this makes the book useful for specialists engaged in treating malignant tumors and developing γ-therapeutic apparatuses. It should be noted that, in presenting the principles of tissue dosimetry in a popular manner, the authors unfortunately did not adhere to strict physical terminology in a number of cases.

ARTICLES

TOKAMAK-BASED LOW-POWER REACTOR

V. I. Pistunovich

UDC 533.9:621.039.61

Recently, there have appeared several papers devoted to an analysis of the possibilities of plasma heating in devices of the "Tokamak" type through injection of fast neutral particles [1-7]. These papers indicate that only the performance of experiments involving the injection of fast particles will make it possible to answer those fundamental questions the solution of which should determine the prospects for the development of a method of plasma heating. The possibility of heating plasma to thermonuclear temperatures is determined mainly by the energy lifetime of the ions, τ_{Ei}. It may be shown that the increase in τ_{Ei} with increase in temperature occurs more slowly than $T^{1/2}$, i.e., it does not correspond to neoclassical theory in the region of infrequent collision [8]. Hence, for ignition of a thermonuclear reaction, it is necessary to construct a device with an increased plasma radius a since the energy lifetime of the plasma $\tau_E \sim a^2$, and consequently to inject a larger flux of neutrals [5]. On the other hand, if it is assumed that the time for transfer of energy from a fast ion to plasma electrons and ions remains classical [9], then even for small τ_{Ei} the "Tokamak-with-injection-of-fast-neutrals" system may be considered as a low-power reactor with positive energy output.

The possibility of producing thermonuclear energy by deceleration of a beam of fast deuterons in a tritium plasma having hot electrons was first proposed in [10] where doubt was expressed with regard to the practical interest of this process. In [11], an analysis was made of the system over a wider range of fast-deuteron energies and conditions were obtained under which a thermonuclear reaction with positive energy output could be achieved.

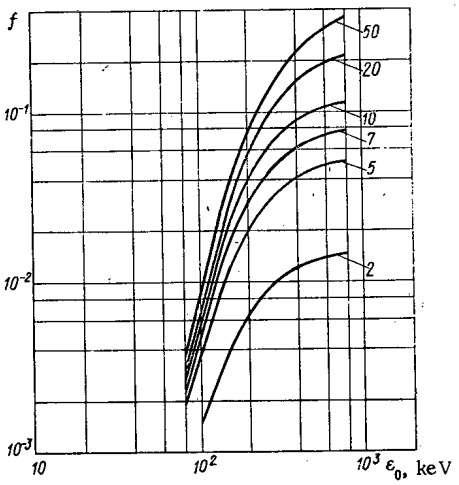

Fig. 1

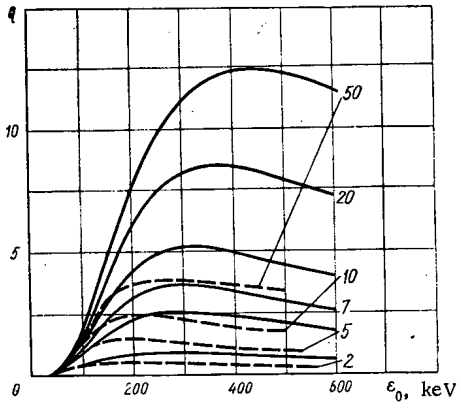

Fig. 2

Fig. 1. Dependence of probability f on deuteron energy ε_0 in tritium plasma. Numbers on the curves in all figures correspond to T_e, keV.

Fig. 2. Dependence of Q on ε_0 for various T_e: ——) this work; - - - -) data from [11].

Translated from Atomnaya Énergiya, Vol. 35, No. 1, pp. 11-14, July, 1973. Original article submitted December 13, 1972.

In this paper, the possibilities of such a system are discussed in more detail using a "Tokamak" device with injection of fast deuterons as an illustration.

Indeed, when fast deuterium atoms are injected into a tritium plasma, a thermonuclear reaction will occur with a certain probability during the deceleration of the deuterons which are formed. If the energy released in the thermonuclear reaction is, on the average, Q times greater than the energy of the injected ion, the condition for the production of electrical power can be written in the form

$$Q \geqslant \frac{1}{\eta\varepsilon} - 1, \tag{1}$$

where $\eta = \eta_T \eta_I$; η_T is the efficiency of the thermal cycle; η_I is the efficiency of the injector; ε is the fraction of the electrical energy which is fed back into the injector. The quantity $Q = fE_T/\varepsilon_0$, where f is the probability that a thermonuclear reaction will occur during the deceleration of a deuteron in the tritium plasma; $E_T = 22.4$ MeV is the total energy of the d–t reaction per fusion event including the capture energy in Li^6 (4.8 MeV) which comprises the blanket; ε_0 is the initial deuteron energy.

We calculate the quantity f for the d–t reaction assuming that the deuteron lifetime τ_α is greater than the deceleration time τ:

$$f = \int_0^\tau n_i \sigma_r v_\alpha \, dt = \sqrt{\frac{2}{m_\alpha}} \int_{\varepsilon_0}^{0} n_i \sigma_r \varepsilon_\alpha^{1/2} \frac{d\varepsilon_\alpha}{d\varepsilon_\alpha/dt}. \tag{2}$$

Here, n_i is the density of the tritium plasma; σ_r is the cross section for the d–t reaction; v_α, m_α, and ε_α are the velocity, mass, and energy of a deuteron which is decelerated in the tritium plasma.

The rate of energy loss by a deuteron in a tritium plasma in the case $T_i \ll \varepsilon_\alpha \ll (m_\alpha/m_e)T_e$ is written in the form [5]

$$\frac{d\varepsilon_\alpha}{dt} = -A\varepsilon_\alpha^{-1/2} - B\varepsilon_\alpha + D, \tag{3}$$

where

$$A = 2\pi\sqrt{2}\,\frac{Z_\alpha^2 Z_i^2 e^4 \Lambda n_i m_\alpha^{1/2}}{m_i}; \quad B = \frac{8\sqrt{2\pi}}{3}\cdot\frac{Z_\alpha^2 e^4 \Lambda n_e m_e^{1/2}}{m_\alpha T_e^{3/2}};$$

$$D = 4\sqrt{2\pi}\,\frac{Z_\alpha^2 e^4 \Lambda n_e m_e^{1/2}}{m_\alpha T_e^{1/2}};$$

$Z_i e$, n_i, and m_i are the charge, density, and mass of the plasma ions; e, n_e, and m_e are the charge, density, and mass of the plasma electrons; $Z_\alpha e$, n_α, and m_α are the charge, density, and mass of the fast ion; T_e and T_i are the temperatures of the plasma electrons and ions; $\Lambda = 20$ is the Coulomb logarithm. It is clear that the quantity f is a function of ε_0 and T_e.

In calculating the probability f for the occurrence of a reaction using Eqs. (2) and (3), the expression for the d–t reaction cross section, in accordance with [10], was taken to be of the following form:

$$\sigma_r = \frac{6\cdot 10^{-17}}{\varepsilon_\alpha} \exp\left(-\frac{1.5\cdot 10^3}{\sqrt{\varepsilon_\alpha}}\right)\left[1 + \frac{(\varepsilon_\alpha - 10^5)^2}{3\cdot 10^{10}}\right]^{-1}, \tag{4}$$

which for energies $\varepsilon_0 < 1$ MeV differs from experimentally measured values by factors of no more than 1.5–2.

Calculated values of $f(\varepsilon_0 T_e)$ determined in this manner are shown in Fig. 1 as a function of ε_0. The corresponding dependence of $Q = fE_T/\varepsilon_0$ on ε_0 is shown in Fig. 2 for various values of T_e. Values for the quantity Q given in [11] are 1.5–3 times less than the values obtained in this work. The reason for such a discrepancy is probably connected with an overestimated value for σ_r used in the present work.

The deceleration time τ for a deuteron in tritium plasma was calculated from the expression

$$\tau = \int_{\varepsilon_0}^{0} \frac{d\varepsilon_\alpha}{d\varepsilon_\alpha/dt} = \int_0^{\varepsilon_0} \frac{\varepsilon_\alpha^{1/2}\, d\varepsilon_\alpha}{A + B\varepsilon_\alpha^{3/2} - D\varepsilon_\alpha^{1/2}}. \tag{5}$$

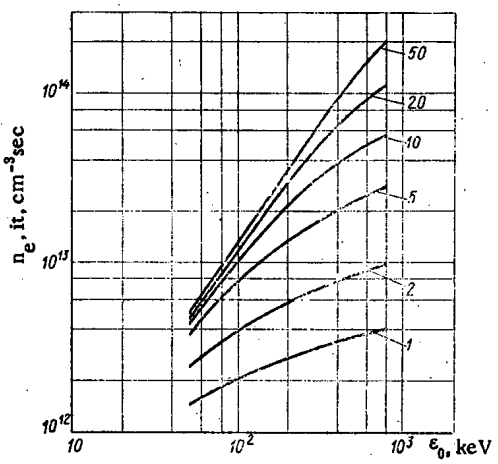

Fig. 3. Values of $n_{e,i}\tau$ for deceleration of a deuteron with energy ε_0 in tritium plasma at various T_e.

The dependence of $n_{e,i}\tau$ on ε_0 obtained from Eq. (5) is shown in Fig. 3 for various values of T_e. The values of $n_{e,i}\tau$ are in good agreement with the results in [11].

Energy balance in the system under discussion can be represented in the form of two relations:

$$\begin{aligned} &\varepsilon_0 n_\alpha \leqslant \eta\varepsilon\,(n_\alpha f E_T + \varepsilon_0 n_\alpha);\\ &\frac{\varepsilon_0 n_\alpha}{\tau} \geqslant \frac{3}{2} n_{e,i}\frac{T_e+T_i}{\tau_E} + P_b + P_M, \end{aligned} \tag{6}$$

where τ_E is the energy lifetime of the plasma; $P_b = 3.34\cdot 10^{-15} n^2\sqrt{T_e(\text{keV})}\,\text{keV/cm}^3\text{-sec}$ is the specific bremsstrahlung power; $P_M = 6.25\cdot 10^{-14} n_e^2 F_M^0 \Phi$ keV/cm^3-sec is the specific power in magnetic radiation from electrons of the Tokamak plasma [12] [$F_M^0 = (T(\text{kev})/25)^2/\beta_e$; $\beta_e = 8\pi nT/H_0^2$; $\Phi = \sqrt{1+9\chi/8}\sqrt{1-r}\,(60t^{3/2}/\sqrt{P_a})$; $t = T/m_eC^2$; $P_a = a\omega_{0e}/c\omega_B$; $\chi = 2a/R\sqrt{2\pi t}$; r is the reflection coefficient; a and R are the minor and major radii of the torus]. In Eq. (6), it is assumed $n_e \approx n_i$ since $n_\alpha \ll n_i$. Eliminating ε_0 in Eqs. (6), we obtain an expression for $n_{e,i}\tau_E$ which is similar to the Lawson criterion for plasma heating by the injection method:

$$n_{e,i}\tau_E \geqslant \frac{1{,}5\,(T_e+T_i)}{\dfrac{\eta\varepsilon}{1-\eta\varepsilon}\dfrac{fE_T}{n_{e,i}\tau} - \dfrac{P_0+P_M}{n_\alpha n_i}}\cdot\frac{n_{e,i}}{n_\alpha}. \tag{7}$$

A second condition for a system with positive energy output is obtained from the first of Eqs. (6) and has the form of Eq. (1).

An advantage of the system under discussion is that only the electrons need be heated in the Tokamak plasma; the ion temperature can be as low as is convenient. In this sense, the modes achieved in present experiments [13] where a considerable difference exists between T_e and T_i are close to those which are necessary for the creation of a reactor based on this scheme.

The dependence of $n_{e,i}\tau_E$ on ε_0 is shown in Fig. 4 for various values of T_e when $T_e \gg T_i$ and $\eta\varepsilon = 1/3$. Shown also is the Lawson dependence on temperature T for n_iT_E without consideration of magnetic radiation during plasma heating by the injection method when $\eta\varepsilon = 1/3$. It is clear that the values of $n_\alpha\tau_E$ lie considerably below the values of $n_i\tau_E$ although, in the calculation of $n_{e,i}\tau_E$, consideration was given to losses because of magnetic radiation from electrons for a reflection coefficient $r = 0$. For comparison, Figure 5 shows the dependence on electron temperature of the nuclear yield of the d–t reaction, $fE_T/n_{e,i}\tau$, for $\varepsilon_0 = 200$ keV, of the magnetic radiation power $P_M/n_in_\alpha\sqrt{1-r}$, and of the bremsstrahlung power P_b/n_in_α.

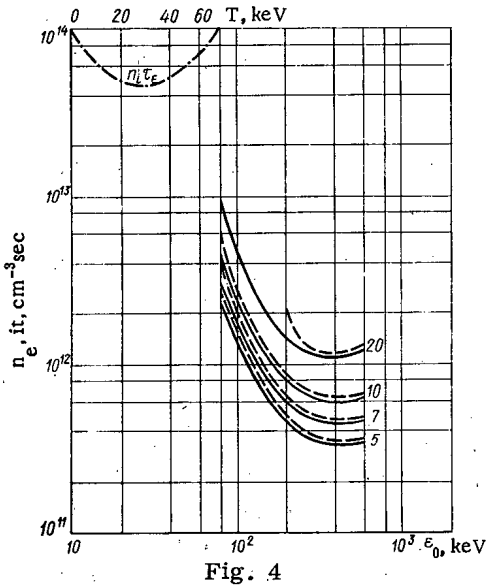

Fig. 4

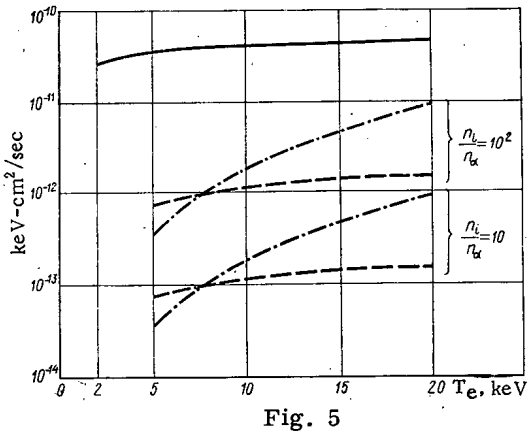

Fig. 5

Fig. 4. Dependence of $n_{e,i}\,\tau_e$ on deuteron energy ε_0 for various values of electron temperature T_e and $\eta\varepsilon = 1/3$: ——) $n_i/n_\alpha = 10$; ----) $n_i/n_\alpha = 10^2$; · - · - ·) Lawson dependence of "Tokamak" reactor for heating by the injection method as a function of plasma temperature T for $\eta\varepsilon = 1/3$.

Fig. 5. Dependence of nuclear reaction power and power losses on T_e: ——) nuclear yield $fE_T/n_{e,i}\tau$ for $\varepsilon_0 = 200$ keV; - · - · -) magnetic radiation power $P_M/n_in_\alpha\sqrt{1-r}$; ----) bremsstrahlung power P_b/n_in_α.

We demonstrate the possibility of building a reactor with positive energy output by the following example. Let the minor and major radii of the Tokamak be respectively $a = 80$ cm and $R = 300$ cm; blanket thickness $r_\delta = 120$ cm; magnetic field $H_{oz} = 50$ kG; the quantity $q = H_{oz}a/H_\varphi R = 3$, hence the magnetic field of the discharge current $H_\varphi = H_{oz}/qA = 4.5 \cdot 10^3$ G; $A = R/a = 3.8$; plasma volume $\Omega = 3.8 \cdot 10^7$ cm^3. Tritium plasma density in the Tokamak is determined from the condition that the flux of deuterium atoms decreases by a factor e because of ionization over a length $l \approx 100$ cm. Let $\eta\varepsilon = \eta_T\eta_I\varepsilon = 1/3$. We find $Q \geq 2$ from Eq. (1). According to Fig. 2, the quantity Q reaches a maximum value for $\varepsilon_0 \approx 300$ keV when $T_e = 5$-20 keV. On this basis, it is advantageous to select an injected deuterium atom energy $\varepsilon_0 \approx 300$ keV. Heating of electrons will occur because of the deposition of Joule heat during the flow of discharge current in the plasma and because of the transfer of energy from fast deuterons. According to [14], electron temperature in Tokamak plasma can be determined from

$$\bar{n}_e k\bar{T}_e(1+\alpha) = 1.8 \cdot 10^{-2}\bar{H}_\varphi^2, \tag{8}$$

where $\alpha = \bar{T}_i/\bar{T}_e$ is the ratio of the temperatures averaged over the cross section of the plasma column. If $\bar{H}_\varphi = 4.5 \cdot 10^3$ G, $\bar{n}_e = 5 \cdot 10^{13}$ cm^{-3}, and $\alpha \ll 1$, $\bar{T}_e = 4.5$ keV.

As is clear from Fig. 2, when $T_e = 4$ keV, $Q \approx 2$, and it is consequently necessary to consider heating of electrons by fast deuterons. To obtain $Q = 3$, an electron temperature $T_e \geq 10$ keV is necessary. We calculate the deuteron current I_α captured in the Tokamak magnetic field which is necessary to heat electrons to $T_e = 10$ keV:

$$I_\alpha = \frac{3}{2} \cdot \frac{n_e T_e \Omega}{\tau_E \Delta E_e}, \tag{9}$$

where τ_E is the energy lifetime of the plasma, which must be no less than the deceleration time τ of a fast ion; ΔE_e is the energy lost by a deuteron during deceleration by plasma electrons. To determine τ_E we used the experimental dependence of lifetime on a and H_φ [15]:

$$\tau_E = 3.6 \cdot 10^{-8} a^2 H_\varphi \approx 1 \text{ sec}. \tag{10}$$

The deceleration time of deuterons with energy $\varepsilon_0 = 300$ keV in a tritium plasma where $n_e = 5 \cdot 10^{13}$ cm^{-3} and $T_e = 10$ keV is $\tau = 0.6$ sec $< \tau_E$ as follows from Fig. 3. We determine the quantity ΔE_e from [5]: $\Delta E_e \approx 0.4\varepsilon_0 = 120$ keV, hence $I_\alpha = 40$ A. The density of fast ions is

$$n_\alpha = \frac{I_\alpha \tau}{\Omega} \approx 4 \cdot 10^{12} \text{ cm}^{-3}, \tag{11}$$

and consequently the value for $n_{e,i}\tau_E$ lies above the corresponding curve in Fig. 4. Finally, we calculate the value of β_φ over the field of the discharge current, which must not exceed R/a from the condition for conservation of equilibrium:

$$\beta_\varphi = \frac{n_e T_e + n_\alpha \varepsilon_0}{H_\varphi^2} \cdot 8\pi = 3.3 < \frac{R}{a} = 3.8.$$

Thus the current of deuterium ions, $I_\alpha = 40$ A, captured in the Tokamak magnetic field is sufficient to heat electrons to $T_e = 10$ keV and to ensure operation of the entire system with positive energy output. The thermal power of such a reactor is $P_T = QI_\alpha\varepsilon_0 = 36$ MW. If it is assumed the injector efficiency $\eta_I = 0.9$ and the thermal cycle efficiency, $\eta_T = 0.5$, we find that a power P_0, equal to $(1-\varepsilon) \approx 0.2$ of the electrical power P_e, will be fed into the grid. The efficiency of the entire system is determined from the expression

$$\eta_0 = \frac{P_0}{P_T} = \frac{(Q+1)\varepsilon_0 I_\alpha \eta_T - \varepsilon_0 I_\alpha/\eta_I}{Q\varepsilon_0 I_\alpha} = 0.3.$$

In this reactor scheme, different variations of its parameters are possible. Looking ahead, the scheme for a thermonuclear reactor considered can be used as an element from which power stations of considerably greater power could be built up.

The author is deeply grateful to I. N. Golovin for numerous discussions of the results and to M. V. Nezlin for valuable comments.

LITERATURE CITED

1. L. A. Artsimovich, Usp. Fiz. Nauk, 91, 365 (1967).
2. G. Kelly et al., Nucl. Fusion, 12, 169 (1972).
3. T. Stix, Plasma Phys., 14, 367 (1972).
4. M. V. Nezlin, Pis'ma v Zh. Éksp. Teor. Fiz., 16, No. 2, 112 (1972).
5. V. I. Pistunovich, Tokamak with Injection of Fast Neutrals [in Russian], Preprint IAE-2209, Moscow (1972).

6. J. Girard et al., Paper at the European Conference on Plasma Physics, Grenoble (1972).
7. D. Aldcroft et al., Paper at the European Conference on Plasma Physics, Grenoble (1972).
8. A. A. Galeev and R. Z. Sagdeev, Zh. Éksp. Teor. Fiz., 53, 348 (1967).
9. B. A. Trubnikov, Problems in Plasma Theory [in Russian], No. 1, Gosatomizdat, Moscow (1963), p. 98.
10. L. A. Artsimovich, Controlled Thermonuclear Reactions [in Russian], Fizmatgiz, Moscow (1961), p. 60.
11. J. Dawson et al., Phys. Rev. Lett., 26, 1156 (1971).
12. B. A. Trubnikov, Pis'ma v Zh. Éksp. Teor. Fiz., 16, No. 2, 37 (1972).
13. L. A. Artsimovich, V. A. Vershkov, et al., Paper CN-28/C8 at Conference on Plasma Physics and Controlled Fusion, Madison, USA (1971).
14. L. A. Artsimovich, Pis'ma, v Zh. Éksp. Teor. Fiz., 13, No. 2, 101 (1971).
15. L. A. Artsimovich, S. V. Mirnov, and V. S. Strelkov, At. Énerg., 17, No. 3, 170 (1964).

POSSIBILITY OF USING A SYSTEM OF TAPERED DIAPHRAGMS FOR THE RECUPERATION OF REACTOR ION BEAMS

O. A. Vinogradova, S. K. Dimitrov,
A. M. Zhitlukhin, A. N. Igritskii,
V. M. Smirnov, and V. G. Tel'kovskii

UDC 621.039.6

The idea of directly converting the energy of charged particles escaping through the stoppers (mirrors) of open adiabatic traps was proposed in [1]. Post also proposed a specific arrangement theoretically yielding a very high conversion efficiency (0.92-0.96).

One of the most important elements in the Post conversion system is an electrostatic device for slowing and collecting the ions, incorporating a steady retarding field and a periodic deflecting field with plane symmetry.

The potential of the combined field is given by:

$$U(x, y) = U_0 \left(\frac{x}{\Lambda} + \frac{A}{2\pi} \sin \frac{2\pi x}{\Lambda} \operatorname{ch} \frac{2\pi y}{\Lambda} + \frac{C}{2\pi} \sin \frac{2\pi x}{\Lambda} \operatorname{sh} \frac{2\pi y}{\Lambda}\right), \quad (1)$$

where Λ is the period of the system along the x axis, U_0 is the potential drop in one period of the system, and the constants A and C regulate the symmetrical (A) and antisymmetrical (C) deflecting fields.

The system chosen in [2] had a potential distribution (1) with A = 0 (i.e., with strong focusing), probably in order to intensify the action on particles traveling close to the axial plane of the beam and reduce the number of returned particles. The parameters U, D/L, C, Λ (D is the channel width of the system) were optimized in advance by computer-calculating the trajectories of ions with different initial velocities V_0 and positions Y_0, the angular deviation of the velocity vector being ± 0.02 radian. As a result of this optimization the calculated number of particles escaping from the system was reduced to 7% (in the energy range $W_{max}/2$ to W_{max}), while the calculated efficiency was 92%, subject to the repeated recuperation of the back-scattered ions, after their reflection from the magnetic field of the stoppers (magnetic mirrors). The results predicted by these numerical calculations were verified by laboratory experiments [2]. The field of the Post system was created in the first retardation section (in which no flow of particles to the walls was expected), using ten pairs of rods charged with respect to the linearly increasing potential on the axis of the system. In the next retarding stage, in which the potential corresponded to the energy of the incoming particles, the negatively charged rods in the modules were replaced by cylindrical grids, so that the particles accelerated by the deflecting field in the transverse direction passed through the grids and fell on plates at a higher potential than that on the axis of the module. The average experimental efficiency over the energy range $W_{max}/2$ to W_{max} for a system of 21 modules was 83% for 5% of back-scattered ions, or 88% if secondary recuperation of the particles escaping into the expander could be achieved. Increasing the efficiency of the Post system to more than 90% is very problematical, even in rarefied beams (neglecting space charge).

For the direct conversion of charged-particle energy in the present investigation we propose a system of tapered diaphragms [3], the experimental efficiency of which is 96% for a rarefied beam, i.e., 13% higher than that of Post el al. [2]. We note that the tapered diaphragm system possesses this high efficiency even without the recovery of the transverse energy $W_\perp$, which was in fact recovered in the Post system.

Translated from Atomnaya Énergiya, Vol. 35, No. 1, pp. 15-18, July, 1973. Original article submitted November 15, 1972.

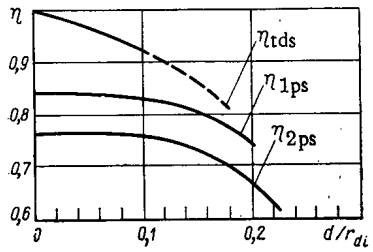

Fig. 1. Dependence of η_{ps} (for narrow and wide beams) and η_{tds} on d/r_{di}.

It follows from the calculations of [4] that the main parameters of the initially parallel beam, which completely determine the geometry of the tapered diaphragm system, are the Debye ionic radius r_{di} and the beam thickness d, the efficiency of the tapered diaphragm system depending on the ratio d/r_{di}. The criterion is clearly common to all recuperation systems, and comparison between these should therefore be made by reference to the efficiency as a function of the ratio d/r_{di} for the entering beam (assuming the same energy and angular spread of the particles). The dependence of η_{tds} on d/r_{di} is shown in Fig. 1. The dependence of η_{1ps} (ps = post system) on d/r_{di} for a narrow beam ($\omega_{0i}\tau = 8\, d/r_{di}$ where ω_{0i} is the plasma ion frequency, τ is the time required for an ion to fly through a distance Λ corresponding to one period of the system with the maximum entrance velocity v) and the dependence of η_{2ps} on d/r_{di} for a wide beam ($\omega_{0i}\tau = 2.67\, d/r_{di}$) with C = 2 are also shown in Fig. 1. The efficiency η_{tds} was calculated from the formula [4]:

$$\varepsilon_{min} = \sqrt{2\varkappa}\left(\frac{d}{r_{di}} + \frac{\theta}{\sqrt{2}}\right), \quad \eta \equiv 1 - \varepsilon, \tag{2}$$

where $\varkappa$ is a coefficient depending on the initial distribution of the particles over the beam cross section; for a uniform particle distribution over the cross section of a plane beam $\varkappa \approx 1/3$; the broken continuation of the line shows the region in which the approximation used ceases to be true ($\varepsilon_{min} = 0.815\, \vartheta/r_{di}$, $\varkappa = 1/3$, $\theta = 0$).

For the reactor conditions considered by Post, in which the deuteron energy was W = 800 keV, the current density at the entrance into the recuperator was $j = 0.4 \cdot 10^{-3}$ A/cm^2, the width of the entrance flux $d = 10^2$ cm, the density of the ions at the outlet from the expander $n = 2 \cdot 10^6$ cm^{-3}, and the total flux intensity from one stopper P = 0.96 million kW, with $d/r_{di} = 0.18$. We see from Fig. 1 that, for d/r_{di} values less than 0.18, η_{tds} is much higher than η_{ps}, reaching approximately 92% for $d/r_{di} = 0.1$ and 96% for $d/r_{di} = 0.05$ (in both cases the Post system gives $\eta \sim 80$–85%).

For large values of d/r_{di} the beam expands considerably as the particles traverse the slowing-down length under the influence of electrostatic repulsion. The simplicity of the present construction favors the introduction of compensating electron fluxes into the tapered diaphragm system (for example, in crossed $\mathbf{E} \perp \mathbf{H}$ fields). However, for $d/r_{di} \leq 0.2$ it is sufficient to use the simplest means of combating beam spread, by focusing the beam in front of the entrance into the recuperator, close to the end of the slowing-down length.

For particles of three energies (W_{max}, $3W_{max}/4$, and $W_{max}/2$) we calculated the distances L from the entrance into the tapered diaphragm system to the centers of the focusing intervals of width δL (giving the maximum η) corresponding to different d/r_{di} ratios. We found that a system of tapered diaphragms in which the particles retained a considerable transverse energy $W_\perp$ [a system with $\varepsilon_{cal} = \sin^2\alpha = 0.1$; the angle between the direction of particle velocity at the entrance into the system and the direction of the field E is $(\pi - \alpha)$; the calculated efficiency is $(1 - \varepsilon_{cal})$] before they intersected the line of the diaphragms was capable of counteracting the effect of space charge up to a value of $d/r_{di} \approx 0.18$ (corresponding to reactor conditions) while still preserving a high efficiency (over 90%).

Focusing of the main part (the center) of the beam may be achieved by the inclination of the magnetic lines of force of the expander; hence it is only necessary to provide extra focusing for the particles in the peripheral parts of the beam, which experience the greatest deflection as the magnetic lines of force pass out of the beam. For this purpose we tried a focusing system with a potential of the form

$$U(x, y) = B \sin\frac{2\pi x}{\Lambda} \operatorname{ch}\frac{2\pi y}{\Lambda}, \tag{3}$$

where the x axis is directed along the axis of the system, Λ is the period of the focusing system, B is the amplitude of the potential fluctuations on the axis of the focusing system, and the potential drop in one period of the system is equal to zero. Using a computer, we calculated the trajectories of the ions in the field (3). The parameters B_1 and B_2 (values of B in the first and second half periods of the field) were varied so as to discover whether it were possible to focus particles of all energies in the desired ranges. The length of the focusing system was taken as $\Lambda = d = 0.3L$ (d = beam width, L = length of tapered diaphragm system) so as to be able to neglect the effect of space charge in the beam for $d/r_{di} \leq 0.2$ (calculations showed that the effect of space charge was unimportant for this length of the focusing system). On

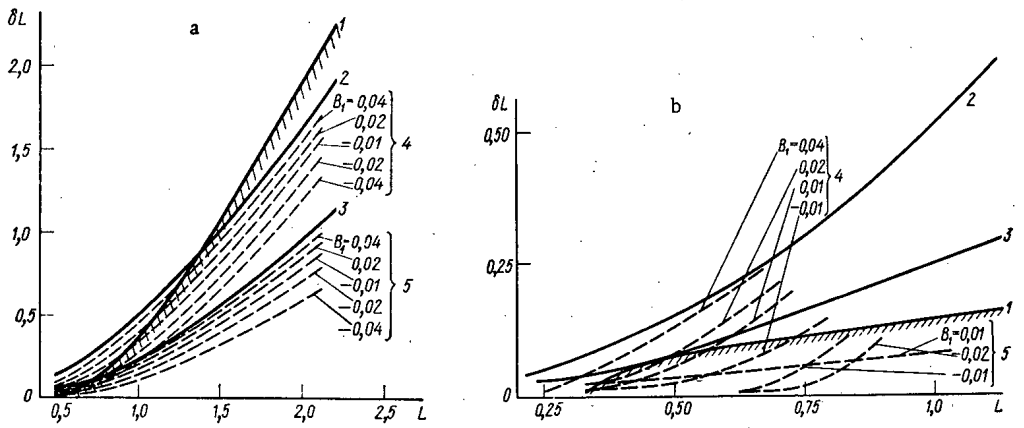

Fig. 2. Possible lengths L and focusing intervals δL in the focusing system: a) $W = W_{max} = 10$ keV, $Y = d/2 = 1.5$ cm; b) $W = W_{max}/2 = 5$ keV; $Y = d/2 = 1.5$ cm; 1) curve defining the boundary of the range of focusing intervals required in order to obtain $\eta_{tds} \geq 0.9$; 2) $\theta = \pm 0.04$, $B_1 = 0.2$, $B_2 = 0$; 3) $\theta = \pm 0.02$, $B_1 = 0.2$, $B_2 = 0$; 4) family of curves with $\theta = \pm 0.04$, $B_1 = 0.2$, and different B_1; 5) family of curves with $\theta = \pm 0.02$, $B_2 = 0.2$, and different B_1.

increasing Λ to L the effect of space charge becomes appreciable; furthermore, particles with an energy $W = W_{max}/2$ which remain for a long time in the field of the focusing system are focused excessively strongly. For a value of $\Lambda < d$ the focusing of a reasonably wide outer region of the beam becomes impossible, since the focusing field falls too rapidly toward the center of the beam.

In Fig. 2a, b, curve 1 is based on calculations of the focusing intervals needed in order to obtain a high efficiency of the tapered diaphragm system, $\eta_{tds} \geq 0.9$, i.e., below this curve is the range of focusing intervals ensuring a high efficiency of the tapered diaphragm system. Curves 2 and 3 in Fig. 2a indicate the possibility of focusing the outer part of a beam with d/r_{di} not less than 0.11 into the desired interval for $\theta = \pm 0.04$, and with d/r_{di} not less than 0.18 for $\theta = \pm 0.02$ when the particle energy equals W_{max}. These curves correspond to a strong-focusing field in the first half period ($B_1 = 0.08$–0.20) and the absence of a field in the second ($B_2 = 0$), i.e., to a single-half-period focusing system. Above these curves is the region corresponding to a defocusing second half period ($B_2 > 0$). The analogous curves in Fig. 2b show that, for beams with energy $W_{max}/2$ and a similar choice of parameters B_1 and B_2, the desired focusing is impossible for $\theta = \pm 0.04$, and for $\theta = \pm 0.02$ is only possible with a narrow range of variation of the ratio $d/r_{di} \approx 0.22$–0.24.

However, by using a slight focusing (or defocusing) field in the first half period and a strong focusing field in the second half period we may secure the desired focusing of beams with energies W_{max} and $W_{max}/2$ for $\theta = \pm 0.02$ and ± 0.04 and a strong space charge (with d/r_{di} not less than 0.23). We see from Fig. 2a, b that the families of curves 4 (for $\theta = \pm 0.04$) and 5 (for ± 0.02) corresponding to this choice of B_1 and B_2 lie in a region giving a high efficiency of the tapered diaphragm system.

By considering trajectory plots of the particles in the focusing system, we may see the manner in which the focusing intervals depend on the entrance radius for energies W_{max} and $W_{max}/2$ with $\theta = 0.02$ and ± 0.04. We find that a focusing system with a field of form (3) only focuses ions from a narrow outer part of the beam (about one third of all the ions).

Recently Barr [5] noted the high efficiency of a tapered diaphragm system for rarefied beams with a small angular divergence; he suggested that the problem of combating the effects of space charge in a tapered diaphragm system was much more complicated than in the Post system, owing to the difficulties of focusing wide beams and the small value of the deflecting field $E_\perp$ by comparison with the space-charge field E_c. The amplitude of the deflecting field in the Post system is of the order of E_c. However, as already remarked, the main preliminary focusing of the wide beam may be achieved by an appropriate inclination of the magnetic lines of force in the expander, while electrostatic lenses at the entrance into the recuperator will only correct the range of focusing. The comment as to the smallness of the $E_\perp/E_c$ ratio loses its meaning in the presence of focusing (as the results of a numerical experiment clearly demonstrate).

In conclusion, let us list the fundamental properties of a system of tapered diaphragms and the possible ways of improving this system.

1. A tapered diaphragm system may work on beams with a wide particle energy distribution W ($^1/_2$ $W_{max} \leq W \leq W_{max}$; W_{max} being the maximum energy of the particles).

2. It is essential for the operation of a tapered diaphragm system that the angular spread in the velocities of the particles in the beam should be small (±0.02 radian).

3. Without preliminary focusing and the recuperation of the transverse energy $W_\perp$, the calculated efficiency of the tapered diaphragm system is only over 90% for relatively rarefied beams ($d/r_{di} \leq 0.1$), reaching 96% for $d/r_{di} \approx 0.05$; an efficiency of 96% for $d/r_{di} = 0.01$ is obtained experimentally.

4. With preliminary focusing of the particles close to the end of the slowing-down length, with an appropriate inclination of the magnetic lines of force in the expander, and with electrostatic lenses at the entrance into the recuperator, a tapered diaphragm system efficiency of over 90% may be obtained for $d/r_{di} \approx 0.2$ (the value of d/r_{di} for the reactor conditions considered by Post was 0.18). Lenses with a periodic electrostatic focusing field of plane symmetry provide the necessary focusing of the particles in the outer part of the beam.

5. The recuperation of $W_\perp$ may reduce the losses of a tapered diaphragm system by approximately a factor of two, i.e., for $d/r_{di} \approx 0.2$ we may obtain an efficiency of 94%.

6. If the width of the plane flow at the entrance is reduced by a factor of N, d/r_{di} is reduced by $\sqrt{N}$ times, while if the flow is divided into N parts it is reduced by N times.

7. The introduction of compensating electron flows (for example, in crossed $E \perp H$ fields) into the tapered diaphragm system yields a high efficiency for $d/r_{di} > 1$.

LITERATURE CITED

1. R. Post, Nuclear Fusion Reactor Conf., UKAEA (1970), pp. 88-111.
2. R. Moir et al., "Experimental and computational investigations of the direct conversion of plasma energy to electricity," UCRL-72879 (1971).
3. O. A. Vinogradova et al., At. Énerg., 33, No. 1, 586 (1972).
4. O. A. Vinogradova, Contribution to the European Conf. on Plasma Physics, Grenoble (1972).
5. W. Barr, Direct Energy Recovery from a Beam of Charged Particles Using Parabolic Ion Trajectories, UCRL-51147 (1971).

VELOCITY PROFILES OF A FLUID AT THE INLET OF A CLOSE-PACKED BUNDLE OF RODS

L. N. Bibikov, Yu. D. Levchenko, V. I. Subbotin, and P. A. Ushakov

UDC 621.1/2

In calculating heat exchangers with a small relative length it is necessary to take into account the characteristics of heat exchange and hydraulics at the inlet, where heat emission and energy loss owing to intense mixing of the fluid are higher than in a stabilized flow. When selecting the method of setting up experiments to obtain data on stabilized fluid flow in channels, it is important also to know the length of the inlet section. Heretofore the characteristics of turbulent fluid flow have been studied only for channels with an axisymmetric cross section. For example, the regularities of stabilization of the velocity profile and pressure gradients were studied experimentally in [1-5] and analytical solutions for a uniform velocity profile at the inlet were obtained in [6-10].

This article describes the results of experimental investigations of the length of the hydraulic inlet section and change of velocity profiles of a turbulent flow over the length of a channel of a close-packed bundle of smooth rods.

EXPERIMENTAL METHOD

In the experiment we used a channel simulating a cell of an infinitely close-packed bundle of rods located in a perfect triangular lattice. The diameter of the circumferences forming the channel was 208.4 mm. The total length of the channel, consisting of three sections, was 4050 mm. The channel sections were joined together in the following order: 450, 1800, and 1800 mm. A diagram of the cross section is shown in Fig. 1.

The measurements were taken for a turbulent flow of air with a maximum flow rate and head equal to 1000 m^3/h and 1000 kg/m^2, respectively. Local flow velocities were measured by glass Pitot tubes with an external diameter of 0.2-0.3 mm; the calibration coefficient of the tubes was assumed equal to unity. The total head was measured by a cup-shaped vertical differential manometer filled with alcohol. The alcohol level was recorded by a cathetometer to within ±0.1 mm. The Pitot tubes were placed in three mutually perpendicular directions by means of a coordinate device with reading microscopes having a scale division of 0.001 m.

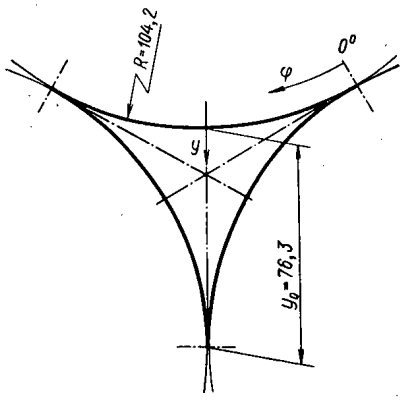

Fig. 1. Diagram of the cross section of the experimental channel.

The stabilization length of the velocity profile is an arbitrary quantity. Strictly speaking, the velocity profile over the channel length approaches asymptotically a limiting profile, which is said to be stabilized. Therefore, in the present study we used as the length of the inlet section the distance from the channel inlet at which the profile of the measured velocities differed from the stabilized profile by not more than 1%. The length of the inlet section was determined both on the basis of the change of the entire velocity profile and on the basis of the change of the velocity of the flow along the channel.

The maximum air velocity in the cross section was measured by a metal Prandtl tube movable over the channel length. The outside

Translated from Atomnaya Énergiya, Vol. 35, No. 1, pp. 19-24, July, 1973. Original article submitted July 24, 1972.

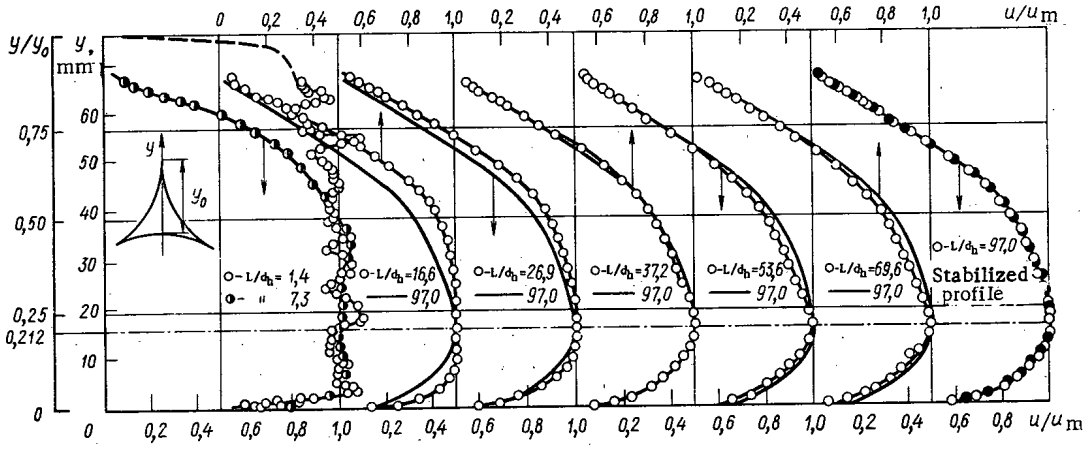

Fig. 2. Velocity profiles along the axis of symmetry of the cross section of the channel of a close-packed bundle of rods for different distances from a smooth inlet, $Re = 59 \cdot 10^3$.

diameter of the tube was 2 mm and the diameter of the total-head hole was 0.6 mm. At a distance of 15 mm from the spherical end of the tube four 0.2-mm-diam. holes were drilled for sampling the static pressure. The Prandtl tube was secured in the center of the channel by means of two plates soldered to a cylinder the outside diameter of which was equal to the diameter of a circle inscribed in the channel cross section; the wall thickness of the cylinder was 2 mm. The leading edge of the cylinder was made sharp-pointed to lessen disturbance. The Prandtl tube projected 110 mm above the leading edge of the cylinder.

Measurements of the maximum velocity in one of the channel cross sections by the movable Prandtl tube and glass Pitot tube showed that the design of the movable probe did not affect the readings of the Prandtl tube. A value of the calibration coefficient of the movable Pitot tube equal to 0.98-0.99 was obtained. The velocity-type transducer in each experiment was placed at the channel inlet and pulled over the channel length by means of a metal cable with a preassigned spacing. The movable Prandtl tube measured the distribution of the maximum flow velocity over the channel length under different conditions of entry of the air into the channel.

The channel inlet is usually made smooth, so as not to reduce the inlet resistance, which is important in real structures, but to obtain a uniform velocity profile in the inlet cross section of the channel. When the inlet is made in the form of a nozzle, the formation of eddies on the inlet edge disappears and the flow becomes more stable.

However, on "constricting" the flow, the transverse intensity of turbulence increases and some rotation of the fluid at the channel entry can occur. For this purpose a diffuser grid is installed at the nozzle inlet, which can be made in the form of honeycombs or can consist of several simple grids.

In the present study we obtained the velocity distribution over the axis of symmetry of the channel for several distances from the smooth inlet and inlet through a diaphragming tube lattice. The plane velocity profile of the air flow was attained by means of diffuser grids installed inside the channel. The size of the cells of the grids and the distance between grids were selected during the experiment. The diffuser grids were selected so that, regardless of the velocity profile of the flow before the grids, the velocities measured over the entire channel cross section immediately after the grids did not differ by more than 10%.

The diffuser grids were welded by contact electric welding to plates curves to match the inside perimeter of the channel. In the corners of the channel the plates were connected together by contact electric welding. A grid with 1.3×1.3 mm cells was the first along the air flow and a grid with 1.0×1.0 mm cells the second. The distance between grids was 25 mm.

During the experimental selection of the grids it was established that the velocity profile after the grids was sufficiently uniform over the cross section with the exception of the channel corners, where the plates occupied a large part of the cross section. Therefore, the corners of the plates on the side of the second grid were partially cut off and the dimensions of the grid in the corners were made larger. The velocity profile measured at a distance of $1.4d_h$ in the channel after the diffuser grids is shown in Fig. 2.

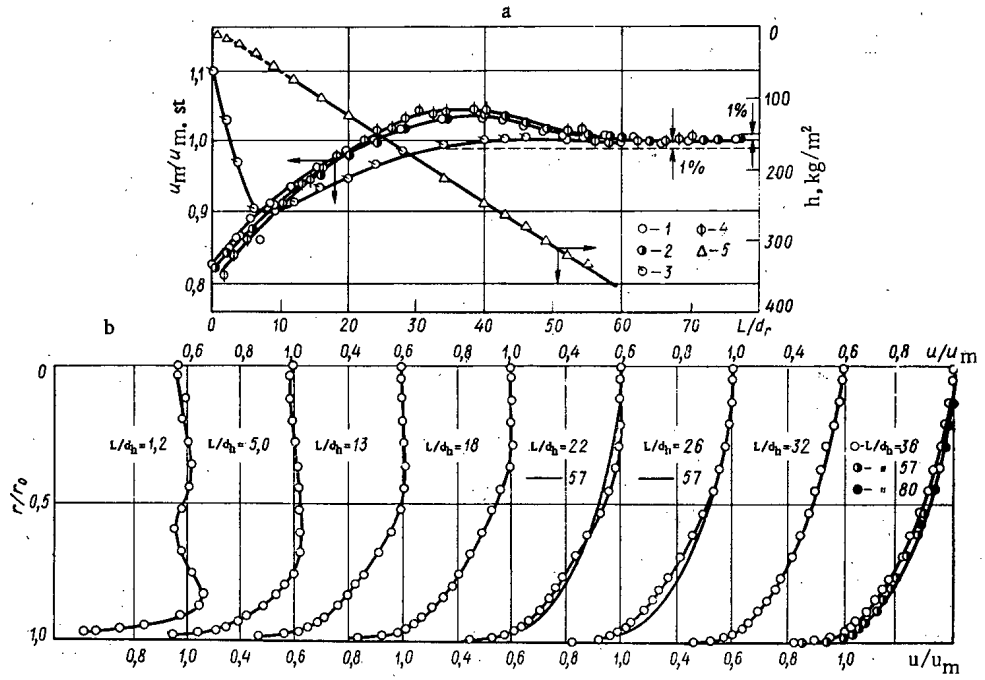

Fig. 3. Velocity profiles at inlet section of round tube. a) Velocity profiles along longitudinal axis: 1-3) measurements by movable probe at inlet with diffuser grids, at smooth inlet, and at inlet with sharp edge, respectively, Re $= 81 \cdot 10^3$; 4) movable diffuser grids, Re $= 60.3 \cdot 10^3$; 5) distribution of static gauge pressure over length of tube with smooth inlet, Re $= 81 \cdot 10^3$ (measurements taken by means of movable probe); b) velocity profiles at inlet section of tube with smooth inlet, Re $= 60.3 \cdot 10^3$.

The velocity profile along the axis of symmetry of the channel was measured in the same cross section of the channel; the diffuser grids were placed at different distances from the selected cross section. The velocity profiles when the inlet conditions simulated a tube lattice were measured in the same way as for an inlet with diffuser grids. The design of the movable simulator of the inlet through a tube lattice differed from the design of movable diffuser grids in that the air flow entered the investigated part of the channel through a tube segment measuring $31.5 \cdot 0.4$ mm with a length of 25 mm installed in the center of the channel cross section. The remaining cross-sectional area of the channel was closed.

Experiments were conducted with a round tube of length 4000 mm and internal diameter 50 mm to develop the measurement method and to establish the legitimacy of simulating the inlet by movable diffuser grids. In the experiments we used diffuser grids specially selected for the tube (the design of the movable Prandtl tube is described above).

The profile of the nozzle providing entry into the tube was calculated by Vitoshinskii's formula [11]. The nozzle length was 200 mm and the degree of constriction was equal to nine. A grid with 1.2×1.2-mm cells was installed at the nozzle inlet.

RESULTS

In the experiments with the tube we measured the distribution of the maximum velocity over the length under different conditions of the inlet and the velocity profiles over the tube diameter for several distances from the inlet with the diffuser grids. The spacing over the length when measuring the maximum velocity by the movable transducer was equal to 2-3 tube diameters. The velocity profiles were measured only for the case of an inlet through grids in cross sections spaced 4-6 tube diameters apart. The measurement results are shown in Fig. 3. We see that the distributions of the maximum velocity over the length of a tube with a smooth inlet and inlet with diffuser grids coincide. For $L/d_h \approx 10$ the greatest difference in values (here L is the distance from the inlet) of the maximum velocity does not exceed 1-2%. The lengths of the stabilization sections of the maximum velocity in the tube obtained for a smooth inlet and an inlet with diffuser grids coincide. Hence we can conclude that an inlet with diffuser grids simulates a smooth inlet.

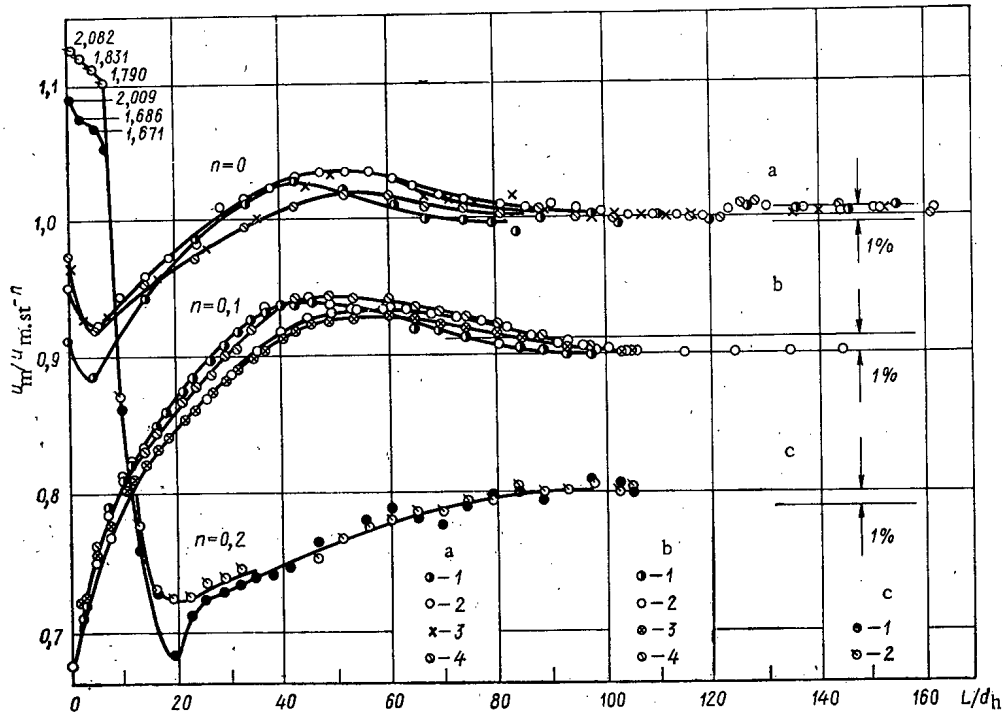

Fig. 4. Distribution of maximum flow velocities at the inlet section of a close-packed bundle of rods: a) inlet with sharp edge, measurements taken by a movable probe: 1-4) $Re \cdot 10^{-3}$ equal to 17.8, 38.1, 52.2, 74.8, respectively; b) simulation of smooth inlet: 1-4) lengthwise movement of diffuser grids for $Re \cdot 10^{-3}$ equal to 19, 29, 52, 59, respectively; c) movement of inlet simulator with tube lattice: 1, 2) $Re \cdot 10^{-3}$ equal to 37.8 and 52.1, respectively.

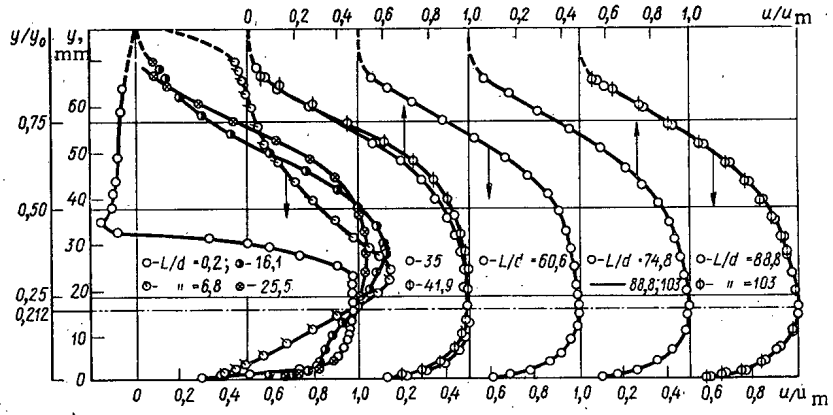

Fig. 5. Velocity profile over the axis of symmetry of the cross section of a channel of a close-packed bundle of rods for different distances from the inlet through a tube lattice, $Re = 52.1 \cdot 10^3$.

In the case of a smooth inlet the velocity distribution measured on the tube axis passes through a maximum at a distance of 35-40 diameters from the inlet. The velocity profile changes nonmonotonically over the tube length. It becomes least filled in the section where the velocity on the tube axis is maximum. Thus, at the inlet section the fluid motion in the center of the tube cross section is at first accelerated and then decelerated.

The maximum velocity apparently corresponds to the instant of joining of boundary layers. Further development of turbulence leads to flattening of the velocity profile.

For an inlet with a sharp edge the velocity distribution along the longitudinal axis of the tube has a maximum at the channel inlet. In this case the maximum velocity is due to constriction of the flow near the inlet edge.

Figure 4 shows the distribution of the maximum velocity over the length of a channel of a close-packed bundle of the rods under different inlet conditions: inlet with sharp edge, smooth inlet, and inlet through a tube-lattice diaphragm. The experimental data for the inlet with a sharp edge had some scatter, and therefore the stabilization length was determined from the intersection of the curve drawn through the experimental points with line $u_m/u_{m.st} = 1.005$ (here u_m and $u_{m.st}$ are the local and stabilized velocities, respectively). We see from Fig. 4 that in the case of a smooth inlet and inlet with a sharp edge the velocity distributions over the length of the channel axis have maxima at a distance of 40-55 d_h. Probably the disturbances caused by the sharp edge for the channel being considered weakly affect the formation of the velocity profiles in the corner zones of the cross section where laminar flow occurs near the inlet. As the fluid advances over the channel length, turbulent disturbances penetrate partially into narrow zones. This process continues also after interferences of the turbulent boundary layers in the wide part of the channel.

In the case of entry of the flow into the channel through a tube-lattice diaphragm, which causes the greatest flow disturbance of the inlet conditions considered, a maximum is not noted in the velocity distribution over the length of the channel axis.

Velocity profiles for different distances from the smooth inlet and inlet to the channel through a tube-lattice diaphragm are shown in Figs. 2 and 5. The velocity profile measured at a distance of $1.4d_h$ from the diffuser grids can be taken as uniform (with an accuracy of ±10%) almost over the entire cross section of the channel. The velocity profile for $37.2d_h$ coincided with the stabilized profiles measured at distances 97 and $106d_h$ from the inlet.

For lengths slightly greater than $37.2d_h$ from the channel inlet the velocity profile deviates from the stabilized profile. This result should be noted because in investigating velocity stabilization by transducers installed in separate sections of the channel erroneous results with regard to the length of the inlet section are possible. As in the experiments with a round tube, the velocity profile approaches the stabilized profile nonmonotonically. It follows from Fig. 5 that in the case of entry through a tube lattice the velocity profile approaches the stabilized profile monotonically. The experimentally obtained distribution $u_{m.st}/\bar{u} = f(Re)$ necessary in order to represent the experimental data in the form of the dependence $\bar{u}/u = f(y/y_0; L/d_h)$ is shown in Fig. 6. Here $\bar{u}$ is the average velocity of the fluid in the channel; y, y_0 are the distance from the wall reckoned along the axis of symmetry of the cross section of the channel and the length of the axis of symmetry of the channel cross section, respectively. The Reynolds number was calculated on the basis of the average velocity and hydraulic diameter of the channel.

In the case of the smooth inlet (with a diffuser grid) we obtained the distribution of tangential stresses over the channel perimeter.

The tangential stress on the wall, as in [11], was measured by Preston's method [12]. For $L = 30d_h$ and $Re = 59.3 \cdot 10^3$ the profile of tangential stresses on the wall was identical to the stabilized distribution obtained by the authors of this article earlier [11].

The presence of a turbulent zone in the flow core and of "stagnant" zones in the channel corners is characteristic for turbulent fluid flow in channels with sharp extended corners (close-packed bundles of rods; triangular channels, eccentric annular spaces). The stagnant zones are characterized by vanishingly small velocities of the fluid flow in these zones.

From the experimentally measured velocity profiles over the axis of symmetry of the channel cross section it was established that the stagnant zone changes depending on the Reynolds number. The results of this analysis, in which the data of [11, 13] were used, are also presented in Fig. 6.

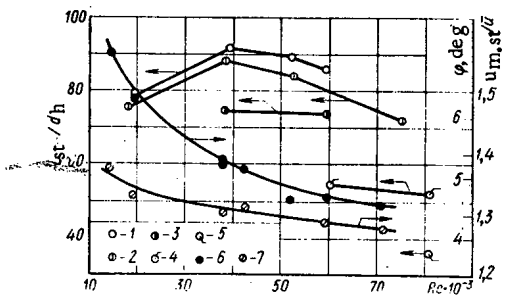

Fig. 6. Length of the inlet channel of a close-packed bundle of rods: 1-3) length of inlet section of channel for a smooth inlet, inlet with a sharp edge, and inlet through a tube lattice, respectively; 4, 5) length of inlet section of round tube with a smooth inlet and inlet with a sharp edge; 6) dependence of the magnitude of the stagnant zones in the channel on the Reynolds number; 7) relation between the maximum and average velocities of a stabilized flow in a channel.

The values of the length of the inlet section where stabilization of the velocity profile of the flow occurs are presented in Fig. 6. It is characteristic that the data for different conditions of entry into the channel of a close-packed bundle of rods differ. This is explained by the different degree of turbulence of the flow in the inlet cross section of the channel. Also in Fig. 6 data for a round tube are shown. The relative stabilization length of the velocity profile L_{st}/d_h for a round tube is considerably less than that for a channel of a close-packed bundle of rods.

LITERATURE CITED

1. A. Barbin and J. Jones, Trans. ASME, 85-D, No. 1, 34 (1963).
2. L. Schilder, Fluid Motion in Pipes [Russian translation], Moscow–Leningrad (1936).
3. M. Cumo et al., Termotechnica, 20, No. 3, 115 (1966).
4. S. S. Filimonov and B. A. Khrustalev, in: Heat Transfer [in Russian], Izd. AN SSSR, Moscow (1962), p. 43.
5. J. Cont-Bello, Turbulent Flow in a Channel with Parallel Walls [Russian translation], Mir, Moscow (1968).
6. H. Latzko, ZAMM, 1, No. 4 (1921).
7. A. S. Ginevskii and E. E. Solodkin, Promyshlennaya Aerodinamika, No. 12, 159 (1959).
8. E. E. Solodkin and A. S. Ginevskii, Trudy TsAGI, No. 701 (1957).
9. P. Oosthuizen, The South African Mechanical Engineer, 16, No. 6 (1964).
10. Y. Nanjundaswamy, J. Inst. Engineers (India), 44, No. 1, 707 (1964).
11. Yu. D. Levchenko, V. I. Subbotin, and P. A. Ushakov, At. Énerg., 22, No. 3, 218 (1967).
12. Preston, in: Mechanics [Russian translation], Per. Obzorov Inostr. Period. Lit., No. 6(34) (1955).
13. Yu. D. Levchenko et al., in: Liquid Metals [in Russian], Atomizdat, Moscow (1967).

DETERMINATION OF THE INTERDEPENDENCE OF VARIOUS REACTOR CHARACTERISTICS USING FACTOR ANALYSIS

G. B. Usynin and A. A. Sennikov

UDC 621.039.526

In the mathematical optimization of a reactor with many independent variables, it is frequently necessary to determine the physical characteristics which are used in calculating the quality function. This is usually achieved by means of a multigroup neutron-physical calculation, which uses considerable computer time, thus substantially limiting the possibility of optimization. Some decrease in computer time can be achieved by the use of simplified methods for calculating the neutron balance but at the same time the accuracy is reduced. Another possible approach is the use of accurate techniques (in the computation programs) to construct mathematical models which describe the interdependence of the various characteristics and parameters and then to use them in the optimization system.

The most important physical characteristics of a reactor are the critical mass of fissionable material, the conversion factors, the distribution of heat release by zones, etc. Fundamentally these all depend on a rather small number of factors which are usually easy to enumerate, since there is sufficient experimental work to allow engineering estimates. Moreover, at the first stage of the calculation, factors of lesser importance which have little influence on the characteristic being investigated may be eliminated.

The use of a neutron-physical calculation to find the characteristic y, which depends on the set of factors $\{x_i\}$, may be regarded as a certain experiment, and one can attempt to describe the $y(\mathbf{x})$ in terms of a specific surface of the response after a small number of such experiments.

Assuming that the number of factors is equal to K, we can write the equation of the response surface in the form of a series:

$$y(\mathbf{x}) = \beta_0 + \sum_{i=1}^{K} \beta_i x_i + \sum_{i \leqslant j}^{K} \beta_{ij} x_i x_j, \tag{1}$$

where the normalized variables x_i are expressed in terms of the X_i by using the relations [1]

$$x_i = \frac{X_i - \overline{X}_i}{S_i}; \quad \overline{X}_i = \frac{\sum_{u=1}^{N} X_{iu}}{N}; \quad S_i = \left(\frac{\sum_{u=1}^{N} (X_{iu} - \overline{X}_i)^2}{N} \right)^{1/2}; \quad -1 \leqslant x_i \leqslant 1.$$

Here X_{iu} is the value of the i-th variable in the u-th experiment, and N is the number of such experiments.

The plan for the experiments can be described in the form of an $N \times k$ matrix, consisting of the values of the independent variables x_i in each experiment (such a matrix is called a planning matrix). By introducing the fictitious variable $x_0 = 1$, and also letting

$$x_{K+1} = x_1^2; \; x_{K+2} = x_2^2, \; \ldots \; x_{2K+1} = x_1 x_2, \; \ldots,$$

we can rewrite (1) in the form

$$y(\mathbf{x}) = \sum_{i=0} \beta_i' x_i, \tag{1a}$$

in which $\beta_0' = \beta_0$, $\beta_1' = \beta_1$, etc. The matrix $\hat{\mathbf{x}}$ consists of the values of these variables in all N experiments, and includes within itself the complete planning matrix. The estimates b_i of the coefficients β_i' (the components of the vector B) may be obtained from the relations [1]

$$\mathbf{B} = (\hat{x}^* \hat{x})^{-1} \hat{x}^* \mathbf{Y}, \tag{2}$$

Translated from Atomnaya Énergiya, Vol. 35, No. 1, pp. 25-27, July, 1973. Original article submitted June 12, 1972.

TABLE 1. Range of Variation of the Variables

Name of variable	Volume fraction of fuel, ε_f	Compression of the active section, $\beta = D_{a.s}/H_{a.s}$	Volume of the active section, $V_{a.s}$, m³
Maximum value	0,5	4	9,55
Minimum value	0,3	1,5	5,2

where $\hat{x}^*$ denotes the transposed matrix. The components of the vector Y are the experimentally observed values of the characteristic y. Advances in experimentation theory [2] make it possible to choose (or construct) linear plans and second-order plans which have a number of optimal properties (orthogonality, rotatability, minimal dispersion of the estimates of the coefficients β_i, etc.). For example, factors for which the coefficients are small can be immediately rejected in the case of orthogonal plans.

A study was made of the dependence of several characteristics of fast reactors on the volume fraction of fuel, the compression, and the volume of the active section. It was assumed that the change in the independent variables was bounded by the surface of a cube:

$$X_{min} \leqslant X \leqslant X_{max}.$$

The boundary values X_{min} and X_{max} are shown in Table 1. In addition, the following assumptions were made: the effective fuel density is 80% of the theoretical value; the heat release field is smoothed with the aid of two sections of different enrichment; the diameter of the central section is $0.72D_{a.s.}$; the ratio of the plutonium concentrations in the two sections is 1.30; and the volume fractions of oxide of the steel and the sodium in the end shields are the same as in the active section, the fraction of steel being half as large as the fraction of sodium. The composition of the lateral shield is the same as in the BN-350 reactor [3]. The thickness of the shields was assumed to be infinite. The two-dimensional 18RZ-4 [4] program was used to make the neutron-physical calculation, and a special program was constructed to solve Eq. (2). The first stage of the calculations resulted in linear saturated simplex-plans [4] with the above-enumerated properties, each plan containing 4 experiments in all. The linear approximation can clearly be made more acceptable if the correct choice of the form of the independent variables is made.

In studying the critical mass, in place of the volume of the active section $V_{a.s.}$, it is evidently preferable to use $V_{a.s.}^{2/3}$, since according to similarity theory it should be approximately proportional to the square of the characteristic reactor dimension. Tables 2 and 3 show the results of two series of calculations. In the second series, in contrast to the first series, the variable $X_2 = \beta$ is replaced by $X_2 = 2/(2 + \beta)$, which is the ratio of the lateral surface to the total surface of the active section. As an example, we list the values of M_{cr} for the first series at points where an experiment was carried out. They are equal to 3507, 3307, 2063, and 3009, respectively. In each series, an additional experiment was set up at the center of a hypercube in order to verify the adequacy of the linear approximation. The quantity $\Delta = [y(0) - b_0]/y(0)$ can serve as an estimate of the contribution of the nonlinear terms in the equation of the response surface.

We denote by CC, CC_a, and CC_l the conversion coefficients (total, active section, and lateral shield); by K_e and K_l the fraction of the power released in the end and lateral shields; and by M_{cr} the critical mass of plutonium, kg. From a comparison of Tables 2 and 3 it is clear that, in calculating the characteristics determined by the neutron leakage from the active section, it is appropriate to use the second series of independent variables.

TABLE 2. Results of the Calculations with a Linear Saturated Plan: $X_1 = \varepsilon_f$; $X_2 = \beta$; $X_3 = V_{a.s.}^{2/3}$

Characteristic	M_{cr}	CC	CC_a	CC_l	K_l	K_e
b_0	2685	1,375	0,852	0,288	0,0460	0,0335
b_1	149	0,105	0,183	−0,015	−0,0063	−0,0114
b_2	100	0,004	−0,014	−0,043	−0,0090	0,0072
b_3	573	−0,035	0,077	−0,023	−0,0025	−0,0105
$y(0)$	2786	1,397	0,828	0,263	0,035	0,042
Δ, %	3,6	1,6	−2,8	−9,5	−31,4	12,5

TABLE 3. Results of the Calculations with a Linear Saturated Plan: $X_1 = \varepsilon_f$; $X_2 = 2/2 + \beta$; $X_3 = V_{a.s.}^{2/3}$

Characteristic	M_{cr}	CC	CC_a	CC_l	K_l	K_e
b_0	2831	1,292	0,708	0,298	0,0414	0,0392
b_1	350	0,140	0,162	−0,028	−0,0049	−0,0021
b_2	−78	−0,025	0,056	0,051	0,0070	−0,0175
b_3	823	−0,025	0,049	−0,039	−0,0055	−0,0049
$y(0)$	2743	1,295	0,747	0,281	0,0393	0,0362
Δ, %	−3,3	0,2	5,2	−6,1	−5,3	−7,6

TABLE 4. Coefficients of the Second-Order Equation of the Response Surface: $X_1 = \varepsilon_f$; $X_2 = \beta$; $X_3 = V_{a.s.}^{2/3}$

Characteristic	x_0	x_1	x_2	x_3	x_1^2	x_2^2	x_3^2	x_1x_2	x_1x_3	x_2x_3	σ, %
M_{cr}	2735,4	231,2	83,5	675,0	—11,4	44,6	33,5	—74,7	11,0	—50,7	1,5
CC	1,408	0,126	0,010	—0,025	—0,043	—0,016	—0,025	—0,005	—0,006	—0,012	2,0
CC_a	0,8626	0,1533	—0,0328	0,0539	—0,0384	—0,0412	—0,0333	0,0139	0,0205	0,0205	2,2
CC_l	0,2632	—0,0196	—0,0606	—0,0304	—0,0046	0,0369	—0,0071	0,0083	0,0041	0,0066	6,1
K_l	0,0348	—0,0047	—0,0096	—0,0028	0.0013	0,0061	0,0015	0,0040	—0,00099	—0,00071	5,3
K_e	0,0399	—0,0023	0,0146	—0,0065	0,0010	—0,0014	0,00030	—0,0028	—0,0051	—0,0068	4,8

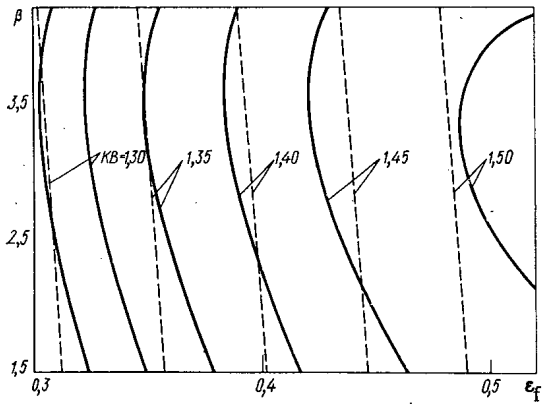

Fig. 1. The dependence of CC on ε_f and the compression, for $V_{a.s.} = 6$ m^3: - - - -) linear approximation; ——) second-order approximation.

The degree of influence exerted on the characteristic by the various factors may be judged from the size of the coefficients of the normalized variables. For example, the overall CC is determined mainly by ε_f, while the change in reactor volume and the compression appear noticeably weaker (the absolute value of the coefficient of x_i is several times larger than the coefficients of x_2 and x_3). On the other hand, M_{cr} depends mainly on the volume of the active section.

The two series of calculations are independent from each other, but lead to results which are qualitatively identical and do not differ very much quantitatively. Results for M_{cr}, CC, and CC_a which are satisfactory as judged by the size of Δ can be obtained by using a linear approximation to the response surface, constructed from only four points. The values of CC_l, K_l, and K_e are not given as well by this approximation. An increase in the planning order causes a decrease in the dispersion of the predicted values of the characteristics. The dispersion is averaged over the region being studied and reduced to one observation.

It seems possible [2], by using the calculations already carried out, and by calculating six more reactor variants, to realize an orthogonal second-order plan and to construct an equation of the response surface which contains squares and pairs of products of independent variables. The results of the series of calculations are shown in Table 4. In Fig. 1 a plot of CC (ε_f, β) for fixed $V_{a.s.}$ is shown. Because the number of experiments is larger than the number of coefficients being determined in a second-order plan, the extra information can be used to estimate the dispersion of the predicted functionals:

$$\sigma^2 = \frac{\sum_i [y_i - y(x_i)]^2}{N - m}, \qquad (3)$$

where m is the number of coefficients (in this case, m = 10).

In the current state of nuclear-physical constants, the error in the calculated determination of the critical mass of plutonium is at least 2-3% and the calculations of CC are still less accurate. We can therefore assume that a second-order equation is a sufficiently good description of the characteristics being considered and can be used for mathematical reactor optimization.

Let us note that increasing the number of factors requires a considerable increase in the amount of calculation. In the case of K = 4, it required the calculation of 24 variants to realize a plan close to the D-optimal one (the plan which ensures that the error ellipsoid for the estimates of the coefficients in Eq. (1a) shall be minimum), whereas for the case K = 6, about 80 variants were required [1].

LITERATURE CITED

1. V. G. Gorskii and V. Z. Brodskii, "First-order simplex-plans and related second-order plans," in: New Ideas in Planning Experiments [in Russian], Nauka, Moscow (1969).
2. V. V. Nalimov, Experimental Theory [in Russian], Nauka, Moscow (1971).

3. G. B. Usynin, At. Énerg., 25, No. 6, 466 (1968).
4. V. V. Khromov et al., Nuclear Reactor Physics [in Russian], Atomizdat, Moscow (1968), p. 159.

COMPUTATIONS OF NEUTRON PROPAGATION, ALLOWING FOR THE RESONANCE STRUCTURE OF THE CROSS SECTIONS

M. N. Nikolaev, T. A. Germogenova, N. V. Isaev, and V. F. Khokhlov

UDC 621.039.51.12

The use of the method of subgroups for calculating the resonance structure of the cross sections in neutron calculations relating to reactors and shielding based on the diffusion approximation was indicated in [1, 2]. It was shown that the method of subgroups gave a higher accuracy in calculating neutron fluxes than the method of "blocked" cross sections normally used in multigroup calculations [3].

In the present investigation we shall consider the use of the method of subgroups for calculating plane shielding on the kinetic approximation; we shall compare the results of calculations carried out on the basis of group-blocked and subgroup cross sections with precision multigroup calculations, which make exact allowance for all the special features characterizing the resonance structure of the cross sections in the energy range under consideration.

Presentation of the Problem and Method of Solution

The spatial–angular distribution of the neutron subgroups in plane-parallel shielding layers irradiated from the left by means of an external source is described by the multigroup equation

$$\mu \frac{\partial \psi_i^g(x, \mu)}{\partial x} + \hat{\Sigma}_{\text{tot}_i}(x)\, \psi_i^g(x, \mu) = \sum_{p=1}^{g} \int_{-1}^{+1} d\mu' \hat{\mathcal{P}}_i^{p \to g}(x, \mu, \mu')\, \psi_i^p(x, \mu') \tag{1}$$

with the boundary conditions

$$\begin{aligned} \psi_1^g(0, \mu) &= S^g(\mu), \quad \mu > 0; \\ \psi_I^g(x_I, \mu) &= 0, \quad \mu < 0 \end{aligned} \tag{2}$$

and the following matching conditions at the internal boundaries between the layers

$$\begin{aligned} \hat{\varepsilon}_{i, i+1}^g \psi_i^g(x_i, \mu) &= \psi_{i+1}^g(x_i, \mu), \quad \mu > 0; \\ \psi_i^g(x_i, \mu) &= \hat{\varepsilon}_{i+1, i}^g \psi_{i+1}^g(x_i, \mu), \quad \mu < 0, \end{aligned} \tag{3}$$

where g is the number of the energy group, $g = 1, 2, \ldots, G$; i is the number of the computing layer, $i = 1, 2, \ldots, I$; x_i is the coordinate of the right-hand boundary of the i-th layer; $\psi_i^g(x, \mu)$ is the vector function of the spatial–angular distribution of the neutron subgroups of the g-th group within the i-th layer, consisting of $\psi_i^{g,k}(x, \mu)$ (k is the number of the subgroup of the g-th layer, $k = 1, 2, \ldots, s_g$); $\mu = \cos\nu$ is the cosine of the neutron scattering angle; $\hat{\Sigma}_{\text{tot}_i}^g(x)$ is the diagonal matrix of the total single-group cross sections of the g-th group of the i-th layer, consisting of the elements $\Sigma_{\text{tot}_i}^{g,k}(x)$; $\mathcal{P}_i^{p \to q}(x, \mu, \mu')$ is the matrix representing the scattering of neutrons from the p-th to the g-th group; the elements $\mathcal{P}_i^{p,l \to g,k}(x, \mu, \mu')$ specify the scattering of neutrons from the l-th subgroup of the p-th group to the k-th subgroup of the g-th group; $S^g(\mu)$ is the vector function of the angular distribution of the external source with respect to the subgroups of the g-th group; $\hat{\varepsilon}_{i,i+1}^g$, $\hat{\varepsilon}_{i+1,i}^g$ are matrices giving the transition from subgroup division in the i-th layer to subgroup division in the i + 1-th layer and back, respectively; if there is only a single subgroup division

Translated from Atomnaya Énergiya, Vol. 35, No. 1, pp. 29-32, July, 1973. Original article submitted October 26, 1972.

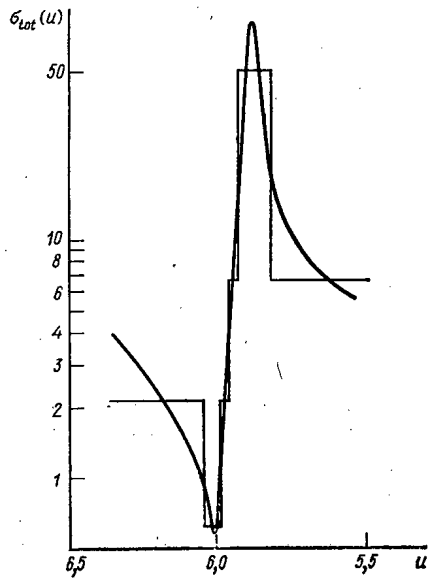

Fig. 1. Subgroup representation of the function $\sigma_{tot}(u)$ for Fe^{56}.

in all the layers of the shielding, then $\hat{\varepsilon}^{g}_{i,i+1} = \hat{\varepsilon}^{g}_{i+1,i} = \hat{E}$, where $\hat{E}$ is a unitary matrix of order s_g (this being the number of subgroups in the g-th group). A detailed description of the methods of calculating the matrices $\hat{\varepsilon}$ is given in [4].

Equation (1) is a matrix vector integrodifferential equation; it requires additional information as to the structure of the cross sections of the substances being calculated. If the number of neutron subgroups in all the energy groups is equal to unity ($s_g = 1$, $g = 1, 2, \ldots, G$), Equation (1) transforms into a kinetic equation for calculating the neutron transport by the group method.

The method of obtaining the subgroup constants is given a detailed description in [2, 4, 5]. It was shown in [5] that, in carrying out practical calculations of reactors and shielding, it was sufficient to distinguish two or three subgroups within an energy group of a system of constants containing resonances [3]. Also in [5] there is a library of the subgroup constants relating to the most important substances used in the calculation of reactors and shielding within the P_1 approximation. At the present time, in order to obtain subgroup constants on the P_1 approximation one uses the ARAMAKO program (versions written in the ALGOL-60 and FORTRAN languages are available for the M-20, M-220, and BÉSM-6 computers). Work is continuing as regards extending the library of the program and creating a subprogram to allow for anisotropy in the scattering of neutron subgroups in the P_N approximation.

Equation (1) is solved by a method analogous to that developed by T. A. Germogenova for the program ROZ [6], taking into account that the coefficients of Eq. (1) are matrices. An algorithm for the solution of the subgroup equation (1) is realized in the program PROZA (standing for "subgroup calculation of one-dimensional shielding") written in the ALGOL–BÉSM-6 language. In order to allow for the neutron-scattering anisotropy, we use the expansion of $\mathcal{P}^{p,l \to g,k}(x, \mu, \mu')$ in a series of Legendre polynomials. In allowing for the neutron-scattering anisotropy in the P_1 approximation, the initial data for the PROZA program

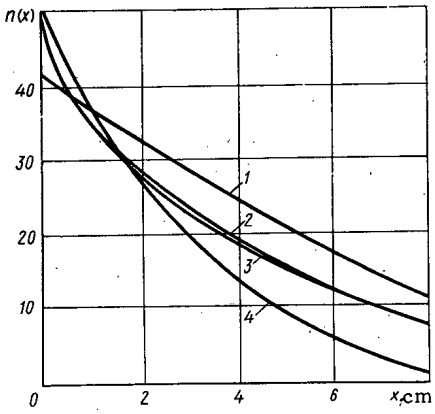

Fig. 2

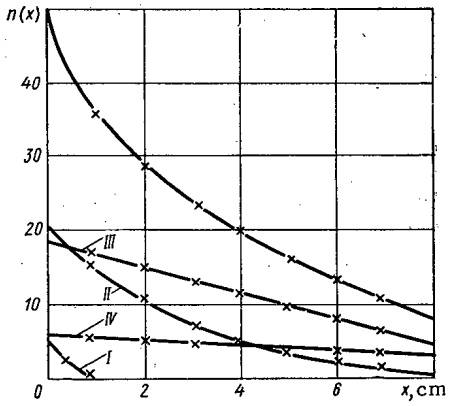

Fig. 3

Fig. 2. Spatial dependence of the neutron flux function n(x) for an iron plate 8 cm thick in the lethargy range 5.54-6.64. The calculations were made using the following constants: 1) group-average blocked; 2) subgroup; 3) group constants, making detailed allowance for the resonance structure of the cross sections; 4) group-average unblocked.

Fig. 3. Subgroup neutron flux functions $n^k(x)$ for an iron plate 8 cm thick corresponding to the first to fourth subgroups (curves I–IV respectively). The top curve gives the group-average neutron flux $n(x) = \sum_{k=1}^{s_g} n^k(x)$; ×) values of the functions obtained from the detailed multigroup calculation.

are prepared by means of the ARAMAKO program. The PROZA program allows a dynamic distribution of the external memory of the BÉSM-6 computer; it may be used for calculating shielding with a large number of energy groups or neutron subgroups.

Results of Model Calculations

When studying the efficiency of the method of subgroups for carrying out shielding calculations, a number of model calculations were made. As a criterion (for purposes of comparison), the integrated group-average neutron fluxes obtained from multigroup precision calculations (allowing for the detailed resonance structure of the cross sections of the constituent materials) were employed. For example, in order to calculate the passage of neutrons through an iron plate 8 cm thick in a region of wide resonance (Fig. 1), the structure of the total cross section in the lethargy range 6.64-5.54 was approximated by thirty groups in the detailed multigroup calculation and by four subgroups in the subgroup calculation. The choice of subgroup division for the resonance in question is also indicated in Fig. 1.

As an external neutron source we used an isotropic source with a uniform lethargy distribution of the neutrons. The neutron distribution was calculated in the $2D_3$ approximation, allowing for the scattering anisotropy, on the P_1 approximation. For comparison we used the spatial neutron distributions n(x) obtained by integrating the functions $\psi^{g,k}(x, \mu)$ with respect to μ from -1 to $+1$ and also with respect to lethargy over the whole range under consideration: $n(x) = \sum_g \sum_k \int_{-1}^{+1} \psi^{g,k}(x, \mu)d\mu$. It is evident from Fig. 2 that the results of the subgroup calculation of the functions n(x) agree closely with the results of the detailed multigroup calculation, whereas the results of calculations based on group-average blocked and unblocked cross sections obtained by the method of [3] differ considerably from the exact calculation.

The spatial dependence of the neutron flux functions $n^{g,k}(x) = \int_{-1}^{+1} \psi^{g,k}(x, \mu)d\mu$ is shown in Fig. 3.

Curve I corresponds to the subgroup with the maximum total subgroup cross section $\sigma_{tot}^{1.1} = 51.297$ b, curve II to $\sigma_{tot}^{1.2} = 6.674$ b, curve III to $\sigma_{tot}^{1.3} = 2.099$ b, and curve IV to $\sigma_{tot}^{1.4} = 0.692$ b. The top curve in Fig. 3, constituting the superposition of four subgroup curves $n^{g,k}(x)$, describes the spatial distribution of the group-average neutron flux in the lethargy range under consideration. To describe such a curve by introducing corrections for the resonance blocking into the quantity σ_{tot} as recommended in [3] is quite impossible. The spatial dependence of the group-average total neutron cross-section function in the resonance

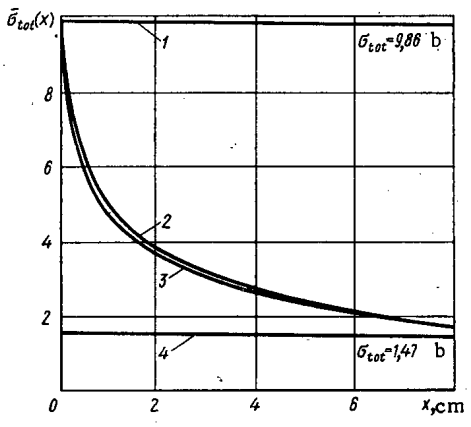

Fig. 4

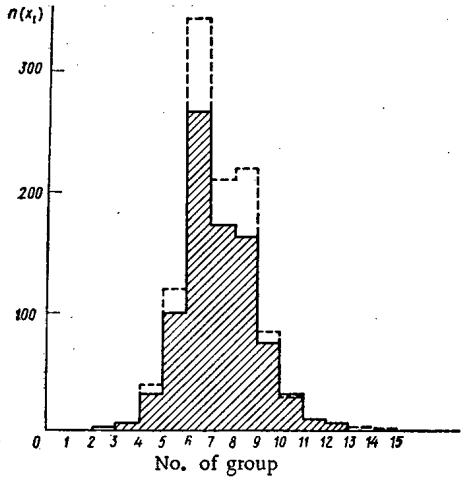

Fig. 5

Fig. 4. Total microscopic cross-section functions $\overline{\sigma_{tot}}(x)$ for an iron plate 8 cm thick obtained from calculations using the following constants: 1) unblocked; 2) subgroup; 3) group constants, making detailed allowance for the resonance structure of the cross sections; 4) blocked group-average.

Fig. 5. Histogram of the radiation emerging from an iron plate 10 cm thick: ——) subgroup calculation; - - - -) calculation using blocked cross sections [3].

region is correctly described in the subgroup calculations. Let us consider the spatial distribution function of the group-average total cross section $\bar{\sigma}_{tot}(x) = \sum_g \sum_k \sigma_{tot}^{g,k}(x) \times \int_{-1}^{+1} \psi^{g,k}(x, \mu)d\mu / \sum_g \sum_k \int_{-1}^{+1} \psi^{g,k}(x, \mu)d\mu$ obtained from detailed multigroup, subgroup, and group blocked and unblocked calculations. We see from Fig. 4 that, for calculations based on the subgroup constants, there is a "spatial" blocking of the total cross section $\sigma_{tot}(x)$. On moving away from the left-hand outer boundary, the quantity $\sigma_{tot}(x)$ tends toward the value of the blocked total cross section, while at distances greater than a few neutron free paths (calculated from the minimum total cross section) it coincides with the latter.

The foregoing calculations were carried out for different plate thicknesses (2, 4, 10, and 20 cm). It should be noted that in all cases good agreement was obtained between the values of the functions under consideration obtained from the detailed multigroup and subgroup calculations.

We see that for neutrons belonging to the same subgroup the effects of resonance blocking are insubstantial, since these neutrons possess very similar cross sections. Hence the propagation of neutron subgroups in the medium may be calculated from the earlier derived subgroup constants, depending solely on the composition of the medium, not on its dimensions. The neutron transmission function is always preserved with great accuracy in the subgroup calculations, since the total subgroup cross sections and the fractions of the subgroups are always chosen by making a mean square approximation of the transmission function.

The results of the foregoing calculations show that shielding calculations in a resonance region (especially in the case of optically thin layers) can only be carried out in an accurate manner within the framework of the subgroup method.

Practical Calculation of an Iron Shield

In order to illustrate the differences obtained in subgroup and ordinary multigroup calculations with blocked cross sections, we calculated the transmission of neutrons from an external source through an iron plate 10 cm thick.

The spectrum of the radiation falling on the plate corresponded to the spectrum of the radiation emerging from the active zone of a fast reactor. The external source of the radiation falling on the plate was unidirectional, the angle of incidence being almost normal ($\mu_0 = 0.9531$). The calculation was carried out with 21-group constants (the first group corresponding to neutrons with an energy of 14-10.5 MeV) in the $2D_5$ approximation. The resonance structure of the cross sections was allowed for by the method of subgroups in groups 2-10 (the total number of neutron groups and subgroups in the calculation was 37). The scattering matrix $\hat{P}$ $p \rightarrow g(x, \mu, \mu')$ was represented by two terms of the expansion in series of Legendre polynomials (P_1 approximation). Multigroup histograms of the radiation emerging from the iron plate are shown in Fig. 5; they were obtained from calculations respectively using subgroup and group blocked cross sections. The difference in the dose beyond the plate equalled 37%.

The calculations based on the PROZA program show that the incorrect allowance for the resonance structure of the cross sections based on the group-average coefficients of resonance blocking recommended in [3] leads to serious errors in calculating the integrated and differential characteristics of the shielding, particularly in the case of optically thin layers. At the same time, the method of subgroups enables us to make a correct allowance for the spatial dependence of the group-average total cross sections in the resonance region, and greatly increases the accuracy of shield calculation in the region of resolved and unresolved resonance.

The authors wish to thank A. A. Ignatov for help in this work.

LITERATURE CITED

1. M. N. Nikolaev et al., At. Énerg., 29, 11 (1970).
2. M. N. Nikolaev et al., At. Énerg., 30, 427 (1971).
3. L. P. Abagyan et al., Group Constants for Calculating Nuclear Reactors [in Russian], Atomizdat, Moscow (1964).
4. V. F. Khokhlov, Taking Account of the Resonance Structure of Neutron Cross Sections in the Subgroup Representation [in Russian], Dissertation, Melekess (1971).

5. M. N. Nikolaev and V. F. Khokhlov, "The subgroup system of constants," in: British–Soviet Seminar on Nuclear Constants for the Calculation of Reactors [in Russian], Dubna (1968).
6. T. A. Germogenova, A. P. Suvorov, and V. A. Utkin, in: Questions of Reactor Shielding Physics [in Russian], No. 2, Atomizdat, Moscow (1966), p. 22.

ACCUMULATION OF Cf^{252} IN THE CENTRAL CHANNEL OF SM-2 REACTOR

V. D. Gavrilov, Yu. S. Zamyatnin,
V. V. Ivanenko, and G. N. Yakovlev

UDC 621.039.531:621.039.572

One of the real problems in the area of transplutonium element (TPE) production is the development of nondestructive methods for monitoring their accumulation in irradiated samples. The high specific neutron yield in spontaneous fission of Cf^{252} offers an opportunity to monitor its accumulation from the increase in neutron activity in an irradiated vial which is periodically removed from the reactor channel. As a rule, the study of such vials is carried out under conditions of high γ background and therefore one of the main requirements imposed on neutron detectors is low sensitivity to γ radiation. This paper gives the principal results obtained in using activation detectors for monitoring Cf^{252} accumulation in the central channel of the SM-2 reactor.

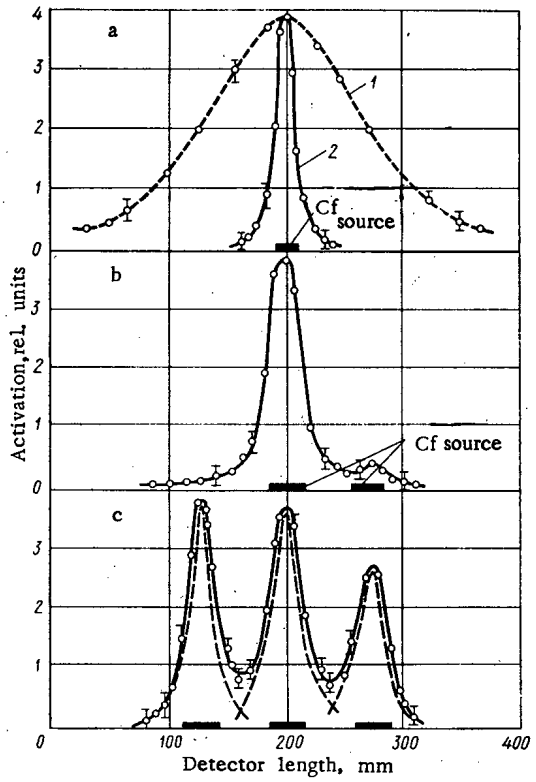

Fig. 1

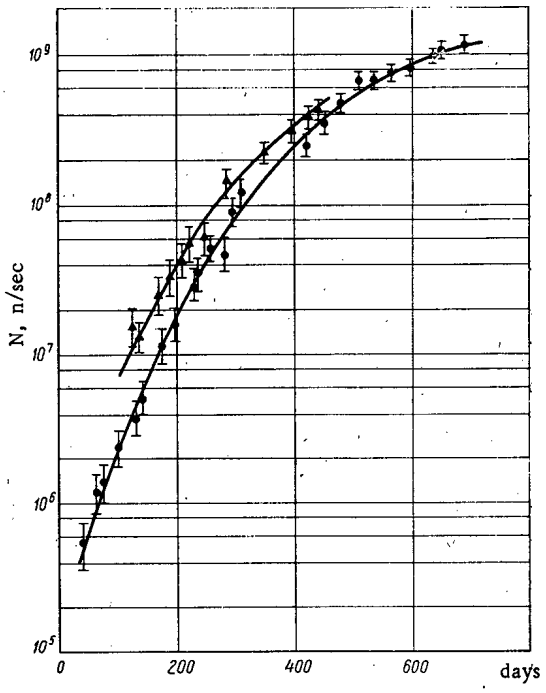

Fig. 2

Fig. 1. Activation of gold (1) and aluminum (2) detectors by californium sources: a) californium source (12 mm long); b, c) compartmented vials (30 mm long).

Fig. 2. Neutron yield from spontaneous fission of transplutonium elements formed by irradiation of 1 g of Pu^{242} and Am^{243} in the central channel of the SM-2 reactor: ▲) Am^{243}; ●) Pu^{242}.

Translated from Atomnaya Énergiya, Vol. 35, No. 1, pp. 33-35, July, 1973. Original article submitted November 17, 1972.

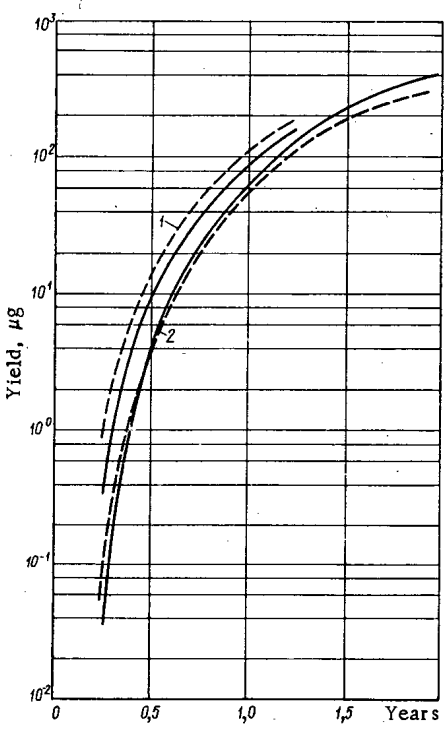

Fig. 3. Buildup of Cf^{252} in the irradiation of 1 g of Pu^{242} and Am^{243} in the central channel of the SM-2 reactor: 1) Am^{243}; 2) Pu^{242}; - - - -) calculation.

Neutron emission from a vial was determined by activation of gold and indium foils in a water pool. The foils were first calibrated with polonium–beryllium and californium sources of known activity. Measurements of induced β activity were made with a 2π proportional counter; the spatial distribution of the neutrons was determined out to distances of 40-50 cm from the axis of a vial. Since the sources were of small dimension (10-15 mm) and the vials were extended sources (~250 mm), a uniformly extended source was simulated in the calibration. Simulation was achieved by rotational–translational motion of the calibration source with oscillation amplitude equal to the length of the active portion of a vial.

Nonuniformity in the distribution of the starting material in the vials and differences in neutron flux density in the reactor lead to nonuniform buildup of californium along the length of a vial. Knowledge of the spatial distribution of neutrons from a point source makes it possible to calculate approximately the error which arises in the study of an extended source with nonuniform distribution of activity. Our calculations showed that displacement of maximum buildup of californium along the length of a vial by 20-30 mm with respect to the geometric center leads to an error of ~3% and a californium accumulation in the center which is double or triple that at the ends leads to an error of ~10%. For a compartmented vial with discrete distribution of the starting material, the error in determination of neutron emission may amount to several tens of percent; it is therefore necessary to study the distribution of neutron activity along the length of a vial.

For scanning, we used the $Al^{27}(n, \gamma)Na^{24}$ reaction, the high threshold for which (3.1 MeV) means that only nearby portions of the aluminum foil are activated by neutrons and activation of more distant portions is small because of neutron moderation in the surrounding medium to energies below threshold value. Measurements of the activity of the aluminum detectors were made with gamma–gamma coincidence equipment which made it possible to decrease the background from impurity emitters contained in the aluminum.

The distribution of neutron activation in aluminum and gold detectors from a point californium source is shown in Fig. 1a. The width of the distribution at half-maximum does not exceed 16 mm for the aluminum detector, which is completely satisfactory for scanning compartmented vials. In Fig. 1b, c the results of a study of vials with sections 30-40 mm long are shown. Since the cross section for the $Al^{27}(n, \gamma)Na^{24}$ reaction is considerably less than the cross sections for (n, γ) reactions in gold and indium, the use of aluminum detectors is advisable in the investigation of samples containing more than 50 μg of Cf^{252}.

The use of activation detectors in combination ensured that growth curves are obtained for neutron activity in vials exposed to integral neutron fluxes from $0.5 \cdot 10^{22}$ to $7.0 \cdot 10^{22}$ n/cm^2 (Fig. 2). The recorded neutron activity resulted from transplutonium elements which accumulated during irradiation. In the initial stages of irradiation, when there is little Cf^{252} in the samples, a large contribution to the total neutron activity is made by Cm^{244}; in the final stages, a large contribution is made by Cf^{254}.

The fraction of neutrons from spontaneous fission of Cf^{254}, which was measured in a supplementary experiment on the ratio of the α-decay and spontaneous fission rates for the californium fraction, was 21% of the total number of neutrons detected in the irradiation of Pu^{242} by an integral flux of $6 \cdot 10^{22}$ n/cm^2. On the basis of this value, a computed correction was applied to the Cf^{252} content in the various stages of irradiation. The curves shown in Fig. 3 characterize the accumulation of Cf^{252} from Pu^{242} and Am^{243}. The error in the determination of the amount of Cf^{252} in the initial stage of irradiation resulted mainly from inaccurate computation of the Cm^{244} content in the samples. Convergence of the curves corresponding to californium accumulation from Pu^{242} and Am^{243} is logical since the burnup of Pu^{242} in the (n, f) reaction can be neglected.

It is practical to compare the experimental curves for Cf^{252} accumulation with calculated curves [1, 2]. It should be remembered that displacement of experimental and theoretical curves is possible because of inexact knowledge of integral fluxes. In addition, variation of neutron flux density in the reactor channel along the length of a vial leads to a situation where the amounts of Cf^{252} formed at the center and ends of the vial may differ considerably. Under such conditions, it is impossible to describe the overall behavior of Cf^{252} accumulation in the entire vial by an average value of the neutron flux. It is therefore only possible to speak of a qualitative agreement between the experimental and theoretical curves (see Fig. 3).

The rate of Cf^{252} accumulation in the SM-2 reactor can be compared with similar data published for the high-flux reactor HFIR [3]. From a comparison of the accumulation curves, it may be concluded that the increase in the rate of accumulation for Cf^{252} observed for the HFIR and SM-2 reactors is not the same, as would be expected on the basis of the ratio of neutron flux densities. This can obviously be explained by the greater hardness of the neutron spectrum in the SM-2 reactor.

The authors are grateful to V. A. Anufriev, A. D. Kusovnikov, A. I. Kushnarenko, V. G. Polyukhov, G. I. Romanov, and E. S. Shevtsova for help in performing various stages of this work.

LITERATURE CITED

1. V. A. Davidenko et al., At. Énerg., 33, No. 4, 815 (1972).
2. V. Ya. Gabeskiriya et al., NIIAR Preprint P-110 [in Russian] (1971).
3. R. Baybarz, Transuranium Elements, Vol. 8, IAEA, Vienna (1970), p. 327.

REVIEW

PRODUCTION OF URANIUM ORE IN CAPITALIST COUNTRIES

N. I. Chesnokov and V. G. Ivanov

UDC 622.2

Geological Reserves of Uranium

A number of sources give conflicting data [1-10] concerning the uranium reserves in capitalist countries. The International Atomic Energy Agency and the European Atomic Energy Agency estimate the total uranium reserves in the capitalist countries as of January 1, 1971 to be 4.5 million tons. However, the minable reserves (in the IAEA's terminology, "certain and available"), i.e., those profitable for exploitation at the commercial rate of about $ 16/kg uranium concentrate, amount to 660 thousand tons* (Table 1), estimated to an accuracy of within ±10%. A large increase (34.6 thousand tons) in the minable reserves occurred in the USA in 1970. The officially stated reserves of uranium in the USA amounted to 190 thousand tons [8, 9, 11] in 1971. Of this total, 143 thousand tons are from the states of New Mexico and Wyoming [9, 10].

The uranium deposits of the USA are concentrated in the sedimentary rocks of the Colorado plateau [2, 12]. The ore bodies are adapted to arkosic sandstones, conglomerates, limestones, and argillites. The reserves are distributed into a rather small number of large deposits and a large number of small deposits. Large deposits, each with reserves of from 50 to 100 thousand tons, are located at Ambrosia Lake (state of New Mexico), the Shirley Basin, the Powder River Basin, the Gas Hills (state of Wyoming), and Laguna (state of Utah). More than 90% of the reserves are concentrated in 120 deposits. Ore bodies of lenticular shape 1-6 m thick often occur at comparatively small depth in several layers (90% of the reserves are found at depths of up to 240 m, and of these, 50% are at depths of up to 100 m); 50% of the reserves can be mined by the open-pit method.

Over 90% of the uranium reserves in Canada are concentrated in uraniferous conglomerates of the pre-Cambrian age [13]. The largest deposit is at Elliot Lake (province of Ontario). Ore deposits 2-4 m thick are as much as 2 km long. Pegmatitic (Bancroft, Faraday) and veiny hydrothermal (Lake Athabaska and the Great Bear Lake regions) deposits are well-known.

About 90% of the uranium reserves of South Africa are found in gold ores in sedimentary–metamorphogenic deposits of the Witwatersrand region. The thickness of the ore-bearing conglomerates varies from several centimeters to 3 m. The biggest strata, which are up to 15 m thick and up to 160 km long, are concentrated at the Main Reef Level. Gold (average content 8 grams/ton) and uranium (content varying between 0.02 and 0.08%) are found in fine-grained cementing material. In addition to those containing gold, there are deposits from which only uranium ores are extracted.

The largest minable uranium deposits in Western Europe are located on the territory of France. The veiny deposits in granitoids located in the Limousin, Forez, and Vendée regions have the highest commercial value. The largest of them (Bois-Noirs) is a zone of uranium mineralization, traced for a length of 8 km; the thickness of the ore vein is 1-3 m.

Australia also has good prospects for reserves of rich uranium ores [9, 14-16]. One of the largest uranium deposits was discovered in 1970 in Northern Australia (in the Nabarlek region, 273 km east of the city of Darwin); the preliminary reserves of this deposit are estimated at 50 thousand tons of uranium oxide with an average content of 270 kg/ton. A deposit has been discovered 255 km east of Darwin which is not so large (reserves eight thousand tons, content 0.272%), but other, comparable deposits may be found.

*Here and in what follows we give values of the content of metallic uranium, rather than U_3O_8 as is given in the foreign sources; the cost indices are also appropriately converted.

Translated from Atomnaya Énergiya, Vol. 35, No. 1, pp. 37-46, July, 1973. Original article submitted July 24, 1972.

TABLE 1. Minable Uranium Reserves in the Capitalist Countries (as of January 1, 1971)

Countries	Average uranium content of ore, %	Uranium reserves, thousands of tons
USA	0,195	190
Canada	0,102	178
South Africa	0,029	158
France	0,187	43
Other countries	—	91
Total	—	660

Thus, the uranium reserves in the principal uranium-producing capitalist countries are concentrated mainly in sheet or sheet-like metamorphogenic (Canada and South Africa) and exogenic (USA) deposits, and only 10% of the ore comes from hydrothermal deposits (Canada, France).

Underground Mining of Uranium Deposits

In all of the capitalist countries, uranium ore is extracted mainly by the underground method. At the present time, the ore is supplied both by mines which were built in the fifties for which the basic technical decisions were based on traditional conceptions, as well as by new or reconstructed mines in Canada and the USA using up-to-date mining techniques and the maximum concentration of labor.

Technical progress in the mining industry is most evident in the construction of new mines, especially the large ones. This is displayed in the layout of surface structures, the methods used for their construction, and in materials and engineering equipment. It is also seen in the use of the newest mining machines in the cutting operations for the main and preparatory workings, as well as in their maintenance operations. The largest mines (producing more than 300 thousand tons of ore per year) are in the USA, at the base of the Shirley Basin, Powder River Basin, and Ambrosia Lake deposits. A mine and ore-processing mill is built in no more than three years [17].

The discovery and preparation of the deposits for underground mining depend on the topography of the locality, the depth of the deposits, and the form of the ore bodies. All of the largest deposits are opened by at least two shafts, using such various arrangements of the main (output) and ventilation shafts as are determined by the specific conditions. In Canada, the United States, and France, the shaft cross sections are usually rectangular, circular cross sections being more common in South Africa [18].

Vertical shafts are used in the United States for ore removal when the ore bodies occur at a depth of more than 60 m. The biggest shafts (the Ambrosia Lake mine) have from three to five branches and are fitted with skip and cage elevators. Vertical holes 914 mm in diameter which are strengthened by casings are drilled to supplement the ventilation of the mine provided by the output shaft. For ore bodies which are on a sloping incline, the shaft usually goes to the lower boundary of the ore body, approximately in the center of the mine field. Next to the shaft, and below the ore-bearing vein, an ore yard and hauling floor are driven, located 20-30 m below the bottom of the ore-bearing level. The hauling level is joined to the cleaning levels by ore chutes and slopes.

Most of the uranium deposits in Canada have been opened by means of two vertical shafts having several sections, with a total cross section of up to 24 m^2. The supports are usually made of wood. Skips with capacities of up to 15 tons are frequently used to lift the ore, while personnel, rock, and material are lifted in cages. Mining fields in blanket deposits are prepared by means of panelled workings, using field panelled workings located at the underside of the ore body for transport.

The preparation of the deposits for the cleaning excavation with a room–pillar development system is designed and executed with consideration of the maximum utilization of power mining and transport equipment and conveyors. Panelled-workings ore are cut along the ore vein to join with the field ore chutes. The ore from the cleaning faces is delivered to electrical power-operated shuttle wagons with capacities of 14 tons or to 8 ton dump trucks and to a panelled conveyor, from which it is transferred to the main conveyor for delivery to the mine shaft. The ventilation system uses either a pressure fan or a combination of pressure and suction.

The deep-lying South African deposits are removed by central vertical shafts with one (for depths of up to 2200 m) or two hoisting stages. Multicable lifting machines and tower headframes are widely used. Stationary surface and underground cooling equipment is used to lower the temperature in the mines. Field preparation of deep levels is used. Preparatory field drifts are driven, then joined to the ore drifts during the ore recovery phase [18].

The French veiny deposits are opened by vertical shafts, the main shafts being located at the center of the deposit and the ventilation shafts at the sides. The main opening developments are located, for the most part, as the underside of the ore body; less frequently, they lie at the upper side or else intersect the ore bed. It is interesting to note that the plan of opening and preparation, the cross section of the workings, and the height of the level are decided upon at the geological prospecting stage. Lightweight prefabricated metal construction is used for the buildings above the mine and elsewhere on the surface. Tower-type headframes are used. These contain the multicable lift engine houses. The material-handling equipment is of a versatile type and is used in the various stages of exploration and exploitation. All the equipment is easy to disassemble and transport. The average depth of a development is 200-400 m; the height of a stage is at most 50 m, usually varying between 30 and 40 m. As a rule, field-type preparation of the mining area is employed (cross-cuts, field drifts, and cross-drifts). The blocks are cut by vertical raising and ore drifts.

Conventional methods are used in all countries to cut large-size shafts. Shafts 5 m in diameter were bored for the first time in the United States in 1970. It can be assumed that the drilling technique for cutting shafts in the uranium mines in this country will undergo development. In South Africa, tests have been made of two new methods for removing rock from the cutting face while cutting deep shafts. The first method involves lifting the rock directly to the surface with large-capacity loaders, while the second makes use of intermediate bunkering of the rock in the shaft. The latter method is evidently of more interest, since it results in a considerable saving in the time required for the sinking process. The utility of opening deep levels of the deposit by running twin shafts simultaneously to the projected mark has been recognized in the past few years in South Africa.

In order to provide for lifting from one level, highly productive mines are frequently equipped with ore by-pass systems, or conveyor ramps, the basic elements of which are highly efficient ore-crushing stations. Drilling has begun to be used for cutting longer main ore slopes, blind shafts, and other vertical developments of increased length. The introduction of drilling assemblies for cutting the raisings accelerates and facilitates the opening and preparation of the deposits, frees the workers from the necessity of being present during the sinking of the stopes, and makes the cutting cheaper. In this connection, many mines have begun using much more widely development systems characterized by larger amounts of preparatory and cutting work. The cost of this system has been greatly lowered by using the drilling technique to cut the raisings. Particular mention should be given to the growth of progressive ideas for modifying the techniques of opening and preparing the deposits to take account of the modern uses of drilling assemblies and material handling machines. The essence of the idea consists in having only one or two cross-cuts, rather than cross-cuts at every level. All of the levels, especially those within the ore zone, can be prepared by using upward sloping and spiral access ramps at their base. Rapid opening and preparation of the deposits can be accomplished in this way, plus a considerable decrease in the extent of the drifts and the overall amount of labor investment in the mining.

One of the recent innovations in lifting technique which should be noted is under construction at the Vaal-Reefs (Witwatersrand) mine. It is a hydraulic lift system for lifting the fines washed out of all of the mining substances which enter the shaft.

High-efficiency and, more frequently, large-scale equipment is widely used in all countries for driving: power-operated drilling carriages with two to three drills, Diesel-powered loading machines with front and side operation (the latter is part of a conveyor-belt system), as well as hauling and load-haul machines of various types. A large quantity of self-propelled equipment is also used for transportation purposes and for performing a number of secondary but important and time-consuming operations. In several uranium mines horizontal workings are cut, intended for the exclusive use of self-propelled transport. However, in many mines rail transport successfully competes with self-propelled transport, especially with the increase in the load-carrying capacity of the cars, improvement in unloading techniques, greater train speeds, and automated train controls.

Various designs of square-set are being used increasingly widely as a means of strengthening the preparatory workings.

The systems for developing the uranium deposits in the principal capitalist countries exhibit a high degree of diversity. In many respects, however, the geological conditions for mining the blanket deposits which are being worked are identical; as a result of this, a rather small number of development systems are in use in the uranium industries of the USA, Canada, and South Africa. At the present time, from 80 to 90% of the ore is mined using systems with an open working space. Thus, selective excavation by means

of open stopes and the room-and-pillar system are the principal systems in use in the United States. In Canada, from 75 to 80% of the ore extraction is based on the room-and-pillar system. In South Africa, only one system of development — continuous extraction — is used. France is the only country in which mining done with the open-working-space system (overhand stoping, subdrifts) is negligible. Some use is made of different variants of systems of development using bracing, gob flushing, and ore storing (France, Canada).

All of the above development systems are characterized by selective ore extraction, which ensures that the impoverishment of the ore due to the enclosing rock and ore-lacking impurities is minimal.

Mining technology in general, and especially the widely used room system of development, is being improved mainly by the introduction of new loading and hauling equipment: large-capacity self-propelled loading machines (especially with horizontal telescopic unloading), and also loading and hauling and other mobile machines. Mobile drilling assemblies, drilling of deep blast holes, the introduction of more durable drilling instruments, the reduction of the diameter of blast holes and other holes to minimum size, the use of ammonium nitrate explosives with petroleum additives, and the employment of square-set have been effectively applied to the technology of cleaning operations. The literature does not given quantitative data concerning the effectiveness of self-propelled equipment, but from isolated publications it may be inferred, for example, that under the conditions existing in the development of the uranium deposits of the Colorado plateau (USA), one loading and hauling machine with a scoop capacity of from 1.53 to 2.48 m^3 is able to replace from four to five ordinary low-output loading and delivery mechanisms.

The Big Back mine (state of Utah, USA) is a typical example of the use of a room-and-pillar system. The rooms are 6 m wide; the pillars which are of rectangular form, are 6 × 15 m. Ore bodies up to 4.5 m thick are finished off on one bench; two benches are used for larger thicknesses (the largest thickness in the deposit is 16.5 m). The cleaning operations are done selectively, using very maneuverable and highly productive self-propelled equipment, such as drilling carriages, Dmimbo assemblies, dump trucks, etc. The pillars are completely recovered when the excavation field is finished off. In digging the pillars, when the roofs are bad, the ore loading is done by a Diesel excavator with a 7.5 m crane arm, which pulls the ore out to a safe place and loads it into dump trucks or front-dumping self-propelled cars. If the roof is sufficiently stable, the ore struck off of the pillars is loaded by self-propelled machines. With such mechanization, the average labor productivity of the mine worker is 10.4 tons/man-shift, and the ore production cost is $ 5.88/ton. The use of self-propelled equipment has made it possible to increase considerably the surface of the cleaning operations within the boundaries of the excavation unit, and thus highly to concentrate the extraction operations. At the Denison mine in Canada, the introduction of self-propelled cars with a lifting capacity of 14 tons, drilling carriages, continuous-motion loaders, and charging machines made it possible to secure the same productivity (1.4 million tons of ore per year) with only one extraction section instead of the 4 to 5 sections formerly required. As a result, high cost-efficiency is achieved; the labor productivity of the mine is 7 tons/man-shift, and the cost of producing one ton of ore is from four to six Canadian dollars. According to the data of Canadian experts, just the use of smaller diameter blast holes and ammonium nitrate explosives with petroleum additives at the Elliot Lake uranium mines lowered the explosives cost by 30% and improved the crushing of the ore [4].

At the French and Canadian uranium mines, where the development is done by systems using subdrifts, horizontal layers with packing, and ore storing, small-size mining equipment is used: drills, vertical supporting columns, hexagonal and rectangular (flexible) steel rods, loaders with a scoop capacity of 0.12 m^3, 5-15 hp scraper winches, and cars with capacities of from 0.5 m^3 to 0.9 m^3. Ore loading without chute drawers is extensively practised, using suitable structures of block floors. Exploded enclosing rocks, rock impurities left in the room, and sometimes preparator tails having definite granule size and definite consistency are used as packing materials in those systems which use packing.

The labor productivity at the Canadian and French mines which use these systems of development is in the range 2.5-5 tons/man-shift. The cost of extracting ore in developing complex hydrothermal deposits is from 10 to 16 dollars per ton [19].

The mining technology at mines using timbering and packing systems is also being improved: self-propelled loaders, loading and hauling machines, and transportation equipment are being introduced. Higher efficiencies are achieved by using hydraulic packing, especially solidifying packing.

Technical progress at the South African mines is coupled with mechanical selective extraction of ore from the ore seam with practically no depletion. It is assumed that in the next few years high-efficiency cutting machines with cutting tools of sufficiently long life will be developed.

Open-Pit Mining of Uranium Deposits

Open-pit mining is presently being carried out at large quarries in the USA which are located in the Shirley Basin and Jackpile regions (the stripping factor is 2-12 tons/ton). There they have adopted development systems using internal terraces (requiring no transport) and external terraces (which require transport).

Friable rock is stripped by means of tractor–scrapers with capacities between 15 and 34 m^3, bulldozers, and dragline excavators with scoop capacities of up to 38 m^3. The height of the open-pit benches is from 10 to 22 m. Rocky varieties are stripped using power shovels with capacities of up to 4.8 m^3. Blast holes are drilled by various rotary boring rigs, immersible air hammers, and heavy drills. The blasting is done with the simplest explosives. Massive explosions during selective excavation are not used. The ore is loaded selectively, using excavators with small scoop capacities (0.5 to 2.0 m^3, occasionally with capacities as high as 3.8 to 4.5 m^3). Occasionally lightweight loaders are used. The only forms of transport used within the quarry are dump trucks, in sizes ranging from 3 to 23 tons. Small-size, but mobile, equipment is widely used at the small quarries. Large quarries (Jackpile, Petromex, etc.) are equipped with up-to-date heavy duty facilities for loading and hauling, drilling, and auxiliary purposes.

The system of ore removal used in the USA for the development of sedimentary deposits, especially where the morphology is complex or where there are separate ore bodies in a thick stratum of rock, involves the use of high-capacity tractor–scrapers. This ensures selective excavation without significant ore loss. The highest efficiency of the recovery work is obtained when the scrapers work in pairs. Experience at the Lucky Mac [20] quarry (with an ore production rate of 500 thousand tons per year, and stripping a yearly volume of 10 million m^3) has shown that the productivity of the scrapers is increased to 84 thousand m^3/month each when they are operated in pairs, for a scoop load of 23 to 25 m^3 of ore and a haulage distance of 2.5 km. An analogous technique is used in the stripping operations at the new uranium deposit in the Shirley Basin region, ores of which will yield 900 tons of uranium concentrate per year, and also at other quarries developing soft (sandy–argillaceous) rocks and ores.

Wheeled scrapers are used at several quarries in the state of Wyoming not only for stripping, but also for ore extraction [21]. In particular, they can be used to stockpile the ore by type. Caterpillar-633 (capacity 24.5 m^3) forming wheeled scrapers are used for ore extraction and to remove rock from the contact section of the ore zone. The productivity of each machine is about 1070 m^3/shift for a haulage distance of 1.2 km. The use of these scrapers results in less ore loss and depletion.

Electric excavators with straight shovels and scoop capacities of 13 m^3 have begun to be used for stripping in the development of deposits with exposed mineralization (the strip mine in the Shirley Basin region). These are used in conjunction with 100-ton autodump trucks and self-contained electric motors built into the drive wheels [22]. In order to reduce the loss and depletion of ore with uranium content of 0.2% and above, each shovel is frequently tested with a radiometer.

The cost of stripping at the open pit mines in the USA varies between 25 cents/ton for the loose types of rock and 65 cents/ton for the rocky varieties. The cost of extracting one ton of ore fluctuates and depends on the size of the strip mine and the stripping factor. According to data furnished by the United States Bureau of Mines, the cost of ore production at small-scale enterprises is from 1.7 to 2.5 times as much as it is at the large-scale enterprises [5], all other things being equal. The cost of extracting one ton of ore is \$4.80, \$6.20, and \$8.00 for stripping factors of five tons/ton, eight tons/ton, and 12 tons/ton, respectively. The productivity of a worker at the largest Jackpile strip mine was 106 m^3/man-shift in terms of mining volume, and 11.2 tons/man-shift in terms of ore. The labor productivity at small strip mines is much lower: in terms of ore, it is at most 8-10 tons/man-shift.

Special Methods for Developing Uranium Deposits

Among the several special techniques for uranium recovery, one should include the method of underground leaching from sedimentary deposits, using special solutions and a new method of hydraulic extraction through holes.

The chemical method for developing deposits, including the various methods of uranium leaching (for the most part, at the place of occurrence), has been developed within the past ten years, and is still in the stage of industrial experimentation. The main problems involved in applying leaching methods arise because the factors which affect the velocity of chemical reactions and the useful work of anaerobic bacteria (for processes in which they are involved) have as yet not been precisely described, and therefore

are not completely controllable. But the prospects for underground leaching are extremely good, so that its investigation and commercial application are becoming widespread.

Commercial experiments on uranium extraction by underground leaching through holes were started in the United States in 1961 at the sedimentary deposits of the Shirley Basin, and have continued on a wide scale up to the present time [23, 24]. From the results of the experimental operations it has been possible to obtain the hydrogeological conditions for the successful application of underground leaching, and to develop methods for determining the geometry of the underground leaching polygon, schemes for locating the injection and discharge holes, operating conditions, the completeness of uranium recovery, and other engineering parameters. The drilling and arrangement of the holes is the principal concern. The holes are drilled as for a heading at first, and are then reamed for the casing. The injection holes are fitted throughout their length with stainless steel casings 76.2 mm in diameter, while 203.2 mm casing is used for the discharge holes (in the latter case, the stainless steel is only installed over the last 12.2 m of the hole). A solution of sulfuric acid with a concentration of 5 g/liter is used for the leaching, and a small amount of sodium chlorate is added to improve the recovery of uranium. The producing solution, containing from 0.1 to 0.3 g/liter of U_3O_8, is transported from the discharge holes to the ion-exchange plant through a pipeline. From three to five polygons are operated simultaneously.

It is difficult to estimate the amount of uranium extracted from all of the operating areas, although it is known that up to 100% of the mineral product is extracted from the polygon within the range of influence of the holes. Company representatives estimate that the total extraction is equal to or even greater than that attained at similar deposits by the use of underground methods of development. However, the complicated composition of the deposit, particularly the multilayered nature of the ore bodies, as well as the fact that there is no waterproof rock lying underneath the ore bed, frequently prevents complete extraction of the uranium.

The cost of extracting uranium by the technique of leaching through holes depends on a large number of factors, particularly natural ones. At the Shirley Basin mine the minimum cost is estimated to be about the same as the cost involved in open-pit operations at similar areas. It can, however, become more than twice as large under unfavorable conditions. In spite of that, it is known that in this region the cost of uranium extraction by the leaching technique is considerably less than the cost when the operations are underground.

The biggest advantage of underground leaching, besides its relatively low production cost, is the safety factor; all production operations are carried out on the surface. In addition, the capital investment in the polygon equipment and the construction of the reprocessing plant is quite moderate. Underground leaching lengthens the useful lives of the miners, as well as making it possible to recover metals from low-grade ores and to reprocess the tails dumps of the low-quality ores and slurries. It should be noted that uranium can also be leached from ores which have first been crushed at the site of their deposit by powerful blasting charges of ordinary (chemical) explosives or nuclear explosions. The main disadvantages of underground leaching are the dependence of the effectiveness of the technique on the porosity of the rocks and other uncontrollable factors of the ore bed, as well as the problems involved in extracting uranium in finishing off ore bodies which have a complicated structure.

Information concerning the amount of uranium being extracted in the USA by the underground leaching technique is incomplete at the present time. The literature contains references to the Utah Corporation and Mining Company and the Pinzh Exploration, which makes use of underground leaching at the Pitch mine in central Colorado [25].

Underground leaching (mostly bacterial) was first employed to mine uranium in Canada at the beginning of the 1960's, at the Elliot Lake mines. It is now being used at all four of the mines in this region; at the Stanrock and Nordic mines it is the principal means of production, while it plays an auxiliary role at the Milliken and Denison mines [25-31].

At the Stanrock mine, underground leaching operations started with uranium recovery during the treatment of the mining waters, using bacterial catalytic agents to promote the ferrous oxide–ferric oxide transition. During the leaching of the uranium, insoluble tetravalent uranium is oxidized by the sulfate of tetravalent iron [27]. A section of a hydrometallurgical plant utilizing ion-exchange is used to recover the uranium from the solution in which it is produced. The Stanrock mine has yielded in this way as much as 5.5 tons of uranium per month, while the total amount of uranium produced by 1968 by bacterial leaching amounted to 250 tons, or 6.5% of the total production.

TABLE 2. Ore Extraction and Production of Concentrates in 1970 [34, 37-44]

Indices	USA	Canada	South Africa	Remaining capitalist countries	Total in capitalist countries
Quantity of ore produced, 10^6 tons	5,6	3,1	13,0	1,0	22,7
Average uranium content in mined ore, %	0,180	0,110	0,025	0,194	0,082
Output of concentrated uranium, thousands of tons	10,00	3,48	3,18	1,94	18,60
Number of active processing plants	15	3	8	19	45
Average yearly output of ore processing plants, thousands of tons	350	700	1560	56	450
Number of plants planned and under construction	8	2	5	7	22
Total output of plants, including those planned and under construction, in terms of metal production (up to 1975), 10^3 tons	17—20	10—13	6	6—7	40—45

The total cost of producing uranium by the bacterial leaching method and by washing the headings averaged $ 8.55 per kilogram [28], which is 36% less than the cost of producing the metal prior to the changeover to the leaching method.

Western experts believe [27, 29] that underground leaching will not replace the usual methods in Canada for the production and processing of ore. However, being cheap, this method may have important consequences for finishing deposits, for recovering metal from ore left in exhausted areas in the form of various wastes, and also for reprocessing low-grade tailings from which it would be economically unfeasible to recover uranium by other methods. Bacterial leaching is also a promising technique for recovering uranium from mechanical enrichment tailings. If necessary, it can be used in recovering valuable metals from the tailings of hydrometallurgical plants. Investigations have shown that under certain conditions bacteria can play the role of oxidizing agents in hydrometallurgical processes. It is assumed that the significance of bacterial leaching in the ore mining and smelting industry will increase in proportion to the study of the mechanism of bacterial leaching.

The technology of underground leaching and the results of adopting it at French mines are thoroughly discussed in the Soviet [32-34] and foreign literature [35].

Another special mining technique which has been projected for adoption at sedimentary deposits in the USA is the method of mining hydraulically through holes drilled from the surface. Hydraulic mining through holes consists essentially of three processes: the usual rotational drilling of a hole 406.5 mm in diameter, hydraulic erosion of the rock mass around the hole, and the lifting of the pulp to the surface. The hydraulic mining equipment, as well as a high-pressure pump with an internal combustion engine which is an original design developed in the USA, have been fully described in the literature [36]. At the present time, the method has been tried in irrigation for building cavities and horizontal branch channels. It has also been tested in the petroleum industry to create conditions for increased oil flow to the wells.

The Economics of the Uranium Industry

In characterizing the present condition of the uranium industry of the capitalist countries, it is first of all necessary to note that it is gradually emerging from a state of crisis. Against the generally moderate background of this transition, there occurred an unprecedented and vigorous development of exploration and prospecting operations, the main purpose of which was to increase the raw material base of the relatively cheap uranium needed to provide nuclear fuel for atomic power stations. The output of the latter should increase from 26 million kilowatts in 1970 to between 234 and 328 million kilowatts in 1980 [1, 2], although the execution of this program is at a standstill at the present time.

Since 1966 appropriations for exploration have steadily increased, especially in the USA and Canada, where the outlook for the growth of reserves is good. It is anticipated that no less than $ 500 million will be spent in the USA alone on exploration operations. The growth in the production and processing of ore is, however, quite small, because the uranium production and processing industry is making deliveries largely on the basis of previously concluded contracts, and the amounts delivered in accordance with new contracts are still small. Table 2 lists the main production indices of the uranium industries in the capitalist countries.

According to an estimate made by Canadian mining industrialists [45], the annual production of uranium in capitalist countries in the period 1971-1972 must have amounted to 30 thousand tons. The USA accounted for 42% of this amount.

3. Cost of Mining Ore and Produc- oncentrated Uranium [45-51]

Indices	USA	Canada	South Africa
Cost of ore mining, dollars/ton	14,0	5—6,5	—
Cost of ore processing, dollars/ton	10,0	6,6—10,4	2—2,5
Extraction of metal, %	92	90	80
Cost of concentrated uranium, dollars/kg	15,0	13—18	10—14

It is difficult to form a sufficiently complete idea of the present expenditures on uranium production in the capitalist countries by using the fragmentary materials available. In 1968 the expenditure in the USA on uranium ore production and processing varied between 80% and 90% of the cost of the concentrated uranium [45]. The remaining 10 to 20% was due to lease payments, taxes, and prospecting. The average cost of exploration operations throughout the country as a whole amounted to 2.33 dollars per kilogram of concentrated uranium. The cost of the main operations in open-pit mining of the deposits is described by the following data [46]:

1. Exploratory drilling: the cost of coreless drilling ranged between 1.15 dollars per running meter for shallow deposits with good drilling conditions, to several dollars per running meter for relatively deep-lying deposits with more difficult drilling conditions (the average expenditures fluctuated between 1.64 and 3.28 dollars/running meter); core drilling costs were as high as 82 dollars /running meter.
2. The cost of removal varied between 0.13 and 0.65 dollars per cubic meter, depending on the distance that the rock which is removed must be transported. Proper distribution of the rock within the strip mine enables the cost of removal to be minimized.
3. Ore production: the cost is 1 or 2 dollars/ton, depending on the technology and equipment used.

The average cost (neglecting the turnover tax) of mining uranium ore by the open-pit method in the United States upon conversion to 1 kg of concentrated uranium is about $ 7 and when processing at the mill is included, it comes to $ 14.5.

We list below the calculated values of the average cost in dollars per kg of concentrated uranium, produced at American mills that process ore from underground mines [46]:

Prospecting	2.07
Lease payment	1.02
Mining	7.80
made up of: work force	3.58
amortization	1.87
supplies, taxes, etc.	2.35
Ore transportation, processing, and selling	4.66
Total	15.55

It can be concluded from the combined data for the year 1968 shown in Table 3 that the expenditures on ore production in the USA and Canada were on the average about half of the total amount spent on the production of uranium concentrates. The expenditures on ore production in South Africa are not considered, since the uranium mills process the tailings of gold mines which do not require crushing and grinding; thus the cost of producing uranium concentrates from low-grade ores is considerably less.

Projections for the growth of the raw material base of the uranium industry in the capitalist countries for the next decade are given in Table 4. These are compiled from data published between 1969 and 1971 by the International Atomic Energy Agency, the European Atomic Energy Agency, the energy department of the Chase Manhattan Bank, and the United States Atomic Energy Commission [11, 43, 44, 52-55].

The total uranium requirements of the USA up until 1980 (excluding that required for military purposes) are estimated to be 510 thousand tons (including reserves for a ten-year period). Of this total, 200 thousand tons are for use in reactors, and 310 thousand tons should make up a 10-year reserve, taking into account the level of consumption in the year 1980. During this period, a number of other capitalist countries will require 340 thousand tons, including 130 thousand tons for reactors and 210 thousand tons

TABLE 4. Predicted Indices of the Growth of the Raw Material Base of the Capitalist Countries for the Next Decade

Indices	Year	USA	C, SA, etc.	Total
Uranium requirement for AEPS, 10^3 tons/yr	1970	5,8	8,4	14,2
	1975	16,1	11,3	27,4
	1980	29,3	37,7	67,0
Calculated production of conc. uranium, 10^3 tons	1970	10,0	8,6	18,6
	1975	13,6	15,4	29,0
	1980	18,7	16,2	34,9
Capital investment, 10^6 dollars	1970	120	80	200
	1975	340	260	600
	1980	600	600	1200
Price of conc. uranium, dollars/kg	1970	17,4	20,1	19,0
	1975	21,2	23,0	22,5
	1980	24,3	25,8	25,6

Note. C) Canada; SA) South Africa. The total is that in capitalist countries.

for a 10-year reserve. The capitalist countries, including the USA, will thus require 850 thousand tons of uranium. Data calculated by the International Atomic Energy Agency and the European Atomic Energy Agency indicate that starting in 1977 the demand for uranium may exceed its level of production.

According to a forecast of the United States Atomic Energy Commission, the total investment in the production of uranium concentrates in the capitalist countries will increase by a factor of six within the next decade. It is assumed that although the share of the USA in the total production will drop to 50% by 1980, for the next 10-15 years this country will still keep its position as the leading producer of atomic raw materials. In the period prior to 1980, combined investment in the capitalist countries in prospecting and exploration of uranium deposits and in constructing mines and mills for producing and processing concentrates may amount to nine billion dollars, including three to four billion dollars in the USA. Many experts estimate that to attract private firms into the development of the uranium industry, the price of uranium in the period from 1973 to 1975 will have to be at least $ 21/kg. The price after 1975 will essentially depend on the results of exploration operations.

LITERATURE CITED

1. Mining Annual Rev. (1969).
2. Uranium Production and Short Term Demand, ENEA–IAEA, Paris–Vienna (1969), p. 29.
3. Annual Report to Congress for 1969, United States Atomic Energy Commission, Washington (1970), pp. 37-39.
4. CIM Bull., 63, 704 (1970).
5. Atomic Energy Clearing House, 15, No. 14, 19 (1969).
6. App. Atomic, 11, 667 (1968); 2, 692 (1969); 1, 711 (1969).
7. Mining J., 272, 452 (1969).
8. Mining Congr. J., 56, 4 (1970).
9. Mining Mag., 122, 5 (1970).
10. World Mining, 24, No. 1 (1971).
11. Nucl. Industry, 18, No. 5, 37 (1971).
12. App. Atomic, 7, 8 (1969).
13. Uranium Canad. Mining J., February (1969).
14. Mining J., July (1970).
15. Mining J., 275, 7050 (1970).
16. Mining J., 275, 7047 (1970).
17. Mining J., November (1968).
18. N. I. Chesnokov and A. A. Petrosov, Uranium Mining Methods [in Russian], Atomizdat, Moscow (1972).
19. N. S. Sadykin, Natural Resources of the Uranium Industries of Capitalist Countries and their Utilization [in Russian], Nedra, Moscow (1968).
20. Eng. Mining J., 170, No. 10 (1969).
21. Eng. Mining J., 169, No. 9 (1968).
22. Eng. Mining J., 169, No. 8 (1968).
23. Mining Congr. J., 53, No. 10 (1967).
24. Mining Congr. J., 54, No. 1 (1969).
25. Eng. Mining J., 170, 3 (1969).
26. Can. Mining J., 87, 64 (1966).
27. Nucl. Applic., 6, No. 1 (1969).
28. Eng. Mining J., 169, 6 (1968).
29. J. Brit. Nucl. Energy Soc., 8, 2 (1969).
30. Eng. Mining J., 168, 10 (1967).

31. Mining Eng., 21, 3 (1969).
32. B. G. Bakhurov, S. G. Vecherkin, and I. K. Lutsenko, Underground Leaching of Uranium Ores [in Russian], Atomizdat, Moscow (1969).
33. A. I. Kalabin, Extraction of Mineral Resources by Underground Leaching [in Russian], Atomizdat, Moscow (1969).
34. Eighth International Congress on the Enrichment of Mineral Resources [in Russian], Proceedings No. E-4, Leningrad (1968).
35. Rev. Ind. Miner., 50, 5 (1968).
36. Mining and Minerals Eng., 10 (1969).
37. Eng. Mining J., 169, 150 (1969); 170, 104 (1969).
38. Nth. Miner, April (1969).
39. Atomwirtschaft, 14, 60, 61 (1969).
40. Ann. Mines, 18 (February, 1969).
41. Lloyd, "The nuclear metals. Uranium," Mining Annual Rev., 83-84 (June, 1969).
42. Can. Mining J., 2, 9 (1969).
43. Commodity Data Summaries, Bureau of Mines, Washington (1971).
44. Uranium: Resources, Production, and Demand, ENEA–IAEA, Paris–Vienna (1970), p. 34.
45. CIM Bull., 62, 692 (1969).
46. Eng. Mining J., 12 (1968).
47. Can. Mining J., 89, No. 8 (1968); 89, No. 9, 19 (1968).
48. Erzmetall, 5 (1970).
49. R. Stochr, Mining Congr. J., February (1968).
50. M. Bonanni et al., Econ. Nucl. Fuels, Vienna (1968).
51. The Outlook for Nuclear Energy and the Uranium Industry, Nuveen Corp., New York (1968), p. 8.
52. The Nuclear Industry – 1968, United States Atomic Energy Commission, Washington (1968), p. 28.
53. "Uranium output must rise 70%," Electr. Times, 155, 14 (1969).
54. Nucl. Industry, 17, No. 7, 22 (1970).
55. Atomwirtschaft, 15, No. 9/10, 413 (1970).

ABSTRACTS

HETEROGENEOUS EFFECTS OF SODIUM AND U^{238} AND OF CERTAIN CROSS SECTION RATIOS IN A BFS-22

L. N. Yurova, A. V. Bushuev,
V. M. Duvanov, A. F. Kozhin,
and A. M. Sirotkin

UDC 621.039:526.519.4

In extrapolating the results obtained in critical models under the conditions in design reactors and also in analyzing the accuracy of the design methods and of the nuclear data, there arises the question of the nature and magnitude of the effects of the heterogeneous arrangement of entrances into the active zone of the materials.

The distribution of the $U^{238}(n, \gamma)$ and $Na^{23}(n, \gamma)$ reactions in disks of natural uranium and metallic sodium were investigated in different zones of a critical BFS-22 station (see Fig. 1). The experiments are based on the detection of γ-radiation from the reaction products, Np^{239} and Na^{24}, which were accumulated during the process of irradiation in the corresponding inserted disks of natural uranium and metallic sodium foil. The distribution of the $Na^{23}(n, \gamma)$ reaction in the volume of the BFS-22 was also investigated through the γ activity of standard sodium disks incorporated into the structure of the installation.

Measurements were performed at the center of a BFS-22 for the determination of the reaction cross section ratios, $\sigma_c(Na^{23})/\sigma_f(U^{235})$, $\sigma_c(U^{238})/\sigma_f(U^{235})$, $\sigma_f(U^{238})/\sigma_f(U^{235})$, based on the detection of γ radiation from the corresponding reaction products. Results of measurements and calculations performed by the method described in [1] are shown in Table 1.

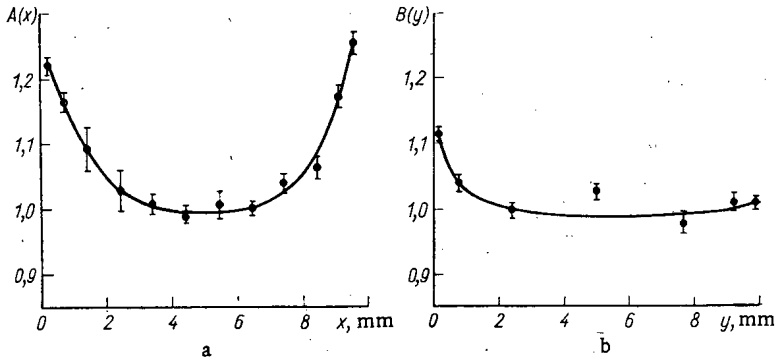

Fig. 1. Distribution of reaction rates inside sodium (a) and uranium (b) disks [A(x) corresponds to $Na^{23}(n, \gamma)$; B(x) corresponds to $U^{238}(n, \gamma)$]: x and y are the distances from the front surface of the disks of metallic sodium and natural uranium arranged in the front shield of the BFS-22 between disks of uranium dioxide (a), and of sodium and uranium dioxide (b).

Translated from Atomnaya Énergiya, Vol. 35, No. 1, pp. 47-50, July, 1973. Original article submitted January 31, 1972; abstract submitted September 18, 1972.

TABLE 1. Calculated and Experimental Cross Section Ratios

Ratio	$\frac{\sigma_c(Na^{23})}{\sigma_f(U^{235})}$	$\frac{\sigma_c(U^{238})}{\sigma_f(U^{235})}$	$\frac{\sigma_f(U^{238})}{\sigma_f(U^{235})}$
Calculation	$0{,}77\cdot10^{-3}$	0,134	0,029
Experiment	$(0{,}580\pm0{,}014)\cdot10^{-3}$	0,128±0,004	0,029±0,001

Taken together, the results obtained indicate that in some cases during calculation of the neutron field it is necessary to take into account the effects of resonance blocking of the cross sections associated with a heterogeneous arrangement of the entrances into the active zone of the materials.

LITERATURE CITED

1. A. M. Sirotkin et al., in: Nuclear Reactor Physics [in Russian], No. 1, Atomizdat, Moscow (1968), p. 106.

INVESTIGATION OF THE SOLUTION OF COMPACT SPECIMENS OF URANINITE IN SULFURIC ACID SOLUTIONS

G. A. Dymkova, L. N. Kuz'mina, G. M. Nesmeyanova, and P. V. Pribytkov

UDC 553.495:532.73

Unlike the methods of dissolving mineral powders used previously [1, 2], mineralogically investigated [3] uraninites in the form of compact prepolished specimens were dissolved. It was established that the rate of solution of the surface in sulfuric acid solutions, determined by the rotating disk method [4], depends not only on the total ratio O:U in the sample [5] but also on the phase composition of the specimens. The investigated uraninites could be divided according to the action of the solvent into three groups differing in lattice parameters, microhardness, and depth of loosening of the surface layer.

Uraninite that forms coffinite on decomposition dissolves the most. It has lattice parameter a_0 = 5.36-5.39 Å, microhardness 200-400 kg/cm^2, and the thickness of the loosened surface layer is 1.1-2.5 μ.

Uraninite having, in polished specimens, a spotty distribution of zones of insignificant dissolution of the surface is characterized by lattice parameter a_0 = 5.40-5.41 Å, microhardness 500-700 kg/cm^2, and loosened layer 0.1-0.5 μ.

The least soluble in sulfuric acid solutions is uraninite with lattice parameter a_0 = 5.43 Å; its microhardness is 950-1000 kg/mm^2; the loosened layer is 0-0.1 μ. In its physical properties this uraninite is apparently a natural analog of synthetic cubic uranium oxide (U_4O_9).

The kinetics of the solution of compact specimens depends on their quantitative relationship of uraninites characterized by different physical properties and belonging to different groups.

LITERATURE CITED

1. G. M. Nesmeyanova and G. M. Alkhazashvili, At. Énerg., 10, No. 6, 587 (1961).
2. G. M. Alkhazashvili, G. M. Nesmeyanova, and L. N. Kuz'mina, At. Énerg., 15, No. 4, 313 (1963).

Original article submitted March 7, 1972; abstract submitted February 22, 1973.

3. Yu. M. Dymkov et al., in: Uranium Deposits. Zonation and Paragenesis [in Russian], Atomizdat, Moscow (1970), p. 274.
4. A. A. Ravdel' and G. I. Gorelik, Zh. Prikl. Khim., 37, No. 11, 65 (1964).
5. I. G. Zhil'tsova and L. N. Karpova, At. Énerg., 31, No. 1, 58 (1971).

EFFECT OF NEUTRON RADIATION AND γ RADIATION ON THE PARAMETERS OF METAL – INSULATOR – SEMICONDUCTOR STRUCTURES

V. A. Girii, V. M. Pasechnik,
V. A. Stepanenko, V. N. Khrapachevskii,
and V. I. Shakhovtsov

UDC 539.125.5.04:539.122.04

Up to the present time, in the study of radiation effects in metal – insulator – semiconductor (MIS) structures, as a rule, the radiation doses absorbed by the components of these structures have not been determined [1]. However, an approach in which only the integrated radiation fluxes are determined is acceptable only when sources that give a single definite form of radiation are used and also in studying objects the radiation sensitivity of which proves to be affected primarily by one of the components of the complicated radiation state. It is known that the radiation sensitivity of MIS structures is determined principally by the ionization effects of irradiation [2]; therefore, for experiments that are carried out in a reactor we must quantitatively take into account the selective action of neutron components and γ components of the radiation. This may be ensured in the determination of absorbed doses of each radiation component.

In the present study we calculate the contribution of the absorbed energy of neutron components and γ components of the reactor radiation in a change of the threshold voltage V_{thr}, and results are presented of an investigation of the behavior of p-channel $Si-SiO_2-Si_3N_4-Al$ structures in fields of reactor and pure γ radiations. The effect of irradiation was estimated on the basis of the change in the magnitude of the threshold voltage V_{thr}, determined from the high-frequency C – V characteristics at the level of the plane bands. MIS structures were realized on n–Si with $\rho_V = 4.5\ \Omega \cdot cm$; the thickness of the layers of SiO_2 and Si_3N_4 were the same and equal to 500 Å.

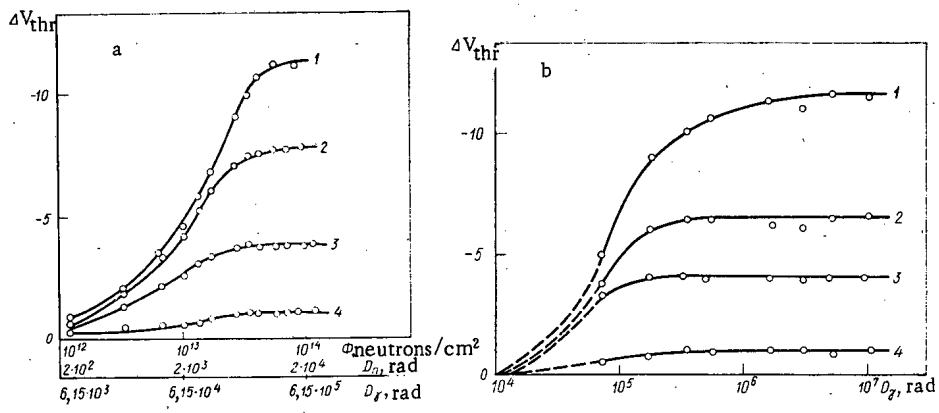

Fig. 1. Variation of threshold voltage as a function of dose of reactor and γ radiations of Co^{60} (a and b, respectively): 1) $V_{CM} = 15$ V; 2) $V_{CM} = 10$ V; 3) $V_{CM} = 5$ V; 4) $V_{CM} = 0$; $d_{SiO_2} = 500$ Å; $d_{Si_3N_4} = 500$ Å.

Original article submitted July 10, 1972.

The data presented in Fig. 1 for the reactor and pure radiation of Co^{60} show that for both forms of radiation for integrated flux density $\Phi_n = 10^{14}$ neutrons/cm^2 and dose $D_\gamma = 10^6$ rad the effects agree both qualitatively and quantitatively. Since the mechanisms of interaction of γ quanta and fast neutrons with a substance are fundamentally different, the indicated effect evidently attests to the predominant effect of γ components of the reactor radiation on the properties of MIS structures. In order to check this conclusion we calculated the absorbed dose of neutrons and γ quanta, and we conducted experiments on different sources.

Calculations showed that for neutrons of the reactor spectrum with energy $E_n \geq 100$ keV for given radiation flux density, the doses absorbed in SiO_2 and Si_3N_4 are 0.08 and 0.053 rad/sec, respectively. For the accompanying γ radiation in these materials the absorbed doses are 2.15 and 2.17 rad/sec, respectively.

From the curve of $\Delta V_{thr}(\Phi_n)$ (see Fig. 1a) – the function of the absorbed dose of each of the components of the reactor spectrum – we see that there is good agreement between the experimental data and the calculated results for pure γ radiation.

The results obtained confirm the ionization character of the radiation effects in MIS structures, and show that the principal factor responsible for the variation of their parameters during irradiation in a reactor is the γ component of the reactor radiation.

LITERATURE CITED

1. G. Messenger et al., IEEE Trans. on Nuclear Science, NS-12, No. 5 (1965).
2. E. H. Snow et al., Proc. IEEE, 55, No. 7, 1168 (1967).

EFFECT OF A PLANE BOUNDARY ON THE β-RADIATION DOSE DISTRIBUTION INSIDE A THICK-LAYERED SOURCE

D. P. Osanov and Yu. N. Podsevalov

UDC 539.12.08

In this paper a calculation is carried out for the dose distribution inside and on the surface of a thick-layered plane tissue-equivalent source with given one-dimensional distribution of concentration of radioactive substance A(x) – powers, exponentials, etc.

We consider what effect the presence of boundaries has on the increase of the dose at the points C_1 and C_2 located to the right and to the left of an elementary infinitesimally thin source S(x). For the case of an "infinite" medium (see Fig. 1) the fraction of β particles emerging from the source S(x) in the direction of the surface (x = 0) would be backscattered and would increase the dose rate at the points C_1 and C_2, i.e., a calculation that does not take account of the effect of the boundaries will give results that are too high. We must stress the difference in conditions of increase of the dose at the points C_1 and C_2. Actually, at the point C_1 the scattered radiation falls after attenuation in the layer of the absorber d_a, and for the point C_2 the scattering and absorption processes take place in the opposite order, i.e., β particles first pass through the absorber and then are scattered near C_2. In view of this, the functions defining the dose from the thin plane source in the direction of the interior of the medium and towards the boundary will differ.

We denote these functions by $D_1(E_0, d_a, d_s)$ and $D_2(E_0, l_a, l_s)$, respectively. The first of these is investigated in [1]. In the present study we investigate experimentally the increase of the dose field at points located between the source and the boundary; this field is described by the function $D_2(E_0, l_a, l_s)$.

Original article submitted October 18, 1972; abstract submitted February 28, 1973.

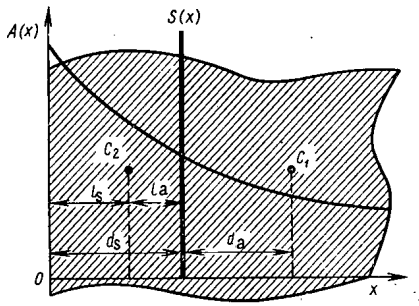

Fig. 1. Diagram of thick-layered source.

In the experiment we used an extrapolation chamber, described in [1]. In the given case the collecting electrode of the chamber had a "window" covered with a thin aluminized Terylene film. For fabrication of the sources we used seven different isotopes with energy limits ranging from $E_0 = 0.43$ MeV (W^{185}) to $E_0 = 3.55$ MeV ($Ru^{106} + Rh^{106}$).

On the basis of an analysis of the experimental data the function $G_2(E_0, l_a, l_s)$ was obtained allowing us to find the unknown function $D_2(E_0, l_a, l_s)$ in the form

$$D_2(E_0, l_a, l_s) = D_\infty(E_0, l_a) G_2(E_0, l_a, l_s), \quad (1)$$

where $D_\infty(E_0, l_a)$ is the dose function of a thin plane source for an infinite medium (see, for example, [2]). In the range under investigation, the quantity $G_2(E_0, l_a, l_s)$ is independent of the energy limit; if the thicknesses of the absorber l_a and of the scatterer l_s (see Fig. 1) are expressed in units of the maximum range R_0, then the quantity $G_2(E_0, l_a, l_s)$ is approximated by the equation

$$G_2\left(\frac{l_a}{R_0}, \frac{l_s}{R_0}\right) = 1 + 0.15 \lg \frac{\frac{l_s}{R_0} + 0.0015}{0.16 - 0.2\frac{l_a}{R_0}}, \quad (2)$$

where

$$0 \leqslant l_s \leqslant 0.1585 R_0; \quad 0 \leqslant l_a \leqslant 0.66 R_0.$$

Since, by definition, $G_2(l_a/R_0; l_s/R_0) \leq 1$, Equation (2) has meaning only for negative values of the logarithm; otherwise, $G_2(l_a/R_0; l_s/R_0) \equiv 1$. The error in Eq. (2) does not exceed 5%, which is quite acceptable for practical purposes.

LITERATURE CITED

1. D. P. Osanov and Yu. N. Podsevalov, At. Énerg., 31, No. 3, 287 (1971).
2. R. Levinger et al., in: Radiation Dosimetry [Russian translation], IL, Moscow (1958).

DETERMINATION OF TOTAL CROSS SECTIONS OF THE RADIATION LOSSES OF ELECTRONS

G. N. Dmitrov

UDC 539.533.7

In order to calculate the total cross sections of radiation losses of electrons we obtain an empirical formula for the dependence of the total cross section of radiation losses of electrons on the energy of the incident electrons and the charge of the damping medium:

$$\sigma_r = 5.373 \cdot 10^{-3} \cdot Z^{1.901} E_k^{0.292 \cdot Z^{-0.047}}, \quad (1)$$

where Z is the charge of the damping medium ($Z \geq 2$); E_k is the kinetic energy of the incident electrons, MeV; σ_r is the total cross section of the radiation losses, barn.

For hydrogen

$$\sigma_r = 7.58 \cdot 10^{-3} E_k^{0.286}. \quad (2)$$

Original article submitted October 23, 1972; abstract submitted October 23, 1972.

The constant coefficients in these equations are determined by the method of least squares.

The values for the total cross sections of the radiation losses of electrons obtained from Eqs. (1) and (2) and as a result of detailed calculations in [1] differ by no more than 7%, which is quite acceptable for engineering calculations on shielding from bremsstrahlung.

The total losses of energy of electrons by radiation are calculated:

$$-\left(\frac{dE}{dx}\right)_{\text{rad}} = \frac{N}{A} E_0 \sigma_r, \tag{3}$$

where N is the Avogadro number; A is the mass number of the damping medium; and E_0 is the total electron energy, MeV.

Values of the total cross sections of radiation losses and losses of electron energy by radiation for a number of structural materials and heat-proof coverings (alloys of metals, plastics, and ablation coverings) are calculated on the basis of Eqs. (1) and (3).

LITERATURE CITED

1. E. L. Stolyarov, V. V. Samedov, and S. N. Volodin, in: Applied Nuclear Spectroscopy [in Russian], V. G. Nedovesov (editor), No. 1, Atomizdat, Moscow (1970), p. 114.

LETTERS TO THE EDITOR

EXPERIMENTAL DETERMINATION OF THE IGNITION TEMPERATURE OF SODIUM AND POTASSIUM

V. A. Polykhalov and V. F. Prisnyakov

UDC 621.039.534.63

It is well known that when an alkali metal interacts with air the rate of oxidation depends not only on the temperature of the alkali metal and the air but also on the thickness of the oxide film. Hence the ignition temperature of the alkali metal depends on the prehistory of the process, so that the theory of thermal explosion [1] is not applicable in determining the ignition temperature of alkali metals.

In [2] an expression for the ignition temperature of alkali metals was derived by an analytical method; however, the necessary data regarding the rate of oxidation were not available, and the solution had no practical use. The experimental determination of the ignition temperature of alkali metals would therefore appear more promising.

In this paper we shall describe experiments relating to the ignition temperature of pure sodium (trade standard TU 1604-50), commercial sodium (GOST 3272-63), and commercial potassium (GOST 10588-68) under the following conditions: 1) slow heating at 1.5-2 and 2.5-4 deg/sec in air; 2) injecting the alkali metal into an experimental section previously heated to the ignition temperature in air; 3) heating the alkali metal to the ignition temperature in argon and then igniting in air or oxygen.

The air experiments were carried out at atmospheric pressure, with a relative humidity of 50-60% (measured by a psichrometer), and a temperature of 18-24°C (under these conditions 1 kg of air contains 5-9 g of moisture [3]). The oxygen experiments were carried out at an oxygen pressure of 1.05 atm; according to GOST 5583-58 the amount of moisture in oxygen is then no more than 0.005 wt.%.

The sodium and potassium were purified by allowing them to settle. Chemical analysis revealed the following oxygen content: in the sodium 0.007-0.008 wt.%; in the potassium 0.12-0.15 wt.%. The weight of the alkali metal sample was 5-10 g.

The experimental apparatus was a vessel 60 mm high made from a tube of external diameter 37 mm and wall thickness 3.5 mm with a welded bottom 5 mm thick; the material was Kh18N10T steel. Glass cloth was used for the thermal insulation of the sides of the experimental section. Heating was achieved by means of an end-type Nichrome heater. In order to convey air and argon to the system, two conduits with an internal diameter of 4 mm were welded to the sides of the vessel, and to measure the temperature a Chromel–Copel thermocouple in a Kh18N10T steel sheath was welded to the bottom of the vessel. In the first and third versions of the experiment the thermocouple was welded to the bottom of the experimental section so that the junction was 6 mm from the bottom. The thickness of the layer of metal above the surface of the junction when carrying out the experiments varied between 2 and 5 mm. In the second version of the experiment the thermocouple junction was welded directly to the bottom of the experimental section. The processes were followed visually through a Pyrex glass roof. The thermocouple readings were recorded with a PP63 potentiometer, and for slow heating in air with an ÉPP-09 potentiometer. In order to determine the temperature-measuring error, a control thermocouple was introduced at the level of the metal while slowly heating sodium at 2.5-4 deg/sec in air to the ignition point. The difference in the readings of the main and control thermocouples was no greater than 2°C. In view of the considerable thermal conductivity of the alkali metal and the existence of convective flows, the measuring error was thus no greater than 3%.

Translated from Atomnaya Énergiya, Vol. 35, No. 1, pp. 51-52, July, 1973. Original article submitted February 16, 1972.

TABLE 1. Ignition Temperature of Sodium and Potassium, °C

Heating sodium in air		Previous heating in a protective argon medium		
1,5–2 deg/sec	2,5–4 deg/sec	sodium on blowing air through	potassium on blowing air through	sodium on blowing oxygen through
454	420	334	428	285
447	414	335	420	286
437	405	347	428	293
462	415	349	416	290

The ignition temperature of sodium on slow heating in air depends substantially on the heating rate. Table 1 gives the ignition temperatures of pure sodium for a heating rate of 1.5-2 and 2.5-4 deg/sec. The heating rate was regulated by varying the thermal resistance of the experimental section.

Slow heating of potassium in air at a rate of 2.5-4 deg/sec leads to vigorous oxidation at 260-270°C, and no ignition occurs. On injecting the alkali metal into the experimental section previously heated in air, commercial and pure sodium ignite at 390-400 and potassium at 450-460°C. Ignition was observed 40-60 sec after the metal had passed into the experimental section. On changing the sodium and potassium sample sizes from 5 × 5 × 5 to 30 × 30 × 30 mm their ignition temperature remains within the same ranges.

The ignition temperature of sodium and potassium on heating in a protective argon medium and subsequently passing air or commercial oxygen over them is shown in Table 1.

The ignition temperature was determined by successive approximations, with a temperature interval of 5°C.

A second ignition of sodium in air after the initial combustion has been halted by blowing in argon takes place at 90-150°C. Thus the temperature of the second ignition in sodium is much lower than that of the first ignition.

We ourselves consider that the ignition temperature falls as a result of the formation of sodium dioxide.

On comparing the ignition temperatures of pure sodium (TU 1604-50) and commercial sodium (GOST 3273-63) purified by settling, the spread of ignition temperature for each type remains within the same range.

LITERATURE CITED

1. D. A. Frank-Kamenetskii, Diffusion and Heat Transfer in Chemical Kinetics [in Russian], Nauka, Moscow (1967).
2. B. I. Khaikin, V. N. Blozhenko, and A. G. Merzhanov, Fizika Goreniya i Vzryva, 6, No. 4, 474 (1970).
3. J. Perry, Handbook of Chemical Engineers [Russian translation], Khimiya, Leningrad (1969).

A NONITERATIVE METHOD FOR SOLVING THE ADJOINT EQUATIONS OF A CRITICAL REACTOR

B. P. Kochurov

UDC 621.039.51.134

Numerical optimization algorithms of the iterative type [1] require an appreciable expenditure of machine time for each step of the iteration to find the adjoint functions. Dozens of steps may be required depending on the number and type of constraints on the problem. When the greatest eigenvalue of the forward (and adjoint) equation is known we can abandon the uneconomical method of group iteration of sources and find the solution in one step forward and one back by using matrix factorization. At first glance it would seem that the degeneracy of the equation and the vanishing of the neutron flux vector at the edge of the reactor would prevent a backward step, but this difficulty is completely surmountable.

Let

$$\tilde{L}_\lambda \equiv \nabla\tilde{D}\nabla - \tilde{S} + \tilde{F}/\lambda$$

be the differential expression for a G-group diffusion problem, where L_λ (without a tilde) is the finite difference representation for a certain fixed partition of the reactor; the matrices D, S, and F determine respectively the diffusion, capture and scattering, and multiplication of neutrons; λ is the greatest eigenvalue; and the eigenfunction N_0 is the discrete G-dimensional flux vector of the problem

$$L_\lambda N_0 = 0;\ \varphi_0(N_0) = 0;\ N_{0,K} = 0. \tag{1}$$

Here the functional φ_0 determines the boundary condition at the left-hand boundary or at the center of the reactor, and the K-th partition point is located exactly at the edge of the reactor where the flux vanishes. For the given partition we introduce the scalar product and use it to define the problem adjoint to (1) (the + signs on S and F denote transposition).

$$L_\lambda^+ \equiv \nabla D\nabla - S^+ + F^+/\lambda;\ L_\lambda^+ N_0^+ = 0;\ \varphi_0(N_0^+) = 0;\ N_{0,K}^+ = 0. \tag{2}$$

The values of N_0, N_0^+, and λ can be found by an iterative method of matrix factorization, Eqs. (6)-(8) given below, where G_k depends on S or S^+, and B_k on $FN_0^{(m)}$ or $F^+N_0^{+(m)}$, each step of which corresponds to the inversion of the operators $P \equiv -\nabla D\nabla + S$, $P^+ \equiv -\nabla D\nabla + S^+$ with appropriate boundary conditions:

$$N_0^{(m+1)} = P^{-1}FN_0^{(m)},\ N_0^{+(m+1)} = (P^+)^{-1}F^+N_0^{+(m)}. \tag{3}$$

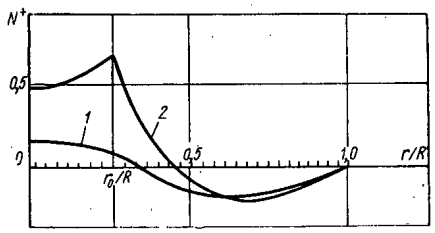

Fig. 1. Green's function (11) obtained by BARSUK program for two-group equation: 1) first group; 2) second group.

Here N_0 and N_0^+ are eigenfunctions of the operators $A \equiv P^{-1}F$ and $A^{+1} = (P^+)^{-1}F^+$, and λ is their greatest eigenvalue. It is clear that the adjoint of A is not identical with A^{+1}; the operator $A^+ = F^+(P^{-1}) = F^+(P^+)^{-1}$ and the adjoint of N_0 is the function $F^+N_0^+$. Therefore the definitions [2]

$$\lambda^{(m+1)} = \frac{\langle F^+N_0^{+(m)},\ N_0^{(m+1)}\rangle}{\langle F^+N_0^{+(m)},\ N_0^{(m)}\rangle};\ \lambda^{+(m+1)} = \frac{\langle F^+N_0^{+(m+1)},\ N_0^{(m+1)}\rangle}{\langle F^+N_0^{+(m)},\ N_0^{(m+1)}\rangle}, \tag{4}$$

guarantee that the error in λ is second order in comparison with the errors in N_0 and N_0^+, and ensure the rapid convergence of the sequences $\lambda^{(m)}$ and $\lambda^{+(m)}$ ($\lim \lambda^{(m)} = \lim \lambda^{+(m)}$ as $m \to \infty$).

We denote by I the result of solving problems (1) and (2) using (3) and (4). λ and N_0 are now known and it is required to

Translated from Atomnaya Énergiya, Vol. 35, No. 1, pp. 52-54, July, 1973. Original article submitted May 18, 1972.

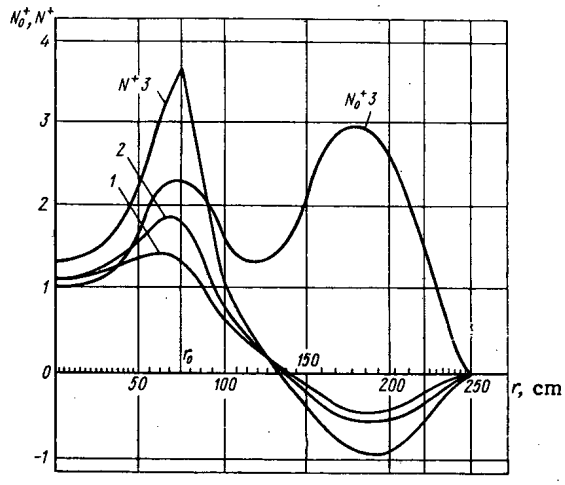

Fig. 2. Third (thermal) component of N_0^+ and the three-group Green's function in a five-zone cylindrical reactor obtained in a single step by the BARSUK program. 1) first group; 2) second group; 3) third group.

find N_0^+, the solution of the homogeneous adjoint problem with $Q^\perp = 0$, and N^+, the solution of the inhomogeneous adjoint problem:

$$L_\lambda^+ N^+ = -Q^\perp;\ \varphi_0(N^+) = 0;\ N_K^+ = 0. \tag{5}$$

We denote by II the solution for N_0^+ obtained by the method described below. N^+ can be found, to the same accuracy as N_0^+, if the vector function $Q^\perp$ is orthogonal to N_0, i.e., if

$$Q^\perp = Q - \frac{\langle N_0, Q\rangle}{\langle N_0, \Phi\rangle}\Phi,$$

the projection of Q in the direction of Φ on the hyperplane orthogonal to N_0. We write (5), in more detail, as

$$A_k N_{k-1}^+ + C_k N_{k+1}^+ - G_k^\lambda N_k^+ = -B_k;\ \ (k = 1, \ldots K-1), \tag{6}$$

where A_k and C_k depend on D, G_k^λ on D and S^+, F^+/λ and B_k on $Q^\perp$. Setting

$$N_k^+ = W_k + V_k N_{k+1}^+ \tag{7}$$

and taking account of (6) we obtain recurrence relations for the forward steps for the $G \times G$ matrices V_k and the G-vectors W_k:

$$\begin{aligned} V_k &= (G_k^\lambda - A_k V_{k-1})^{-1} C_k; \\ W_k &= V_k C_k^{-1}(A_k W_{k-1} + B_k), \end{aligned} \tag{8}$$

where the initial values V_0 and W_0 are determined by the form of φ_0 in (1). The solution for N_0^+, strictly positive for $k < K$, must be satisfied by Eqs. (7) and (8) (for $B_k = 0$, $W_k = 0$) and therefore the matrices V_k and V_k^{-1} must be nonsingular for $k < K-1$. However

$$N_{0,K}^+ = V_{K-1}^{-1} N_{0,K-1}^+ = 0.$$

This implies that the matrix $U \equiv V_{K-1}^{-1}$ is singular, but $F = N_{0,K-1}^+$, its eigenvector corresponding to a zero eigenvalue, is unique, since the positive solution N^+ is unique. From the solvability of Eq. (5) for $Q^\perp \neq 0$ it follows that the vector $Z \equiv UW_{K-1}$ is orthogonal to the vector $y: U^+Y = 0$. As a matter of fact, in order to ensure the solvability of (5) for $Q^\perp = 0$ and for $Q^\perp \neq 0$, it is necessary to take for F the eigenvector of the matrix $U_\varepsilon = U - \varepsilon$, where ε is the lowest eigenvalue of the matrix U:

$$U_\varepsilon F = 0, \tag{9}$$

and instead of Z to take the vector Z_1:

$$\begin{aligned} Z_1 &= Z - \frac{(Y_\varepsilon, Z)}{(Y_\varepsilon, Y_\varepsilon)} Y_\varepsilon;\ \ U_\varepsilon^+ Y_\varepsilon = 0; \\ U_\varepsilon N_{K-1}^+ &= Z_1. \end{aligned} \tag{10}$$

ε is different from zero because of the inaccuracy in λ, or, if λ is obtained with computer accuracy, because of the rounding off in the transformations (8). The accuracy of determining the factor $\langle N_0, Q\rangle / \langle N_0, \Phi\rangle$ in $Q^\perp$ in (5) depends on the accuracy of determining N_0. It can be shown, by taking into account that N^+ may not be unique, and assuming that the operators A and A^+ have discrete spectra, that the accuracy of N^+ is of the same order of magnitude as the accuracy of N_0. The transition $U \to U_\varepsilon$ and $Z \to Z_1$ denotes a certain redefinition of the operator L_λ^+ due to the inaccuracy in λ, and of the source $Q^\perp$ because of the inaccuracy in N_0.

Thus for known λ and N_0 the solutions for N_0^+ and N^+ can be found in one step by the following scheme; a forward step (8), the determination of ε and F in (9) and the vectors Z_1 and N_{K-1}^+ in (10). A backward step (7) beginning with the vector F for $W_k = 0$ and a backward step beginning with N_{K-1}^+ for W_k determined from (8) give N_0^+ and N^+ respectively.

On the basis of the above we wrote the BARSUK program in FORTRAN for a BÉSM-6 computer to calculate cylindrical or slab reactors with an arbitrary number of zones and an arbitrary number of groups

TABLE 1. Errors in λ, N_0^+, and N^+ as functions of the Number of Iterations of Method I

Error	Number of iterations, m			
	12	25	35	45
λ	$2\cdot10^{-5}$	$2\cdot10^{-7}$	$3\cdot10^{-10}$	0
$N^+_{0(I)}$	$3\cdot10^{-2}$	$2\cdot10^{-3}$	$3\cdot10^{-4}$	$5\cdot10^{-5}$
$N^+_{0(II)}$	$2\cdot10^{-3}$	$1\cdot10^{-4}$	$1\cdot10^{-5}$	0
N^+	$1\cdot10^{-2}$	$2\cdot10^{-3}$	$5\cdot10^{-4}$	0

$G \leq 4$-5. Using the BARSUK program we obtained the Green's function (Fig. 1) for the two-group equation

$$(\nabla^2 - S + F^+/\lambda)\, N^+ = -\begin{pmatrix}0\\1\end{pmatrix} \delta(r-r_0)/r_0 + \frac{N_0^{-2}\, \mathrm{rp}\,(r_0)}{\langle N_0,\ N_0\rangle} N_0,$$

having the following analytic form, to within the accuracy of N_0^+:

$$N^+ = \begin{cases} \varphi(r) + I_0(\bar{K}_0 - \bar{I}_0\check{K}/\check{I}_0)(1-\gamma_2/\gamma_1)^{-1}\begin{pmatrix}\gamma_2\\1\end{pmatrix}, & r < r_0; \\ \varphi(r) + (\bar{\mathcal{J}}_0 Y_0 - \bar{Y}_0\mathcal{J}_0)\frac{\pi}{2}(\gamma_1/\gamma_2 - 1)^{-1}\begin{pmatrix}\gamma_1\\1\end{pmatrix} \\ \quad + (K_0 - I_0\check{K}_0/\check{I}_0)\,\bar{I}_0(1-\gamma_2/\gamma_1)^{-1}\begin{pmatrix}\gamma_2\\1\end{pmatrix}, & r > r_0; \end{cases} \tag{11}$$

$$\varphi(r) = (1-\gamma_1/\gamma_2)^{-1}\left[r\mathcal{J}_1\bar{\mathcal{J}}_0/R_2^2\check{\mathcal{J}}_1^2\begin{pmatrix}\gamma_1\\1\end{pmatrix} + \frac{2(1+\gamma_1\gamma_2)}{s_{21}(\gamma_2+\gamma_2^{-1})}\mathcal{J}_0\begin{pmatrix}0\\1\end{pmatrix}\right],$$

where $\gamma_1 = -s_{21}(1+s_{11})^{-1}$; $\gamma_2 = (1+s_{11})s_{12}^{-1}$; $\beta^2 = 1 + s_{11} + s_{22}$; $\mathcal{J}_0(R) = 0$; the Bessel functions $\mathcal{J}_0$, $\mathcal{J}_1$, and Y_0 are functions of r, and I_0 and K_0 are functions of βr; a bar over a function indicates that $r = r_0$, and a tilde that $r = R$. In our case $r_0 = 0.633$

$$S = \begin{pmatrix}3 & 0\\ -4 & 1\end{pmatrix};\quad F = \begin{pmatrix}0 & 2\\ 0 & 0\end{pmatrix};\quad N_0 = \mathcal{J}_0\begin{pmatrix}1\\2\end{pmatrix};$$

$$N_0^+ = \mathcal{J}_0\begin{pmatrix}1\\1\end{pmatrix}.$$

In Fig. 2 N_0^+ and the Green's function obtained from a three-group calculation of a five-zone cylindrical reactor of intermediate size (4% leakage) are shown and in Table 1 the maximum errors in $N^+_{0(I)}$, $N^+_{0(II)}$, and N^+ relative to $N^+_{0(II)}$ and N^+ for m = 45 are presented as a function of the number of iterations m of method I. It is clear from Table 1 that the accuracy of N^+ is of the order of $N^+_{0(I)}$ and $N_{0(I)}$; the accuracy of $N^+_{0(II)}$ is higher than that of $N^+_{0(I)}$. This is because $N^+_{0(II)}$ is determined for a value of λ calculated with a greater accuracy than $N^+_{0(I)}$. Therefore calculations by method II may also be considered as a means of speeding up the convergence of the iterative solution I, and it is expedient to do this also with respect to N_0 so as to obtain greater accuracy in N^+.

LITERATURE CITED

1. V. V. Khromov et al., in: Physics of Nuclear Reactors [in Russian], No. 2, Atomizdat, Moscow (1970), p. 3.
2. L. N. Usachev, First Geneva Conference (1955). Reactor Engineering and Theory [in Russian], Izd. AN SSSR, Moscow (1955), p. 251.

PROTOTYPE TESTS OF GAMMA SPECTROMETER WITH SEMICONDUCTOR DETECTOR FOR BOREHOLE RADIOMETRY

G. A. Nedostup and F. N. Prokof'ev

UDC 539.1.55:550.83

At the present time, a great deal of attention is being directed toward the use of germanium semiconductor detectors (SCD) for solving a number of geological and geophysical problems and primarily for analysis of the elemental composition of rocks. However, SCD are not being used for measurements in boreholes as of the present writing. This is primarily related to the complexity of developing a cryogenic system that will keep an SCD at liquid-nitrogen temperature (78°K) in an enclosed volume of the detector for an extended period of time (6-8 h). In [1, 2] it was proposed to solve this problem by using ordinary Dewar vessels of liquid nitrogen evaporating into the cavity of a dry borehole or to the surface along a special hose line. Some brief data are given below on a prototype borehole γ spectrometer using an SCD for measurements in deep boreholes (up to 3 km and more) and on the first test results.

Workers at the All-Union Scientific-Research Institute of Nuclear Geophysics and Geochemistry have prepared a special cryogenic system in which the SCD is cooled by solid nitrogen obtained from the liquid phase by adiabatic freezing before the instrument is lowered into the borehole.

The cryogenic device (Fig. 1) consists of an integral cryogenic system and a removable chamber with a germanium SCD located in it. Such a design makes it possible to keep the chamber with the SCD in a standard ASD-15 container during transportation and storage.

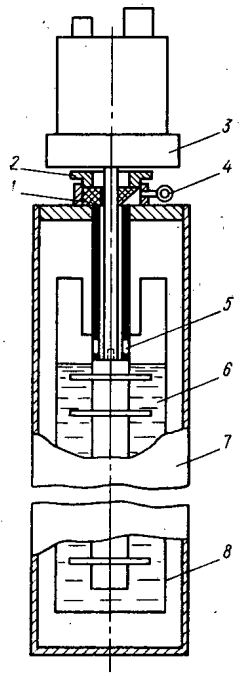

Fig. 1. Cryogenic device: 1) sealing gasket; 2) tightening nut; 3) removable chamber containing SCD; 4) valve for pumping out nitrogen vapor; 5) channel for nitrogen filling; 6) nitrogen (liquid or solid phase); 7) external cylindrical housing; 8) internal container.

Translated from Atomnaya Énergiya, Vol. 35, No. 1, pp. 54-55, July, 1973. Original article submitted May 18, 1972; revision submitted October 23, 1972.

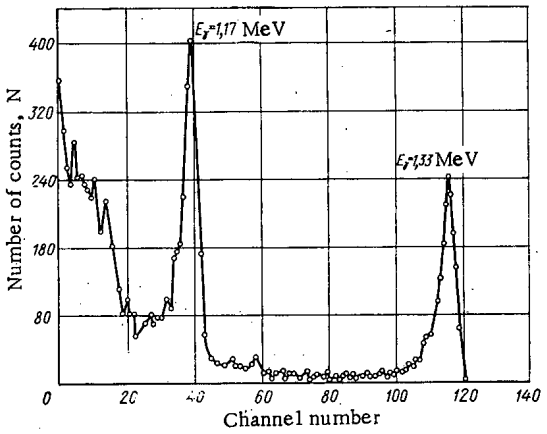

Fig. 2. Co^{60} spectrum taken with γ spectrometer in a borehole.

The integral cryogenic system consists of an external cylindrical housing and an internal container protected by vacuum insulation. For the installation of the chamber containing the SCD in the cryogenic system, the internal cavity, which is filled with nitrogen, is hermetically sealed by a sealing gasket and tightening nut. The nitrogen solidifies after its vapors are pumped out through a valve and channel.

The external diameter of the cryogenic system and detector is 85 mm and the length 1500 mm. As tests have shown, preparatory operations for adiabatic freezing of the nitrogen in the cryogenic system take 1.5-2 h and provide solidification of 3-4 liters of nitrogen, which makes it possible to carry on investigations for 5-7 h.

Preamplified signals from the SCD travel along a logging cable to the surface, where they are analyzed. With such a technique, the electronic circuit of the borehole device is considerably simplified and the recording of spectra is ensured with sufficient accuracy for evaluation experiments when the total count is $(2-3)\cdot 10^3$ sec^{-1} and a KTB-6 logging cable 2-3 km long is used. The intrinsic energy resolution of the borehole preamplifier was $(5.5 + 0.05C_{in})$ keV and the maximum signal amplitude at the circuit output was 30 V.

At the beginning of 1971, the prototype γ spectrometer using an SCD was tested in the experimental borehole of the Ramenskii branch of the All-Union Scientific-Research Institute of Geophysics. Operation of the SCD and the electronic circuit of the prototype was monitored by periodic recording of the spectrum from Co^{60} located in the borehole instrument near the SCD.

Spectra were recorded with an AI-128-2 analyzer after preliminary expansion. Multiple borehole measurements over a period of 5-7 h demonstrated high stability of prototype operation. Spectrometer resolution for the Co^{60} lines was 10-12 keV and was determined mainly by the resolution of existing SCD (Fig. 2).

In addition, the prototype developed was used for measurements in simulated rock strata for comparison of the instrumental spectra obtained from the prototype with spectra obtained in [3] for the same simulated strata. In these measurements, 3 km of KTB-6 cable was simulated by a special dummy cable with similar amplitude and frequency characteristics.

In the simulated strata, γ-ray spectra were obtained for uranium in equilibrium with decay products and for radiative capture in strata of water-bearing and oil-bearing sandstones. As in the borehole measurements, resolution of the equipment using SCD was 10-12 keV for the Co^{60} lines.

A comparison of the simulation measurements for radiative capture γ-ray spectra obtained with the borehole prototype and similar data [3] confirmed the high efficiency of SCD application for quantitative evaluation of the content of hydrogen, iron, silicon, calcium, and other rock-forming elements.

In conclusion, the authors express their gratitude to G. N. Flerov and Yu. S. Shimelevich for constant interest and valuable advice in the course of this work, and also thank staff members N. V. Popov, V. V. Miller, and E. M. Kadisov of the All-Union Scientific-Research Institute of Nuclear Geophysics and Geochemistry for practical help in the simulation measurements, and staff members V. G. Garkalns and E. E. Pakhomov of the All-Union Scientific-Research Institute of Radiation Instruments for participating in the construction of the borehole cryogenic system.

LITERATURE CITED

1. R. Dumesnil and C. Andrieux, Inds. Atom., 14, No. 11/12, 29 (1970).
2. J. Dewan, US Patent 3496360, Cl. 250-83.3 (Golt 1/16).
3. Yu. F. Baryshev et al., JINR Preprint 13-5199 [in Russian], Dubna (1970).

COLLISION DENSITY IN INTERMEDIATE RESONANCES

A. P. Platonov and A. A. Luk'yanov

UDC 621.039.51.12

The slowing down of neutrons in a two-component homogeneous medium near resonance energies is characterized by a strong dependence of the collision frequency $\Psi(u)$ on the character of the energy structure of the neutron cross sections. This appears particularly clearly near so-called intermediate resonances with widths close to the magnitude of the energy loss in the elastic scattering of a neutron by nuclei of a resonance component [1, 2].

Taking account of the energy structure of the collision density close to such resonances leads to an appreciable difference in the magnitudes of the resonance integrals in individual energy groups, and can be significant in the calculation of group-averaged characteristics in the resonance region [3].

The accuracy and practical possibilities of known approximate schemes for representing the collision density in resonances and effective resonance capture integrals (NR, NRIM, and IR approximations [4, 5]) were investigated for the energy range 160-230 eV by numerical solution of the equation of deceleration in a homogeneous medium of $U^{238}O_2$ and in an equivalent mixture of uranium and hydrogen nuclei having a total potential scattering cross section equal to that of the $U^{238}O_2$ medium. There are two adjacent intermediate U^{238} resonances in this energy interval with parameters $E_1 = 189.6$ eV, $\Gamma_1 = 168$ eV, $\Gamma_{1\gamma} = 23$ eV; $E_2 = 206.6$ eV, $\Gamma_2 = 80.6$ eV, $\Gamma_{2\gamma} = 24$ eV, $\sigma_p = 11$ b [6, 7].

The slowing down of neutrons in a multicomponent homogeneous medium is described by the equation

$$\Psi(u)=\sum_{j=1}^{2}\int_{u-r_i}^{u}\Psi(u')\,h_j(u')\,f_j(u-u')\,du'+\delta(u),$$

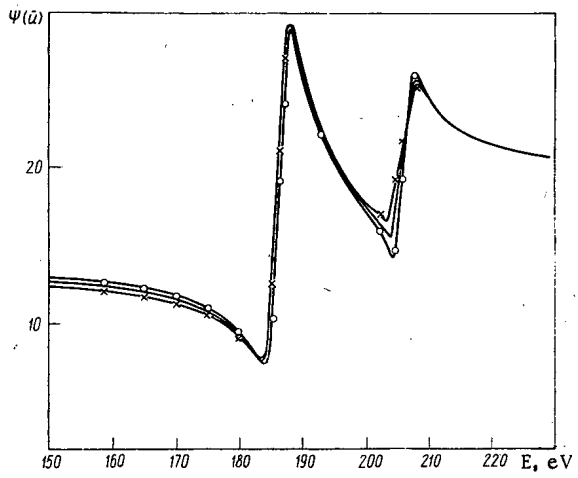

Fig. 1. Neutron collision density $\Psi(u)$ in a homogeneous mixture of U^{238} and O_2 for the energy range 150-230 eV. Temperature, °K; ○) 300; ——) 900; ×) 2100.

where $f_j(u) = \alpha_j e^{-u}$ is the neutron energy distribution function for elastic scattering from nuclei of the j-th component; $h_j(u)$ is the relative probability of neutron scattering; $\alpha_j = (A_j + 1)^2/4A_j$; $r_j = 2\ln(A_j + 1)/(A_j - 1)$; A_j is the atomic number of the j-th nucleus.

The equation is solved by the numerical integration of a first-order differential equation equivalent to the integral equation [8], and the relative scattering probabilities $h_j(u)$ are calculated in accord with the URAN program [7], i.e., by the one-level Breit–Wigner formulas taking account of the interference of resonance and potential scattering and the temperature dependence of the resonance shapes.

Calculation shows that the collision density in this region is rather strongly energy dependent and there appears a structure that correlates with the structure of the scattering cross section (Fig. 1).

Accurate values of the resonance integrals were obtained for the calculated values of $\Psi(u)$ and compared with the NR, NRIM, and IR approximations [4, 5, 9] (Table 1).

Translated from Atomnaya Énergiya, Vol. 35, No. 1, pp. 56-57, July, 1973. Original article submitted August 22, 1972.

TABLE 1. Resonance Capture Integrals for U^{238} Levels (Dilution cross section 7.6 b)

T, °K	Medium	Method of calculation							
		accurate	IR	NRIM	NR	accurate	IR	NRIM	NR
		$E_0 = 189{,}6$ eV				$E_0 = 208{,}6$ eV			
300	UH	0,1797	0,1561	0,1712	0,2835	0,1153	0,1100	0,1132	0,1019
	UO_2	0,1689				0,1127			
900	UH	0,1803	0,1584	0,1808	0,2312	0,1229	0,1175	0,1181	0,1041
	UO_2	1,1693				0,1199			
2100	UH	0,1827	0,1653	0,1998	0,1840	0,1400	0,1347	0,1421	0,1158
	UO_2	0,1713				0,1363			

TABLE 2. Total Resonance Capture Integrals for Two Levels of U^{238} with Energies of 189.6 and 208.6 eV (Dilution cross section 7.6 b)

T, °K	Medium	Method of calculation				
		accurate	accurate	IR	NRIM	NR
		taking account of overlapping of levels	in the one-level approximation			
300	UH	0,2932	0,2950	0,2661	0,2844	0,3854
	UO_2	0,2657	0,2816			
900	UH	0,2966	0,3032	0,2759	0,2989	0,3353
	UO_2	0,2728	0,2892			
2100	UH	0,3172	0,3227	0,3000	0,3414	0,2998
	UO_2	0,2899	0,3076			

The values of the resonance integrals calculated for individual levels with various moderators are appreciably different from one another for all temperatures. The approximate results differ from the values calculated with the accurate collision density by from 5 to 30%, and in the NR approximation for the 189.6 eV level the temperature dependence of the resonance integral is different. The NRIM approximations are closest to the accurate values of the resonance integrals, but even here the average spread is as much as 10%.

It is interesting to note that the divergence of the values of the resonance integrals both for various moderators and calculated by the approximate formulas is larger for the broader resonance ($E_1 = 189.6$ eV). Table 2 shows the values of the total resonance integrals for two levels calculated accurately for different moderators, and also the total resonance integrals determined for each level both with the accurate and with the approximate value of the collision density. The differences in the results can be accounted for by the interference of the resonances, leading to a change in the energy dependence of the collision density between resonances.

LITERATURE CITED

1. G. I. Marchuk and F. F. Mikhailus, Atomnaya Énergiya, 4, No. 6, 520 (1958).
2. A. A. Luk'yanov and M. Yu. Yusef, Atomnaya Énergiya, 26, No. 6, 540 (1969).
3. L. P. Abagyan et al., Paper No. 357 [in Russian], Third Geneva Conference (1964).
4. L. Dresner, Resonance Absorption in Nuclear Reactors, Pergamon, New York (1960).
5. R. Goldstein, Nucl. Sci. and Engng., 20, 384 (1965).
6. Neutron Cross Sections, BNL-325, 2nd Edition, Vol. 3 (1965).
7. L. P. Abagyan, M. N. Nikolaev, and L. V. Petrova, Byul. ITsYaD, No. 4, Atomizdat (1968), p. 392.
8. A. P. Platonov, Preprint NIIAR, P-90 [in Russian], Melekess (1970).
9. L. P. Abagyan et al., Supplement to ITsYaD Bulletin [in Russian], Atomizdat (1968).

INVESTIGATION OF THE SYSTEM $UO_3 - UO_2(NO_3)_2 - H_2O$

V. S. Efimova and B. V. Gromov

UDC 576.791.6-31+546.791.6'175-38+546.212

When uranium is precipitated by ammonia from solutions of uranyl nitrite at a molar ratio of uranium to ammonia of 1:2, according to the reaction $UO_2^{2+} + 2NH_4OH \rightarrow UO_2(OH)_2 + 2NH_4^+$, the uranyl hydroxide produced is not pure. The precipitate, as a rule, contains a certain (sometimes substantial) amount of NO_3^- and NH_4^+, which is explained by the formation in solution of more stable ions $[(UO_2)_2(OH)_5]^-$ and $[UO_2(OH)_3(H_2O)_n]^-$ together with the dihydroxouranyl ions [1].

An interrelationship between the complexes in solution and the composition of the precipitate was indicated in [2]. This question was discussed in greater detail in [3], which is devoted to a study of the process of hydrolysis of UO_2^{2+} in uranyl chloride solution.

To determine the conditions of formation of uranyl hydroxide, in this work we investigated the phase equilibrium in the system $UO_3 - UO_2(NO_3)_2 - H_2O$. The production of UO_3, $UO_2(NO_3)_2$ and the solutions was outlined in [4].

In an investigation of the phase diagram of the $UO_3 - UO_2(NO_3)_2 - H_2O$ system, solutions of uranyl nitrate with uranium trioxide, placed in hermetic vessels, were exposed at room temperature for 1.5 years (to reach equilibrium, the UO_3 had to be in contact with the solution of $UO_2(NO_3)_2$ for eight months). The mixtures were shaken to mix them. The composition of the solid phase was established according to the Schreinemakers method. The uranium content was determined by a gravimetric method, while the nitrate ion was determined by back titration of iron (II) with potassium bichromate.

The precipitates were washed with acetone and dried over sulfuric acid to constant weight; they were subjected to x-ray diffraction study on a URS-50IM diffractometer, using filtered copper radiation.

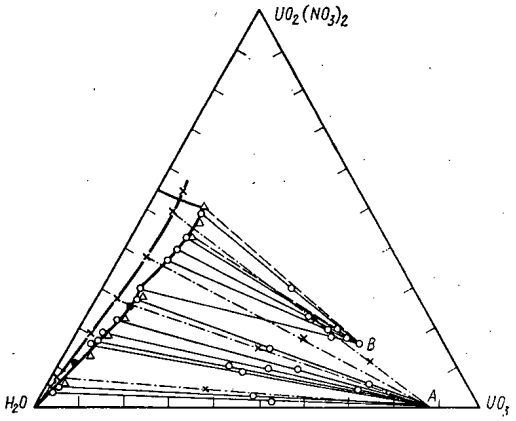

Fig. 1

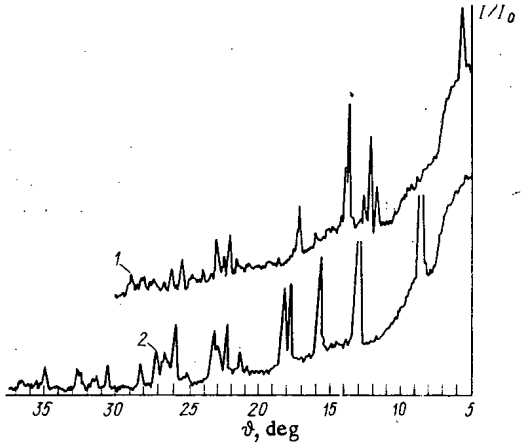

Fig. 2

Fig. 1. Phase diagram of the system $UO_3 - UO_2(NO_3)_2 - H_2O$: ○, ×) results obtained at 20 and 95°C, respectively: ●) data of [5]; Δ) data of [6].

Fig. 2. Diffraction patterns of phase A and the products obtained by washing phase B with acetone (curves 1 and 2, respectively).

Translated from Atomnaya Énergiya, Vol. 35, No. 1, pp. 57-59, July, 1973. Original article submitted February 3, 1973.

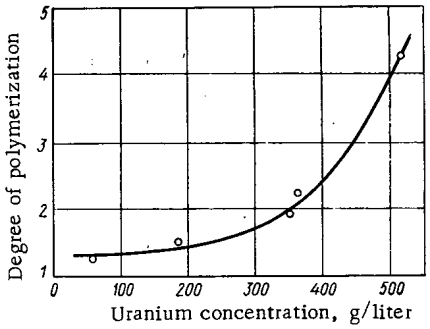

Fig. 3. Dependence of the degree of polymerization of the uranyl ion in equilibrium solutions of the system $UO_2(NO_3)_2-UO_3-H_2O$ on the uranium concentration in solution.

The results of experiments on the determination of solubility in the system $UO_3-UO_2(NO_3)_2-H_2O$ are shown in Fig. 1. In the region studied at room temperature the existence of two solid phases, A and B, was detected. The composition of phase A corresponds to the formula $UO_3 \cdot 2H_2O$ or $UO_2(OH)_2H_2O$. The phase B is the basic nitrate of uranyl, containing 64.20 ± 2.70 mass % UO_3 and 16.6 ± 1.20 mass % $UO_2(NO_3)_2$, which corresponds to the formula $6.1UO_3 \cdot 0.5N_2O_5 \cdot 25H_2O$.

The values of the solubility of uranium trioxide obtained agree with the data of [5, 6]. However, the composition of the solid phase in the region of interest to us was not studied in [5]. In [6] the formation of the phase A and the metastable state of uranyl nitrate in a narrow region of the system was indicated (see the dashed curves in Fig. 1). The data obtained are evidence that the phase B exists in a broader region and is not broken down during the entire time of exposure of the solutions of $UO_2(NO_3)_2$ with UO_3, i.e., for a period of 1.5 years. In contrast to phase A, it is difficult to isolate phase B, since the NO_3^- ion is almost entirely washed out of the solid substance, and $UO_3 \cdot H_2O$ is obtained. The diffraction patterns of phase A and the products obtained by washing phase B with acetone are cited in Fig. 2.

As can be seen from the diagram of the system $UO_3-UO_2(NO_3)_2-H_2O$ (see Fig. 1), a substantial amount of UO_3 dissolved in uranyl nitrate solution. Data on the dialysis of equilibrium solutions at 20°C (Fig. 3) show that primarily dimers exist at equilibrium with the phase A, and tetramers at equilibrium with the phase B.

Thus, the precipitation of uranyl hydroxide is accompanied by the formation of dimer complexes, while the subsequent association of uranyl ions probably leads to trapping of the NO_3^- ion in the solid phase.

In the system under consideration, $UO_3-UO_2(NO_3)_2-H_2O$, thermostatically controlled at 95°C for 9-10 h, the existence only of the solid phase A was determined (see Fig. 1). With increasing temperature, there is a complete breakdown of phase B as a result of the intensification of the process of complex formation of the uranyl ion with the nitrate ion in solution [7].

As a result of decomposition of the phase B into $UO_3 \cdot 2H_2O$ in the solid phase and into nitrate complexes of uranyl in the liquid phase (the ratio NO_3^-/UO_2^{2+}, expressed in gram ions, increases from 1.40-1.44 at 20°C to 1.65-1.70 at 95°C), the solubility isotherm under these conditions is shifted in the direction of an increase in the uranyl nitrate concentration in solution.

LITERATURE CITED

1. Chernyaev (editor), Complex Compounds of Uranium [in Russian], Nauka, Moscow (1964).
2. V. Baran and M. Tympl, J. Inorg. and Nucl. Chem., 28, 89 (1966).
3. M. Aberg, Acta Chem. Scand., 24, 2901 (1970).
4. B. V. Gromov and V. S. Efimova, Tr. Mosk. Khim.-Tekhnol. Inst. im. D. I. Mendeleeva, 73, 99 (1973).
5. J. Lacher, Inorg. Chem., 1, 4 (1962).
6. E. Cordfunke, J. Inorg. and Nucl. Chem., 34, 531 (1972).
7. B. G. Pozharskii, Radiofizika, 4, No. 5, 561 (1972).

INVESTIGATION OF THE POSSIBILITY FOR THE APPLICATION OF THE KEEPIN METHOD IN ORDER TO DISTINGUISH FISSIONABLE ELEMENTS IN MIXTURES, UTILIZING A BEAM OF GAMMA-QUANTA

M. M. Dorosh, N. I. Kovalenko, A. M. Parlag, and V. A. Shkoda-Ul'yanov

UDC 539.173.3

Possibilities of utilizing photonuclear reactions in order to analyze the contents of fissionable elements without damaging the specimens analyzed were studied in [1-3]. In particular, it is mentioned in [1] that photonuclear reactions have considerable advantages over other reactions, e.g., those induced by 14 MeV neutrons. Possibilities utilizing methods based on the detection of photofission and delayed neutrons were studied in [2]. The measurements were conducted in the 5.5-9.5 MeV energy range. It was shown that it is possible to discard such conditions whenever it is possible to distinguish U^{235} and U^{238}, and U^{235} and Pu^{239}. However, an effective discriminatory relation for U^{235} and U^{238} is obtained only during the irradiation of the specimen under investigation by 14 MeV neutrons and measurement of the retarded neutron yields in different time intervals.

G. Keepin [4] proposes an original method for distinguishing fissionable elements and their isotopes on the basis of differences in the kinetics of the retarded neutrons. Equations are shown for the calculation of discriminatory factors and the determination of the relative content of isotopes in a mixture, after measurement of the retarded neutron yields in different time intervals.

In order to ascertain the possibility of applying the Keepin method, the $R_{f\pm}$ and $S_{f^+/\Delta}$ curves were calculated for several elements according to the equations:

$$R_{f+}=\Sigma_{a_i}e^{-\lambda_i f};$$

$$R_{f-}=\Sigma a_i(1-e^{-\lambda_i f});$$

$$S_{f+/\Delta}=\Delta^{-1}\Sigma(a_i/\lambda_i)e^{-\lambda_i f},$$

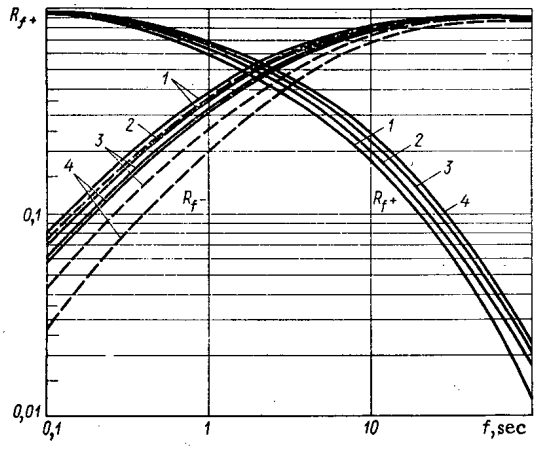

Fig. 1. The R_{f+} and R_{f-} curves for photofission with $E_{\gamma max}$ = 15 MeV (solid curves) and fission by 14 MeV neutrons (dashed curves): 1) U^{238}; 2) Th^{232}; 3) U^{235}; 4) Pu^{239}.

where Δ is a time interval shorter than τ_i (τ_i is the lifetime of the i-th group); a_i is the relative intensity of the i-th group; λ_i is the decay constant of the i-th group; f is an instant of time the duration of which runs from zero to infinity (in practice, up to a time reasonable for the detection of retarded neutrons).

The curves are calculated for the photofission of Th^{232}, U^{235}, U^{238}, and Pu^{239} by γ quanta with a maximum energy of 15 MeV for given a_i and λ_i [5], and also for the photofission of U^{235} and U^{238} by γ quanta with energies of 8 and 10 MeV for given a_i [2]. All of the curves are calculated over the time interval f in the limits 0.02-300 sec.

The discriminatory relations (relations of the same parameter for different isotopes characterizing the

Translated from Atomnaya Énergiya, Vol. 35, No. 1, pp. 59-61, July, 1973. Original article submitted November 27, 1972.

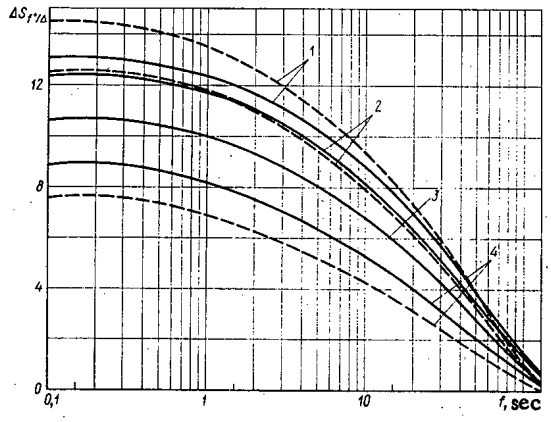

Fig. 2

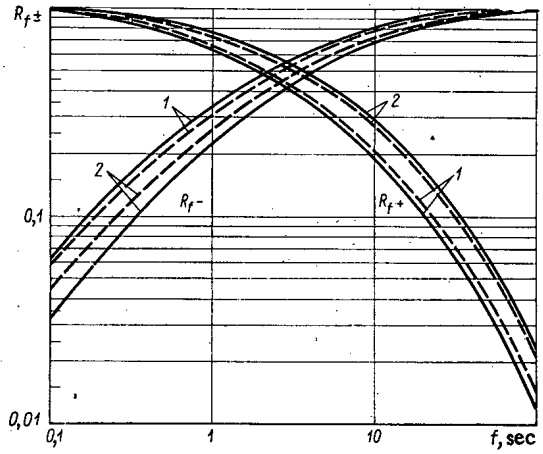

Fig. 3

Fig. 2. The $S_{f+/\Delta}$ curves for photofission with $E_{\gamma max}$ = 15 MeV (solid curves) and fission by 14 MeV neutrons (dashed curves): 1) Pu^{239}; 2) U^{235}; 3) Th^{232}; 4) U^{238}.

Fig. 3. The R_{f+} and R_{f-} curves for photofission with $E_{\gamma max}$ = 8 MeV (dashed curves) and 10 MeV (solid curves): 1) U^{238}; 2) U^{235}.

TABLE 1. Discriminatory Relations for Pairs of U^{235} and U^{238} during Photofission and Neutron Fission

f, sec	$S_{f+/\Delta}$				R_{f+}				R_{f-}			
	$E\gamma$ 8 MeV	$E\gamma$ 10 MeV	$E\gamma$ 15 MeV	En 14 MeV	$E\gamma$ 8 MeV	$E\gamma$ 10 MeV	$E\gamma$ 15 MeV	En 14 MeV	$E\gamma$ 8 MeV	$E\gamma$ 10 MeV	$E\gamma$ 15 MeV	En 14 MeV
0,1	1,44	1,58	1,39	1,68	1,01	1,03	1,02	1,04	1,27	1,88	1,33	1,75
1	1,47	1,62	1,42	1,73	1,11	1,17	1,10	1,21	1,30	1,49	1,19	1,49
10	1,56	1,76	1,56	1,90	1,42	1,54	1,26	1,64	1,04	1,15	1,06	1,14
100	1,76	2,19	2,08	2,18*	1,57	1,92	1,75	1,88*	1,01	1,01	1,11	1,01

*For $f = 50$ sec.

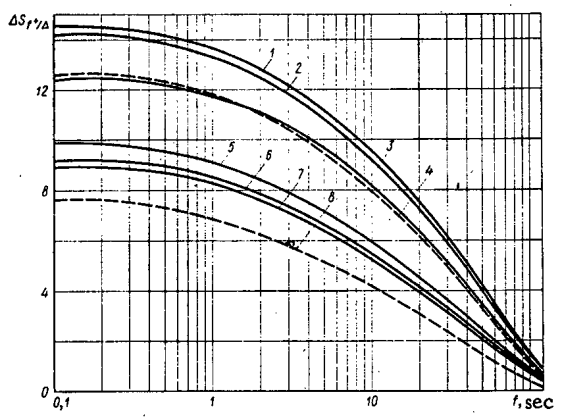

Fig. 4. The $\Delta S_{f+/\Delta}$ curves for the fission of U^{235} and U^{238}: 1) U^{235}, $E_{\gamma max}$ = 10 MeV [2]; 2) U^{235}, $E_{\gamma max}$ = 8 MeV [2]; 3) U^{235}, $E_{\gamma max}$ = 15 MeV [5]; 4) U^{235}, E_n = 14 MeV [4]; 5) U^{238}, $E_{\gamma max}$ = 8 MeV [2]; 6) U^{238}, $E_{\gamma max}$ = 10 MeV [2]; 7) U^{238}, $E_{\gamma max}$ = 15 MeV [5]; 8) U^{238}, E_n = 14 MeV [4].

separability of the isotopes) are obtained for different pairs from the data in [2, 5].

The corresponding $R_{f\pm}$ and $S_{f+/\Delta}$ curves, calculated from the data in [5], and, for comparison, the R_{f-} and $S_{f+/\Delta}$ Keepin curves are shown in Figs. 1 and 2. The curves for the photofission of two uranium isotopes by γ-quanta with maximum energies of 8 and 10 MeV, calculated from the data in [2], are shown in Fig. 3. The $S_{f+/\Delta}$ curves for the photofission of U^{235} and U^{238} with maximum energies of 8, 10, and 15 MeV and fission by 14 MeV neutrons are shown in Fig. 4. The discriminatory relations for U^{235} and U^{238}, obtained from the data of various authors, are presented in Table 1.

As is seen from Figs. 1 and 2, the $R_{f\pm}$ and $S_{f+/\Delta}$ curves, calculated from the data in [5], are bunched significantly closer than the Keepin curves. The curves calculated from the data in [2] are less densely bunched (see Fig. 4); at the same time, for U^{235} and U^{238}, they are separated with the transition in energy from 8 to 10 MeV (see Figs. 3 and 4). According to this, the discriminatory relations which were obtained for photofission are less accurate than those of Keepin for neutron fission. However, the discriminatory relations for U^{235} and U^{238} during photofission at a maximum

energy of 10 MeV are close to the discriminatory relations obtained by Keepin; while for the parameter R_{f-}, they even surpass the data associated with fission by 14 MeV neutrons.

The discriminatory relations for all three parameters associated with photofission by 10 MeV γ quanta are extremely encouraging in the sense of the application of the Keepin method for the analysis of fissionable elements.

However, owing to the large errors in the determination of a_i, λ_i, and correspondingly the $R_{f\pm}$ and $S_{f+/\Delta}$ associated with photofission, it is impossible to give a definitive conclusion concerning the behavior of these parameters with the transition from neutron to photofission and their dependence on the energy of the γ quanta. The formulation of an experiment on the direct measurement of the $R_{f\pm}$ and $S_{f+/\Delta}$ curves is probably the next step in the solution of this problem.

LITERATURE CITED

1. J. Beyster, The Use of Photonuclear Reaction Processes for Nondestructive Nuclear Material Safeguards Applications, WASH-1076 (1967), p. 138.
2. T. Gozani, Prompt and Delayed Neutron Experiments, WASH-1149 (UC-15) (1970), p. 76.
3. T. Gozani et al., New Developments in Nuclear Material Assay Using Photonuclear Reactions, IAEA-133/45 (1970), p. 143.
4. G. Keepin, Nondestructive Detection, Identification, and Analysis of Fissionable Materials, WASH-1076 (1967), p. 150.
5. O. P. Nikotin et al., At. Énerg., 20, No. 3, 268 (1966).

YIELDS OF Ba^{133m} AND Ba^{133} AND ISOMERIC RATIOS FOR $Cs^{133}(p, n)Ba^{133m,g}$ AND $Cs^{133}(d, 2n)Ba^{133m,g}$

P. P. Dmitriev, G. A. Molin, and M. V. Panarin

UDC 539.172.12

The isotopes Ba^{133m}($T_{1/2}$ = 38.9 h) and Ba^{133}($T_{1/2}$ = 7.2 yr) are widely used in pure and applied research. The most effective method for producing Ba^{133m} and Ba^{133} is irradiation of cesium by deuterons and protons.

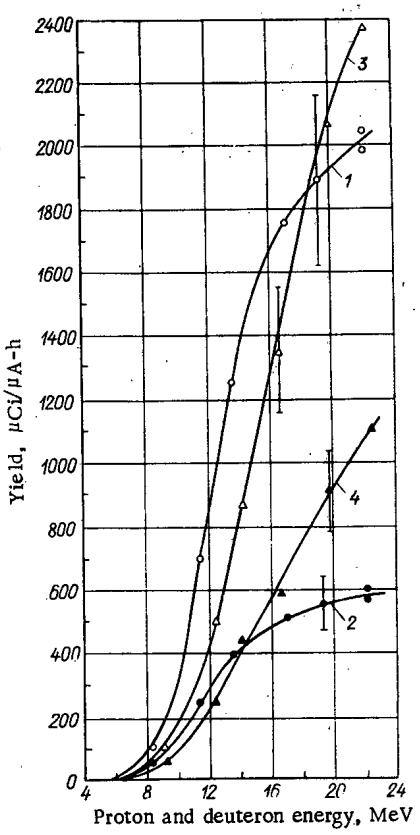

Fig. 1

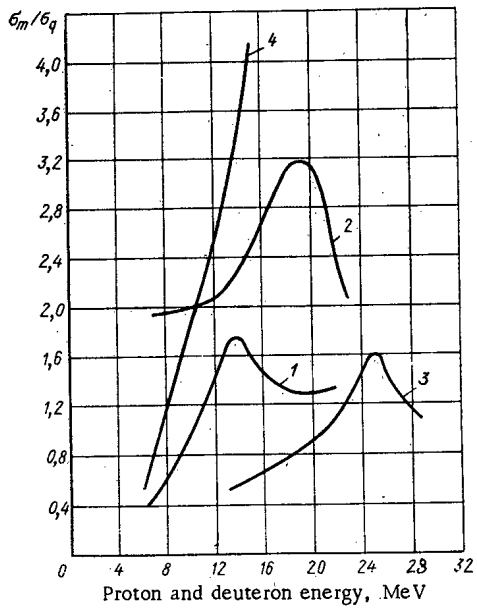

Fig. 2

Fig. 1. Dependence of Ba^{133m} and Ba^{133} yields on particle energy for irradiation of thick cesium targets by protons and deuterons: 1) $Cs(p, n)Ba^{133m}$ (×4); 2) $Cs(p, n)Ba^{133}$ (×1000); 3) $Cs(d, 2n)Ba^{133m}$; 4) $Cs^{133}(d, 2n)Ba^{133}$ (×500).

Fig. 2. Isomeric ratios σ_m/σ_g in nuclear reactions: 1) $Cs^{133}(p, n)Ba^{133m,g}$ (this work); 2) $Cs^{133}(d, 2n)Ba^{133m,g}$ (this work); 3) $Cs^{133}(d, 2n)Ba^{133m,g}$ [5]; 4) $Cs^{133}(d, 2n)Ba^{133m,g}$ [4].

Translated from Atomnaya Énergiya, Vol. 35, No. 1, pp. 61-62, July, 1973. Original article submitted February 17, 1973.

In this work, we measured the dependence of Ba^{133m} and Ba^{133} yields on the energy of the bombarding particles for irradiation of thick cesium targets by protons and deuterons. The method for measuring the Ba^{133m} and Ba^{133} yields was similar to that described previously [1]. Cesium is an alkali metal and therefore its compounds CsCl and $CsNO_3$ were irradiated. The coefficients for conversion from the values of the Ba^{133m} and Ba^{133} yields for CsCl and $CsNO_3$ to the values of the yield for pure cesium were calculated by the method given in [2] and were 1.40 for CsCl and 1.86 for $CsNO_3$. In measurements of Ba^{133m} and Ba^{133} activity with a γ spectrometer, the following values were used for the quantum yields of the γ lines [3]: Ba^{133m} has a γ line at 276 keV with a yield of 0.17 quanta/decay; Ba^{133} has γ lines at 356 and 382 keV with a total yield of 0.77 quanta/decay. The Ba^{133} activity was measured a month (or more) after irradiation using radiochemical separation of Ba^{133} from the irradiated samples. Measured values of Ba^{133m} and Ba^{133} yields are shown in Fig. 1; the systematic error is ±15%.

Data on the yields of Ba^{133m} and Ba^{133} is lacking in the literature. Only the excitation functions for the reactions Cs^{133}(d, 2n)Ba^{133m} and Cs^{133}(d, 2n)Ba^{133m+g} have been measured up to E_d = 15 MeV [4]. Numerical integration of these excitation functions carried out in this work gave the following yield values for E_d = 15 MeV: Ba^{133m}, 980 μCi/μA-h; Ba^{133}, 0.85 μCi/μA-h, which agree with the data in Fig. 1 within the limits of experimental error.

The isomeric ratio σ_m/σ_g for the same reactions has been measured [5] in the deuteron energy range 13.5-28.5 MeV. For comparison, the ratio σ_m/σ_g was calculated from the excitation functions in [4]. Both isomeric ratios are shown in Fig. 2 (curves 3, 4) and, as is apparent, they are greatly different. Since the production of a number of isomers (for example, Sc^{44m}, Zn^{69m}, Tc^{95m}, In^{114m}, Sn^{117m}, Sn^{119m}, Te^{121m}, Te^{123m}, Ba^{135m}, and others) is of great practical interest, it is desirable to know isomeric ratios in nuclear reactions for as large a number of isomers as possible. Because of this, an attempt was made to evaluate the ratio σ_m/σ_g by using the Ba^{133m} and Ba^{133} yield curves measured in the present work. By differentiation of the Ba^{133m} yield curve, the curve $\sigma_m(E_a)$ is obtained, and by differentiation of the Ba^{133} yield curve, the curve $\sigma_T(E_a) = \sigma_m(E_a) + \sigma_g(E_a)$ (since the isomeric state Ba^{133m} decays completely into the ground state of Ba^{133}). The curve $\sigma_g(E_a)$ is found by subtraction ($\sigma_g = \sigma_T - \sigma_m$).

The σ_m/σ_g ratios for the (p, n) and (d, 2n) reactions in Cs^{133} obtained as the result of these calculations are shown in Fig. 2 (curves 1, 2). We feel that with an accuracy of 20-30% they represent the values of the isomeric ratios and the nature of the variation of the σ_m/σ_g ratios with particle energy.

The authors thank Z. P. Dmitrieva and G. N. Grinenko for help with the work and Yu. G. Sevast'yanov and V. G. Vinogradova for the radiochemical separation of Ba^{133}.

LITERATURE CITED

1. P. P. Dmitriev et al., At. Énerg., 32, No. 5, 426 (1972).
2. G. Friedlander et al., Nuclear Chemistry and Radiochemistry, 2nd ed., Wiley, New York (1964).
3. C. Lederer et al., Tables of Isotopes, J. Wiley and Sons, New York (1967).
4. F. Perlman and R. Wolke, Nucl. Phys., 86, 429 (1966).
5. A. Macoroa et al., J. Inorg. and Nucl. Chem., 28, 5 (1966).

THE EFFECT OF RESONANCE SCATTERING ON THE DISTRIBUTION OF NEUTRONS IN ROCKS

D. A. Kozhevnikov

UDC 550.83

In [1] the author suggested that the resonance structure of the cross sections for the scattering of neutrons by nuclei of rock-forming elements in rocks might explain the nonmonotonic dependence of the reading of a moderated neutron detector located far from a fast neutron source on the hydrogen content. This idea, which was developed in a number of seminars on nuclear geophysics, encountered objections from many specialists.

When the experimental data of various authors were reduced to comparable conditions a nonmonotonic dependence was found [1], but, because of the various sizes of the models, and the edge effects which appear at large distances, this conclusion required special verification.

Analysis based on [2], experimental studies performed on models of uniform slabs of sandstone and limestone at the I. M. Gubkin Moscow Institute of the Petrochemical and Gas Industry, and Monte Carlo calculations made at the Institute of Applied Mineralogy of the Academy of Sciences of the USSR showed that the resonance structure of the scattering cross sections affects the character of the dependence of the neutron readings on the hydrogen content m for $m < 20\%$, but cannot cause its nonmonotonic nature.

At the same time it was shown that, for rocks studied by stationary neutron methods (neutron–neutron method with thermal neutrons, and neutron–gamma method) under borehole conditions, the readings vary nonmonotonically with the hydrogen content of the rock. However this has a different physical cause – the change of mineralization of stratified liquid in a neighboring zone in the transition from nonporous impermeable strata to permeable as a consequence of the demineralization of the latter by the filtrate of the drilling mud [3]. This phenomenon was used to separate water-bearing from oil-bearing strata-collectors in sections of boreholes [4].

Thus it can be concluded from the studies performed that the effect of the resonance structure of the cross sections for the scattering of neutrons by nuclei of rockforming elements is of no practical importance in the quantitative interpretation of the results of borehole measurements.

LITERATURE CITED

1. D. A. Kozhevnikov, in: Nuclear Geophysics. Reports from All-Union Conference: Twenty Years of the Production and Use of Isotopes in the National Economy of the USSR, Minsk, 1968 [in Russian], Atomizdat, Moscow (1972).
2. D. A. Kozhevnikov and V. S. Khavkin, Atomnaya Énergiya, 27, No. 2, 142, 143 (1969).
3. D. A. Kozhevnikov, N. N. Mar'enko, and V. I. Markhasin, Neftegazovaya Geologiya i Geofizika, No. 10, 30 (1971).
4. Ya. S. Vitvitskii et al., Neftegazovaya Geologiya i Geofizika, No. 9, 43 (1972).

Translated from Atomnaya Énergiya, Vol. 35, No. 1, pp. 62-63, July, 1973. Original article submitted December 28, 1972.

CHRONICLE OF THE COUNCIL OF MUTUAL ECONOMIC AID

DIARY OF COOPERATION

A Symposium of Specialists of Member Nations of the Council of Mutual Economic Aid (CMEA) on Problems of Radiation Sterilization of Materials and Medical Articles

The symposium, held in Baku on November 13-14, 1972, was attended by specialists from Bulgaria, Hungary, East Germany, Poland, Rumania, USSR, and Czechoslovakia.

The results of sanitary–chemical investigations of a number of materials (PVC, polymethyl methacrylate, dacryl-4B, divinylstyrene thermoelastic plastics DST-30, etc.) and medical articles (blood transfusion systems, syringes) were considered at the sessions of the radiation chemistry section; data on diffusion and mass transfer in polymer–ambient environment systems, which determine the sanitary–chemical properties of polymeric materials and articles made of them, were discussed. The theoretical basis of the procedures and the setting up of sanitary–chemical experiments were discussed. Several analytical methods of determining small concentrations of toxic compounds in liquids were examined, together with the results of investigations of radioscopy and relaxation spectroscopy of aging processes of irradiated polymeric materials.

Methods of studying posteffects in polymeric systems were also considered, as well as experimental data on the change of physical and mechanical properties of irradiated materials (PVC, polymethyl methacrylate, dacryl-4B, polyethylene, etc.) and medical articles (blood transfusion systems). The methods of sanitary–chemical and physical and mechanical tests of irradiated materials and articles developed by specialists of the USSR were discussed and in the main approved.

Eighteen reports on the radiosensitivity of contaminating microorganisms, the initial contamination of medical products subject to radiation sterilization, the scale of the dependence of the irradiation dose on initial contamination and control of the sterility of irradiated articles, and ways of reducing the sterilizing dose of irradiation were heard and discussed at the session of the biomedical section. In addition, reports devoted to the testing of plastics and plastic articles for pyrogenicity and toxicity were presented.

In the majority of reports attention was given to cardinal problems of the radiation sterilization of disposable medical articles. Special attention was focused on the radioresistance of contaminating microorganisms and its significance when selecting an effective sterilizing dose of irradiation. Experimental data on the development of methods of determining the radioresistance of microorganisms isolated from articles and in production were presented. In view of the importance of the problem discussed, all specialists expressed the opinion that it was expedient to create a microbiological reference laboratory with a collection of radioresistant strains of microorganisms.

The Polish specialists proposed a method of establishing the sterilizing dose by studying the radiosensitivity of microflora contaminating materials, articles, and production rooms of a given plant (index D_{10}), and also methods of evaluating the initial contamination of articles and the value of the safety coefficient, which is set by health agencies. This method was evaluated favorably by specialists of the member nations of the CMEA.

The reports of representatives of East Germany and the USSR stressed the importance of providing suitable sanitary and hygienic conditions in the production of medical articles. The existence of a relation between the magnitude of the initial contamination of articles and the sanitary and hygienic conditions in

Translated from Atomnaya Énergiya, Vol. 35, No. 1, pp. 65-67, July, 1973.

production and the need to take sanitary and hygienic measures, even though considerable expenditures are required for this, were emphasized.

A decrease of initial contamination of articles will allow the sterilizing dose of irradiation to be reduced; this will lessen the cost of radiation sterilization and thus compensate the expenditures for sanitary and hygienic measures.

In discussing the problem of checking the sterility of radiation-sterilized medical articles, all specialists expressed the opinion that it is not necessary to check the sterility of the articles if there is a guarantee that the articles received the necessary sterilizing dose of irradiation. In this case the check of the sterility of the articles should be replaced by a check of the effectiveness of sterilization using a highly radioresistant test – by means of microorganisms. A periodic check of the sterility of the radiation-sterilized articles was recommended (once or twice a quarter). Daily checking of the sterility of irradiated articles in each batch of products is also rejected because of economic considerations, since such checking requires the sampling of a large number of finished, poststerilized products and a long incubation of the cultures in the sterility test, which entails prolonged storage of the products. All this, however, does not pertain to naturally highly contaminated articles, such as catgut.

The reports on the method of checking irradiated articles for pyrogenicity and toxicity did not evoke a special discussion. The tests selected for this, which were proposed by specialists of the USSR, were considered correct. But in the opinion of the delegations from Hungary, Poland, East Germany, and Czechoslovakia, the toxicity of finished articles should not be checked. Materials should be subjected to such testing at the stage of their development and introduction into practice. Neither is a regular check for pyrogenicity necessary; in the opinion of the specialists it should be done periodically, once or twice a year.

Thus the symposium reviewed the results of investigations into the radiation sterilization of disposable plastic medical articles conducted in the member nations of the CMEA and planned further ways of cooperation of the countries in this field.

The Conference of Specialists of Member Nations of the CMEA on Initial Data of the Technical Design of the Soviet-Developed VVER-1000 Reactor Plant

The conference was held in Moscow on February 6-9, 1973 in conformity with the operations plan of the Research and Development Institute of Atomic Energy of the CMEA.

A report on the initial data and information reports of specialists of member nations of the CMEA on the course of works for implementing the plan of cooperation were discussed in detail, and specific organizational measures were outlined.

The conference was attended by specialists from Bulgaria, Hungary, East Germany, Poland, Rumania, USSR, Czechoslovakia, and co-workers of the Secretariat of the CMEA.

The Conference of Specialists on Problems of the Transportation of Spent Atomic-Power-Plant Fuel Elements

The conference was held in Berlin on March 13-16, 1973.

Reports were given by the East German and Soviet delegates on the experience of transporting spent fuel from the atomic power plant in Reinsberg. The state of development was discussed and problems of the construction and unification of means of railroad transport for the haulage of the spent fuel elements of the VVER-440 reactor were examined, as were the technical requirements on the containers and cars for transport and problems of manufacturing the means of transport. It was noted that in their further development it is necessary to take into account the requirements of the International Atomic Energy Agency and the corresponding documents of the CMEA. General principles in evaluating the content of fissionable materials in spent fuel element assemblies were discussed. In East Germany and the USSR, calculation methods have been developed which may now be used for determining the quantity of fissionable materials in the assemblies being transported. It was considered necessary to improve the methods of nondestructive inspection of the fuel elements.

In connection with the discussion of the draft of the technical specifications for spent fuel element assemblies from atomic power plants with VVER-440 reactors, developed by Soviet specialists, it was noted that, after corrections, this draft can be used as a standard when concluding contracts for the delivery of spent fuel elements to radiochemical plants.

Taking into account the importance of the problem, the specialists suggested drawing up instructions for hauling spent fuel by different type of transport, envisaging the solution of all problems (requirements imposed on packing and shipping, provision of a good state of preservation, responsibility, and guarantees, prevention and elimination of possible accidents, customs procedures, and order of solution of disputable problems).

The conference was attended by delegations from Bulgaria, Hungary, East Germany, Poland, Rumania, USSR, and Czechoslovakia. The conference aroused great interest in the specialists, as manifested by their active participation in the discussion on many problems.

The Third Meeting of the Committee of the Scientific and Technical Council for Fast Reactors

The meeting was held in Prague on March 27-30, 1973.

The meeting was attended by specialists from Bulgaria, Hungary, East Germany, Poland, Rumania, USSR, and Czechoslovakia, and by a co-worker of the Secretariat of the CMEA.

The course of work on the technology of a sodium heat exchanger and heat exchange in a steam generator was examined. Problems of the preparations for holding the symposium on fast reactors and other problems of an organizational character connected with implementing the operations plan of the Committee were discussed.

The participants heard with interest the report on the results of the startup and adjustment works on the main lines of the BN-350 reactor and on investigations of its nuclear-physical characteristics following physical startup. The great scientific and technical value of the works conducted and of the experience of the practical utilization of this plant was noted.

The Fifth Conference of the Council of the International Economic Union Interatominstrument (IAI)

The conference was held in Warsaw on April 10-14, 1973. It was chaired by Council member M. Baba, deputy general director of the GAMMA Combine (Hungary).

The Council heard the report of the director of IAI on the work of the Union in 1972, refined the nomenclature of the articles entering the sphere of activity of the Union, and examined problems relating to long-range planning and coordination of research and development. Some financial problems and suggestions on opening branches of the IAI for service in territories of countries the economic organizations of which are members of the Union were discussed. Appropriate decisions were made for all the problems considered.

The chairman of the Department of the Secretariat of the CMEA attended the conference.

The Council decided to hold its next meeting in August 1973 in Budapest and outlined a preliminary agenda.

The meeting was held in a businesslike atmosphere in the spirit of complete mutual understanding.

IAEA SYMPOSIUM ON INSTRUMENTATION AND CONTROL OF ATOMIC POWER PLANTS

E. A. Zherebin, L. V. Konstantinov, V. D. Nikolaev, and V. I. Petrov

The symposium took place in Prague on January 22-26, 1973. It was opened by the Assistant Director General of the IAEA Yu. F. Chernilin (USSR). This was the first symposium dedicated to this field of nuclear engineering, which has become quite important in connection with the vigorous developments in the design and building of atomic power plants based on various types of reactors. The symposium was attended by nearly 250 specialists from 29 countries and six international organizations. The symposium heard 62 reports (from 14 countries and the IAEA) including five from the USSR. The reports were discussed at meetings dedicated to the following eight topics:

1) operation of atomic power plants, past experience and future plans;

2) control of atomic power plants; application of modern control methods;

3) measurement of dynamic characteristics;

4) system and equipment reliability;

5) detection of local anomalies in sodium-cooled fast reactors;

6) measurement of coolant temperature and flow rate;

7) measurement of neutron flux;

8) detection of damaged fuel elements.

Most reports either directly or indirectly reflected the use of computers in monitoring and control of neutron flux distribution in the core, and also the results obtained with various neutron detectors. These topics were given much attention in reviews presented at the beginning of the symposium by J. Furet (France) and R. Cox (UK).

The modern theory of automatic control and supervision of atomic power plants, as well as most new projects under development, foresee the use of central control computers (this has been in some measure already implemented in certain operating plants). The reports stressed that the use of computers directly connected to primary elements eliminates the need for intermediate processing devices, thus improving the control system reliability and reducing capital investments. However, one should not forget the place of human operators in computerized systems. Even in the most highly automated supervision and control system the final decision rests with the human operator. The algorithms, their correction in the course of operation, the evaluation of results, and, in the final result, the quality and effectiveness of control are in the hands of the operator. Thus, special attention is being devoted to the development of control models as closely as possible reproducing the actual operating conditions and the various possible abnormal situations.

Great importance attaches to the computer–operator interaction, the technical problems of data and program input into the computer, and the optimization of the display of information about the plant operation.

The experience of using computers in atomic power plants occupied a prominent place in several reports of the first group. D. Habler (FRG) reported on the simultaneous use of two computers for processing the information from primary elements (for nuclear and thermodynamic parameters) at the State

Translated from Atomnaya Énergiya, Vol. 35, No. 1, pp. 69-71, July, 1973.

Atomic Power Plant. For two months the trouble-free operating time of each computer (Siemens-305) amounted to 98%, and the total concurrent "nonoperating" time was less than 1 min per month. The two planned Biblis plants will also be equipped with two improved computers having a higher memory capacity (Siemens 306).

The experience gained with "on-line" computer operation for centralized information processing in several British reactors has been described by M. Jarvis and F. Dickson, and by B. Low. Failure-free operating time of the computers varied between 95.3 to 99.9%.

M. Langlaid and M. Leroy (France) discussed the advantages and disadvantages of supervision systems, using as an example three atomic power plants with different degrees of computerization. In the authors' opinion, the experience gained with a central computerized supervision system does not yet fully justify the economical expense. This opinion is based on the cost of equipment and its operation. Repair and replacement of faulty components and units is frequently quite difficult.

The first attempt to use a computer not only for supervision but also for control (with the computer included in the common loop) of an entire atomic power plant has been made at the Pickering Plant (three units 512 MW each). This was reported by E. Yaremy and D. Anderson (Canada). The reactor and its ancillary equipment are controlled by two digital computers that duplicate one another. During the operating time, computer failure caused three shutdowns (in three units). The utilization factor of the plant as a whole fell by 0.5%. The concept of two duplicated computers seems to be optimal and is to be used also in the Bruce Plant with four 750 MW units. The heavy-water reactor with boiling light-water coolant of the Gentley Atomic Power Plant is equipped with a similar control system.

Notwithstanding the initial difficulties, the advantages of widespread incorporation of computers in atomic power plants have been stressed in all reports, addresses, and discussions. These advantages are obvious in view of the enormous flow of information involved, in particular in case of deviation from normal operating condition or during the onset of emergencies. It should be noted that there is no agreement among specialists as to the character of computer application: some advocate the use of decentralized control branches with small computers (U. Heinis, FRG; M. Langlaid et al., France), others suggest the use of two or three large computers for centralized monitoring only, while still others consider it most important to use large computers for "closed-loop" control. Obviously, the last point of view will prevail as soon as the reliability of the entire instrumentation and equipment of power plants becomes sufficiently high, and more experience with plant operation is gained.

Monitoring of the neutron flux distribution in reactor cores and neutron detectors were also widely discussed.

The report of I. Ya. Emel'yanov et al. (USSR) on the monitoring of the energy release in the boiling multichannel reactor (RBMK) of the Leningrad Atomic Power Plant* met with considerable interest.

D. Habler (FRG) described positive results obtained with a system for measuring the neutron flux in the core of the Stade reactor. This composite system includes 32 vertical channels for periodical automatic measurements by the activation method (30 points at different heights) and six channels with six fixed detectors each (18 fission chambers and 18 cobalt electron-emission neutron detectors) for continuous monitoring. The use of two measuring methods provides highly reliable results with a reproducibility better than 0.5%, and makes calibration quite easy (to within 0.5%). The highly reliable operation of the system was stressed. The system was accepted as a standard and is included in the plans of two new plants of the Biblis type.

The satisfactory performance of neutron detectors with a cobalt emitter (fast response, high reliability, linearity, and small size) makes them suitable for in-reactor measurements as well as for reactor control and protection systems. D. Anderson et al. (Canada) reported on the application of 28 such detectors in an automatic control system including two computers (14 detectors per computer) in Pickering reactors. Regulation and redistribution of power in the reactor core is accomplished automatically by varying the amount of ordinary water in 14 chambers located near the detectors. It is noted that, after several years of operation, cobalt neutron detectors require the introduction of systematic corrections (for the accumulation of Co^{60} and Co^{61} isotopes) and that the determination of the exact value of this correction after 4-5 years is rather difficult as it depends on the entire history of reactor operation. To avoid this problem, electron-emission detectors with platinum emitters are now used at the Pickering and Gentley plants; these detectors are thought to have an operating time of nearly 30 years.

*See also Atomnaya Énergiya, Vol. 34, No. 5, 331 (1973).

K. Mochizuki et al. (Japan) reported the results obtained with electron-emission neutron detectors in liquid-metal reactors. Special emphasis was placed on temperature resistance and on the elimination of gamma background. The detectors contain two emitters in a compensation circuit with approximately the same atomic numbers but with different activation cross sections (e.g., rhodium and palladium or molybdenum, vanadium and nickel). The current of such a twin detector remained practically constant up to 430°C. Test proved that in fast reactors the ratio of the useful signal to the gamma background is nearly ten times lower than in thermal detectors (using rhodium emitters).

P. Gebureck et al. (FRG) compared electron-emission neutron detectors with different compatible emitters (hafnium, erbium, and cadmium on the one side and rhodium, cobalt, and vanadium on the other). Experiments proved that detectors with cobalt emitters have the best parameters.

Experience gained at the Mont d'Arret Power Plant with a power monitoring system using 120 detectors with vanadium emitters (reported by F. Decole, France) proved good operating performance of these detectors. No diminishing of detector sensitivity has been observed during 450 days of operation.

Several papers discussed the application of miniature fission chambers as in-reactor neutron detectors. Such chambers can operate at temperatures up to 600°C (K. Mochizuki et al., Japan; C. MacMinn, UK). In comparison with electron-emission detectors, fission chambers have a much broader dynamic range (of nearly 10 orders of magnitude), but are less durable and more complicated, and require that burnup is allowed for. The general opinion expressed in most papers was that electron-emission detectors are preferable.

The important role of noise immunity of cables connecting electron-emission detectors with recording equipment has been stressed. This is especially true in connection with the widespread use of detectors with cobalt emitters which have a relatively low sensitivity (10 to 15 times lower than detectors with rhodium emitters). E. Wilson et al. (UK) discussed the necessary extent of cable shielding as well as the optimum cable design. They recommended the use of double shields made of copper and stainless steel, and two internal conductors that cross at specified intervals.

System and component reliability has been the topic of many papers. P. Kovanik (Czechoslovakia) considered a theoretical analysis of the reliability of analog and digital systems. He suggested recommendations for choosing estimation algorithms that are applicable also to computerized safety systems. Theoretical problems of system reliability were discussed in papers by E. Sobor (Hungary) on the degree of reliability of two out of three safety systems with automatic checking and replacement, and by B. Kuklin (Czechoslovakia) on an algorithm for calculating the reliability of complex systems from the point of view of dependent failures. The results of the last work were checked in an analysis of the reliability of a system for automatic control of coolant temperature at the A-1 atomic power plant. Tables of safety system reliability obtained with the aid of a computer were discussed by H. Hoermann (FGR).

Several papers described experimental results on the determination of local anomalies in light-water and fast reactors by analyzing fluctuation or frequency spectra provided by acoustic or neutron detectors in the core. The beginning of coolant boiling indicates a departure from normal operating conditions, in particular in sodium-cooled fast reactors. K. Mochizuki et al. (Japan) described the development of an acoustic detector with a crystal capable of operating in strong gamma and neutron fields (of up to 10^{20} neutr /cm^2) and at high temperatures (up to 600°C), and discussed the operating characteristics of such a detector. M. Dunc (USA) described the results of a study of coolant boiling in the 20-50 kHz range with the aid of acoustic detectors. In this frequency range the measurements are not affected by pump and cavitation noise. It was noted that the noise spectrum of boiling sodium is similar to that of boiling water.

The study of coolant pressure fluctuations with the aid of a piezoelectric pickup in a light-water reactor of the Stade Plant has been discussed by W. Bauernfeind (FRG). The studied frequency range of up to 100 Hz characterizes the operating noise of the main circulation pumps and the vibrations of the core elements.

The study of the state of the first circuit and of the core by acoustic noise analysis is still in an experimental stage. No instruments are now available for a quantitative interpretation of noise spectra, but this direction is of considerable practical importance for reactor instrumentation and should be further developed.

The use of electron-emission neutron detectors with cobalt emitters in an analysis of noise fluctuations of the neutron flux in the core of light-water reactors has been discussed by P. Gebureck et al. (FRG).

Experiments in the Lingen boiling reactor proved that the "noise" increases from the core bottom to about one half of its height; this is associated with the fluctuation of coolant density along the core height and, in turn, characterizes the local fluctuations in the core. The authors suggested that the variable component of the neutron detector current can be used for early detection of core anomalies.

Systems monitoring the airtightness of fuel-element jackets have been discussed in six reports.

Conventional methods of monitoring the airtightness of fuel element jackets employed in various French reactors have been reviewed by J. Graftieau. Reports of English workers indicate that the earlier trends in the design of airtightness monitoring systems developed for gas–graphite reactors, i.e., the use of special sampling lines for each channel, is continued also in modern reactors such as channel-type boiling reactors which have to be fitted with facilities for sampling each channel (A. Hoodings). This considerably complicates airtightness monitoring and reduces reactor reliability. L. Burton et al. (UK) described cases in which emergency situations were caused in gas–graphite reactors by untimely triggering of airtightness monitors based on the detection of fission products of noble gases. As shown experimentally, the method of monitoring delayed neutrons at the reactor channel outlets gives more satisfactory results both as to sensitivity and to correct triggering time. The last method is suitable for systems monitoring the airtightness of fuel jacket elements in gas–graphite reactors.

Special interest was aroused by the report of V. A. Aksenov et al. (USSR) on the fuel-jacket airtightness monitoring system of the VVER-1 reactor which is based on the detection of delayed neutrons and includes taking coolant samples from each loop of the first reactor, and the report of E. A. Zherebin et al. (USSR) on the detection of damaged fuel elements after shutoff of a water-moderated water-cooled reactor by placing the extracted samples into cans, automatic separation of iodine and cesium isotopes from water samples, and their radiometry with a simple setup consisting of a scintillation detector, discriminator, and scaler.

The various opinions expressed in addresses and discussions indicate that specialists of different countries do not agree as to the principle and desired extent of monitoring the state of fuel elements in the core of light-water reactors. For example, West German and Canadian workers doubt the effectiveness of operational monitoring in the primary circuit and consider that operational analysis of the coolant with the aid of reference isotopes is sufficient.

The Symposium was followed by the Third Meeting of the IAEA Working Group on Instrumentation and Control of Atomic Power Plants; the meeting was attended by 21 representatives of 16 countries and two international organizations. Representatives of Bulgaria, Hungary, Poland, the USSR, and Czechoslovakia actively participated in the meeting. All present praised the high level of the Symposium and noted the timeliness and urgency of the topics discussed. The working group scheduled the next Symposium on these topics for the end of 1975 or the beginning of 1976. The subjects of Special Conferences and the associated organizational problems were discussed. All participants strongly recommend that meetings be held on such topics as in-reactor measurements and the control of neutron flux, temperature, and flow rates (basic concepts, sensors, and instrumentation), and the detection of damaged fuel elements. The assistance to underdeveloped countries as well as certain other organizational problems were discussed.

The IAEA expects to prepare the Symposium proceedings for publication in July-August 1973, and to send them to the participating countries.

The excellent organization of the Symposium by the Czechoslovak Atomic Energy Commission which greatly contributed to its success has been noted by all participants.

IAEA PROGRAMS ON NUCLEAR SAFETY AND ENVIRONMENT PROTECTION

R. M. Aleksakhin

The IAEA programs foresee in the next few years (1973-1978) a great expansion of research in radiation safety and the protection of the human environment. The protection of the biosphere is especially urgent in connection with the expanding net of atomic power plants and the ever-increasing amounts of nuclear waste.

The IAEA activity in environmental protection and nuclear safety includes the following basic directions: radiological research, improvement of waste-handling methods, study of radiation safety, and investigation of the effects of nuclear explosions for peaceful purposes.

Radiological research is called upon to provide and coordinate norms and standards on the protection of personnel working with radiation and radioactive materials and on the protection of the population and the environment; they make it possible to develop safe methods for the transportation of radioactive materials, to provide adequate radiation protection in radioisotope laboratories, and to organize prompt help in case of radiation accidents. It also involves the assessment of radiation hazards in uranium and thorium mines, in fuel processing plants, in the operation of accelerators and neutron generators, and in work with transuranium elements; the use of chelate compounds to prevent the deposition of inhaled transuranium elements, and radiation surveys of the air. In IAEA places special emphasis on dosimetry of surrounding objects; on the physical aspects of the migration of radioisotopes in the atmosphere, in soil, and hydrosphere; on the study of the transfer of radioactive materials along biological and food chains that culminate in the penetration of these materials into the human organism. The program also foresees an examination of the principles and methods for establishing norms on the permissible content of radioactive materials in foodstuffs.

The basic object of studies in handling waste materials is to find new effective ways to ensure maximum isolation and prevention of the leakage of radioactive materials to the environment. The program contemplates a study of the sorption capacity of various natural media for different artificial radioactive materials (including an evaluation of the rate of migration of radioisotopes in soil, water, etc., and of the effect of prolonged exposure of these media to radiation). The study of the capacity of various natural media to absorb radioisotopes calls for an evaluation of ecologically safe irradiation doses. Special emphasis will be placed on studying the behavior of such mobile radioisotopes as tritium, Kr^{85}, and iodine isotopes.

One of the most important aspects of the protection of the water environment is the determination of criteria and principles of the disposal of wastes into the seas and oceans. As is known, the International Conference on Prevention of Pollution of Seas by Radioactive Wastes and Other Materials (London, October-November, 1972) decided to ban the burial of highly radioactive wastes in seas. The IAEA has been charged with the development of criteria by means of which the toxicity of radioactive materials can be judged from the point of view of their effect on sea plants and animals. Besides developing the principles of standardization and classification of radioactive wastes it will be necessary to gather and analyze information on the biological effects of the wastes. Primary attention should be given to the effect of ionizing radiations on fishes, which are among the most important components in hydrobiocenosis.

An important factor in considering the effect of atomic energy on the surroundings is the thermal contamination of the biosphere and in particular the effect of elevated water temperature on sea plants

Translated from Atomnaya Énergiya, Vol. 35, No. 1, p. 72, July, 1973.

and animals, as well as the combined effect of heat and ionizing radiation. In the next few years the information gathered is to be systematized so that further research in this direction can be precisely outlined.

The program calls also for a study of the disposal of nonradioactive wastes that accompany the implementation of various nuclear programs, and the application of isotopic techniques and nuclear instrumentation in studying the behavior of different chemical substances in the environment.

The principal point of the program of radiation (technical) safety is to assist in a successful solution of the problems of safe disposition, design, construction, and operation of research reactors, atomic power plants, and nuclear-material storage and processing plants. Of special importance is the analysis of earthquakeproof characteristics of nuclear installations built in regions of high seismic activity, and the development of principles for the ecologically safe location of nuclear reactors.

Much more information is available on the possible harmful effect of dumped radioactive isotopes on the surroundings and on the behavior of radioisotopes in biological and food chains than on the migration of other pollutants in natural environment and on their effect on the biosphere. In comparison with other industries, nuclear power engineering is in a much more advantageous situation from the point of view of protection of the environment from pollution. However, the contemplated growth of the net of atomic power plants and the sharp increase of the amount of radioactive wastes urgently require the continuation of research in this field.

SESSION OF INTERNATIONAL COMMUNICATION GROUP ON MHD GENERATORS

Yu. M. Volkov

The Ninth Regular Session of the International Communication Group on MHD Power Generators was held on January 17-19, 1973 in Paris at the headquarters of the Organization of Economical Cooperation and Development. The Session was attended by representatives of 13 member-countries and invited experts.

The agenda included problems of protocol, exchange of information on National Conferences held during the passed year, and a discussion of the state of affairs and national programs on MHD generators.

The Soviet delegation reported on the continuing advances in all three basic directions in MHD generator design; open-cycle combustion generators, closed-cycle generators with nuclear (or thermonuclear) heat sources, and liquid-metal generators. The results of an analysis of the engineering and economical prospects of these MHD generator types were cited. It was shown that in the USSR, preference should be given to open-cycle generators operating on the combustion products of petroleum or gas, which can provide an efficiency of up to 50% (first-generation plants) or 60% (second-generation plants). MHD plants are economically competitive with thermal plants provided the cost of fuel exceeds 8 rubles per ton ideal fuel. MHD plants require a capital investment not very much higher than that required by conventional thermal plants but allow a 1.5- to 2-fold reduction of thermal pollution of the environment, which is particularly important in the European USSR.

Although the construction of closed-cycle nonequilibrium MHD generators with a gas temperature of 1500-2000°C is now physically and technologically feasible, the future prospects of such plants depend on which type of high-temperature reactor (nuclear or thermonuclear) will be developed first. An analysis of a nonequilibrium MHD generator with a thermonuclear reactor of the "Theta-pinch-and-liner" type indicates that this kind of heat-to-electricity converter has good prospects. In spite of some still-outstanding scientific and technological problems, the construction of such a nonequilibrium MHD generator seems to be quite practical.

Liquid-metal generators merit consideration only in conjunction with conventional low-power thermal plants. This is economically justified provided the MHD plant efficiency exceeds 6% as the cost of an installed kilowatt of energy produced by a liquid-metal MHD plant is very low because of the simplicity at such a plant.

American workers reviewed the research in the above three MHD generator types conducted in several large industrial companies and universities in the USA. They noted that the Avco–Everett Company directed its efforts to the demonstration of the operation of an equilibrium MHD plant at an acceptable power level (the Mark-VI plant generated 560 kW for 5 h), a theoretical and technological investigation of the possibility of a full-scale MHD plant, and a preliminary study of an experimental 50 MW plant. In addition, experiments were continued on the Mark-VII plant with a high conversion efficiency, as well as on certain other programs.

Several companies and universities investigated the operation of combustion MHD generators using coal dust. General Electric continues research on nonequilibrium MHD generators. Energy conversion efficiencies of up to 20% have been achieved. Experimental and engineering design work proceeds also in other companies and universities.

Translated from Atomnaya Énergiya, Vol. 35, No. 1, p. 73, July, 1973.

Research into MHD generators is actively pursued in Poland. Some drop of activity in this field has been observed in certain countries (FRG, Italy) partly because of the transfer of efforts to thermonuclear research and partly for economical reasons.

A technological and economical analysis carried out in the FGR indicates good prospects for open-cycle MHD generators as stand-by plants for emergency situations at atomic power plants but further studies in this direction have been discontinued.

Organizational problems associated with the Sixth International Conference on MHD Generators, to be held in the beginning of 1975, were also discussed. The exact location of the Conference will be decided upon at the Tenth Session to be convened in February-March, 1974.

SOVIET – FRENCH SYMPOSIUM ON FUEL ELEMENTS OF FAST REACTORS

L. P. Zavyal'skii

In accordance with the protocol of negotiations between the State Atomic Energy Commission of the USSR and the French Atomic Energy Commission from October 14, 1969 on further cooperation in peaceful uses of atomic energy, a Soviet–French Symposium on Fuel Elements of Fast Reactors was held in the Soviet Union on December 10-20, 1972. The meeting was attended by 12 members of the French Delegation and 11 delegates and 26 experts of the Soviet Union. Throughout the visit, the French delegation was accompanied by the Scientific Attaché of the French Embassy in the USSR, Mr. J. Chapper.

Each side presented 13 reports which were followed by an interesting and useful debate on the discussed topics. The reports can be grouped as follows in accordance with their subjects:

1. design models and operating principles of fuel elements;
2. properties of fuel elements;
3. properties of structural materials of fuel elements;
4. results of fast reactor operation;
5. prospective types of fuel, carbides and carbonitrides;
6. manufacture of fuel elements.

The first part of the Symposium was held in Dimitrovgrad (December 12-15); the reports presented dealt with the design principles and construction of fuel elements, their properties, the interaction of fuel with fuel jackets in case of high burnup, the results obtained with regular and experimental fuel elements in the Rapsodiya and BOR-60 reactors, and with carbide and carbonitride fuels. A French report on the manufacture of plutonium fuel for the Phoenix reactor was also heard.

An interesting feature of French reports was that they dealt mainly with mixed uranium–plutonium fuel.

The second part of the Symposium, held at the Physics and Power Institute in Obninsk, was devoted primarily to topics concerning the behavior of fuel-jacket materials and hexagonal casing tubes. The topics included a discussion of the effects of radiation on the mechanical properties, structure, and swelling of steel, an evaluation of the properties of fuel-jacket steel in sodium-cooled reactors based on the results of prereactor and in-reactor tests, and a discussion of problems associated with simulating radiation porosity with the aid of accelerators. Other papers dealt with the effect of steel treatment on the behavior of hexagonal casing tubes in neutron fluxes.

The exchange of information on all these topics was very valuable to both sides. It is interesting to compare the construction of fuel elements and assemblies of Soviet and French reactors. Neither the Rapsodiya nor the Phoenix reactors use displacers in the outside cells of their fuel assemblies and this causes a temperature difference of the order of 100°C in the fuel elements near the walls. The temperature drop along the fuel assembly perimeter can be reduced to 40-50°C by using displacers. French workers reported interesting data on the behavior of fuel elements in the BOR-60 reactor at a burnup factor of 10% and a jacket temperature of 700°C, and on the use of Soviet niobium-alloyed steels which are less affected by swelling in radiation doses of up to $2.5 \cdot 10^{22}$ neutr/cm^2.

Translated from Atomnaya Énergiya, Vol. 35, No. 1, pp. 73-75, July, 1973.

In view of the satisfactory results obtained with carbide and carbonitride fuels, French workers are no advantage in using vibration-compressed oxide and metallic fuels. Both French and Soviet scientists stressed the need of further investigation of swelling, and including a detailed study of the effects of the structure and state of steel, temperature, neutron spectrum, and other pertinent factors.

Soviet specialists were especially interested in the production technology of oxide fuel pellets from mixed uranium–plutonium oxides. This technology uses behenic acid salts as plasticizers. Solid plasticizers give better results as to the porosity and geometry of pellets than aqueous plasticizers. The French workers designed an automatic oven for sintering mixed-fuel pellets. The oven is divided into three zones: a drying zone, a zone where the plasticizer is removed, and the sintering zone. The process is fully automatic and takes 28 h. Simple manual operations can be performed only during repairs. The entire production area is 5000 m^2, and the production rate is about 10 tons per year. It was reported that the first charge of fuel elements for the Phoenix reactor is fully completed.

Mixed oxide fuel gives a better interaction between fuel and jacket both in depth and along the perimeter than a core of uranium oxide only. The interaction of mixed fuel and jacket has been examined in detail on the basis of much factual material; all the possible mechanisms of such interaction have been investigated: oxidation of the jacket by oxygen released from fuel, the formation of a liquid phase consisting of eutectic cesium oxide compounds, transport of jacket iron and chromium to fuel, etc.

Soviet scientists noted the high standard of French research and the excellent instrumentation of French hot laboratories. The latter are equipped not only with first-class electron microscopes and x-ray spectral microanalyzers but also with ion microscopes by means of which it is possible to identify different phases in fuel and jackets, and to determine the presence of Cs, I, Te, Rb, and other fission fragments, as well as of oxygen, on the steel jacket surface, along the grain in case of intercrystalline corrosion, and in fuel. All this provides much valuable information about the irradiated sample which is particularly important in view of the fact that irradiation experiments are expensive and very time consuming.

An investigation of the development of defects in fuel elements of the Rapsodiya reactor indicates that as long as sodium does not penetrate the jacket the development is quite slow. As soon as this point is reached, sodium starts to react with fission products especially in fuel elements with a high burnup fraction. This information provoked a lively discussion.

The results of French studies of structural changes in fuel and of the formation of a central hole, as well as a comparison of theoretical and experimental data, agree with Soviet data.

French workers obtained valuable information on fuel-assembly materials and noted that the development of Kh16N15M3B steel is an outstanding Soviet contribution to the selection of fuel-jacket materials which ensure reliable operation of fast reactors.

Unlike American and British scientists who prefer cold-worked type 316 steel, Soviet and French workers agree in using type Kh16N15M3B and tempered 316 steel as fuel-jacket materials.

Tentative results of an investigation of fuel elements filled with mixed uranium–plutonium carbide fuel irradiated in the Rapsodiya reactor were described. Programs were reported on the study of carbide and nitride fuels in the Rapsodiya and BOR-60 reactors. The common approach to advanced fuel composition and fuel element construction has been noted. The construction of fuel elements with a layer of sodium has been acknowledged as being optimal.

Cold-worked 316L steel is used in France in the manufacture of hexagonal casing tubes. In the opinion of French workers such steel is less prone to swelling than tempered steel, the more so after thermomechanical treatment. In the Soviet Union hexagonal casing tubes for fast reactors are made of thermomechanically treated 0Kh18N10T steel (20% cold deformation with subsequent annealing for 1 h).

Summing up the six days of the Symposium, the heads of the delegations noted its contribution to further advances in the design of fast reactors. All participants stressed the need of frequent meetings such as this Symposium, and the advisability of exchanging personnel of Rapsodiya and BOR-60 reactors, of research laboratories, and "hot" chambers.

SOVIET–SWEDISH SYMPOSIUM ON ATOMIC POWER PLANT SAFETY

V. A. Sidorenko

A Soviet–Swedish Symposium on Atomic Power Plant Safety was held on March 5-7, 1973 at the Scientific Research Center in Studsvik (Sweden). Many timely topics concerning the safe operation and location of atomic power plants were discussed at the Symposium.

One Swedish and one Soviet report discussed the hazards of locating atomic power plants in populated areas. The potential hazards of atomic plants resulting from a possible major breakdown have been considered by workers of the I. V. Kurchatov Atomic Energy Institute who used as an example a water-moderated water-cooled reactor of 1400 MW thermal power. They proved that an escape of the entire activity contained in the primary coolant, even in case of a large number of nonhermetic fuel elements, presents no danger to the surrounding population. Foremost considerations should be given to the design of emergency cooling systems so as to prevent damage to fuel elements in the reactor core.

The design of systems for containing the escaping radioactivity must take into account the efficiency of the emergency cooling system and the power plant location.

S. Bergström discussed the risks involved in locating an atomic power plant within the bounds of a large city. He considered the hazards presented by a normally operating plant, and the danger of recurring failures and of a major (but not very probable) breakdown. The dangers were evaluated on the basis of an analysis of somatic and sociomedical effects. The author stressed that in his opinion, the equipment reliability required (and put into practice) for economically efficient power plant operation exceeds that necessary for demonstrating the plant safety. The most important unknown factor in estimating the hazards presented by atomic plants is a correct evaluation of the probability of large-scale breakdowns. This makes it difficult to obtain relevant data on the safety of locating atomic plants in cities.

Methods of ensuring the safety of atomic power plants were discussed in three reports. A. M. Bukrinskii described the measures taken in the Soviet Union in the design of atomic power plants to prevent radiation danger in case of a major breakdown. It was stressed that primary consideration must be given to high equipment quality, and to extensive periodical and continuous monitoring of its performance in the course of operation. The main efforts should be directed to preventing emergencies and only then to limiting their scale and localizing their consequences.

I. Tiren discussed the approach to safety of boiling light-water reactors now under development in Sweden. This approach is characterized by setting up multiple barriers on the possible escape paths of radioactive products from the fuel elements to the environment, and by the development of reliable reactor shielding and emergency cooling systems.

Workers of the F. E. Dzerzhinskii All-Union Heat-Engineering Institute described the design and analyzed the efficiency of the safety system of an atomic power plant with a water-moderated water-cooled reactor in which provision is made for discharging the low-active fraction of the primary coolant into the surroundings and confining highly active products that are liable to escape from the core at an advanced stage of breakdown.

The probabilistic approach to evaluating the potential hazards of an atomic plant and to breakdown analysis has been discussed by A. I. Klemin and E. F. Polyakov (USSR) and Per Linder (Sweden). On the basis of a comparative safety analysis, the probabilistic approach makes it possible to choose the most suitable version from among the various possible designs of operational, safety, and confinement systems.

Translated from Atomnaya Énergiya, Vol. 35, No. 1, pp. 75-76, July, 1973.

The Swedish report proved that at the present level of safety systems, the most probable and most dangerous failure, melting of the reactor core, is associated with an explosion of the reactor vessel. The probability of such a disaster is estimated as 10^{-6} per year.

Actual emergency core cooling systems and the behavior of a reactor in case of failure involving core circuit rupture have been discussed in papers by S. Ericson (Studsvik) and V. P. Stekol'nikov et al. (read by G. I. Biryukov). The same topic has been touched upon by Yu. V. Rzheznikov et al., who described an evaluation of dangerous mechanical effects associated with breakdowns involving loss of hermetization.

Two Soviet papers discussed the results of an experimental study of discharge of hot water through holes and pipes in a pressure range 20-221 bar (V. D. Keller, B. K. Mal'tsev, and D. A. Khlestkin) and of an analysis of the transport and deposition of nongaseous fission products by simulating a leakage in the primary circuit of a water-moderated water-cooled reactor (V. I. Pavlenko).

Jungham described a system for monitoring the state of the reactor vessel in the course of operation which was developed in Sweden and is being incorporated in new reactors. The system operation is based on remote ultrasonic control by means of special devices and mechanisms mounted outside the reactor which are inserted into the reactor vessel in case of overloads. The state of the vessel metal (in particular near welded seams) is checked periodically in the course of reactor operation and compared with a reference state recorded by the same remote control system before starting the reactor.

R. Margen and S. Menon reported on joint Scandinavian studies on the construction of vessels for light-water reactors of prestressed concrete. All the data necessary for designing a commercial high-power reactor in a concrete vessel will be available after the third phase of the investigation is completed in 1975. Besides purely economical merits, the principal advantage of such a reactor is that, in the opinion of the authors, it provides a cardinal solution to the problem of reactor safety: such a vessel cannot explode and each of its power units can be checked and repaired individually.

Two Swedish papers dealt with fuel-element damage in power reactors. S. Dürle summarized the results of a series of studies on the mechanism of failure of zircalloy jackets of uranium dioxide fuel elements. The author concludes that the most likely mechanism of failure is corrosion under stress which causes the appearance of initial cracks on the inside of fuel-element jackets. This is followed by mechanical broadening of the cracks at weakened spots.

J. Fogt gave a detailed analysis of the causes of fuel-element failure in the Agesta reactor and described the work on reconstructing the reactor core.

Two Soviet papers described safety problems in sodium-cooled fast reactors associated with reactor dynamics (Yu. E. Bagdasarov and I. A. Kuznetsov) and discussed the experience gained with the BOR-60 reactor in the Scientific-Research Institute of Atomic Reactors.

All papers read at the Symposium aroused great interest and lively debates that were continued during visits at Swedish atomic reactors and companies that were organized for the Soviet Delegation by the Swedish Academy of Engineering Sciences after the Symposium.

BOOK REVIEWS

NEW BOOKS FROM ATOMIZDAT (SECOND QUARTER OF 1973)

F. Kedrov, Irene and Frederic Joliot-Curie. The book familiarizes the readers with the life and scientific creativity of the famous French scientists Irene and Frederic Joliot-Curie. Special attention is given to their main discoveries — artificial radioactivity, neutron moderation, etc. The scientific activities of Irene and Frederic Joliot-Curie are shown against the general background of the development of physics, beginning with the discovery of radioactivity. Considerable space is given to the contribution of the French scientists to the development of scientific relations between the USSR and France. Information is given on their participation in the French Resistance Movement during the Second World War and in the struggle against the use of atomic weapons and for peace and friendship during the postwar years.

The book is intended for a wide range of readers interested in the history of nuclear physics, particularly for youths trying to become acquainted with the most important scientific events of our time.

A. Beiser, Concepts of Modern Physics. Modern physics is a field of knowledge attracting the close attention not only of physicists but also of workers of the most diverse allied fields. The author begins the account with the principles of the special theory of relativity and relativistic dynamics. There follows a description of the particle properties of waves and the wave properties of particles. After a presentation of the principles of quantum mechanics, the hydrogen atom, complex atoms, atomic spectra, the chemical bond, and the structure and spectra of molecules are considered. The principles of classical and quantum statistics are presented. Four chapters familiarize the reader with solid-state physics: problems of the crystal lattice, Debye theory of specific heat, band structure, dislocations, and conductivity are examined. The concluding part of the book is devoted to the atomic nucleus, nuclear forces and models, nuclear reactions, and elementary particles. An excellent feature of the book is the successful combination of a popular nature of the presentation with a high scientific level.

The book is designed for readers interested in the achievements of modern physics and its problems.

Atomic and Nuclear Physics

V. P. Krainov, Lectures on the Microscopic Theory of the Atomic Nucleus. The simplest theoretical concepts of the structure of the atomic nucleus are given. Main attention is given to a popular description of microscopic methods widely used in scientific literature on nuclear physics. Mainly ground and the lower excited states of nuclei are presented. The methods of analyzing nuclear reactions are regarded as auxiliary in investigating the structure of the nucleus.

The book can be recommended as an introductory text for senior and graduate students specializing in theoretical and experimental nuclear physics. It will be useful also for university teachers of theoretical physics and nuclear physics.

Plasma Physics. Thermonuclear Research

Yu. V. Gott and Yu. N. Yavlinskii, Interaction of Slow Particles with Matter and Plasma Diagnostics. Processes occurring in the interaction of particles with matter play a major role in science and engineering. The book considers the interaction of particles (with energies less than 50-100 keV) with solid matter; the current state of theoretical and experimental investigations of energy losses and particle paths in matter is presented; the charge exchange of protons and their scattering on passing through a layer of material and experimental methods are described. Methods of producing and using as targets ultrathin layers of the

Translated from Atomnaya Énergiya, Vol. 35, No. 1, pp. 76-79, July, 1973.

investigated material without a substrate are presented in detail. The last section is devoted to the use of the phenomena considered for particle diagnostics of laboratory and cosmic plasma.

The book is designed for engineers and physicists engaged in problems of the radiation damage of semiconductors and of the production of semiconductor materials, working in the field of plasma physics, studying cosmic space, and occupied with problems of emission electronics, as well as for senior students of the pertinent specialities.

I. P. Stakhanov, V. P. Pashchenko, A. S. Stepanova, and Yu. K. Gus'kov, Physical Principles of Thermionic Energy Conversion. A large number of papers have appeared in the past 10-15 years on physical processes in a low-temperature, weakly ionized plasma because of the practical need for the creation of more effective electrical energy sources. The monograph examines the structure of the near-electrode layer in plasma, the mechanism of ionization of atoms in a discharge, and the stability and occurrence of oscillations in weakly ionized plasma. Methods of calculating the volt–ampere characteristics of a gas discharge and a calculation of the kinetic coefficients of low-temperature, three-component plasma in a magnetic field are presented. Particular attention is given to the use of a low-voltage arc discharge. The effect of various admixtures to cesium on the operation of a thermionic energy converter is also considered.

The monograph is intended for physicists and engineers interested in problems of the direct conversion of energy, plasma physics, and gas discharge.

G. A. Kasabov and V. V. Eliseev, Spectroscopic Tables for Low-Temperature Plasma. Handbook. The tables present the most reliable data on oscillator strengths and the parameters of Stark broadening for a large number of spectral lines of 19 elements used widely in devices and instruments with low-temperature plasma.

The handbook is useful for researchers studying methods of direct energy conversion, high-temperature hydrodynamics, the physics of shock waves, gas lasers, and gas-discharge light sources.

Nuclear Instrument Manufacture

W. Meyling and F. Stary, Nanosecond Pulse Techniques. The book contains a sequential presentation of the principles of nanosecond techniques and various aspects of its application. It considers in detail various circuits of the nanosecond range, including circuits with tunnel diodes and other high-speed semiconductor elements. Considerable space is given to important problems of testing and adjusting these circuits. The physical principles of the operation of fast ionizing-radiation detectors are presented, and various areas of the use of nanosecond electronics in modern physics are discussed broadly.

The book is designed primarily for experimental physicists working in the electronics field and university teachers and students. The extensive and systematized bibliography will be a great help to physicists and engineers engaged in the development of such circuits.

Neutron Physics. Theory and Physics of Nuclear Reactors

T. A. Germogenova, V. P. Mashkovich, V. G. Zolotukhin, and A. P. Suvorov, Albedo of Neutrons. The book is the first monograph on the backscattering (albedo) of neutrons of various energies from real media (concrete, iron–water shields, etc.). The available information and the authors' data on the differential and integral characteristics of the albedo of neutrons are systematized and analyzed, and methods of studying them are considered.

Using a computer the authors have obtained information on the differential characteristics of the albedo of unidirectional monoenergetic sources (in the area of isotopic and reactor sources), the greater part of which is published here for the first time.

The book is intended for engineers, graduate students, students, and all scientific and technical workers specializing in problems of protection against ionizing radiations or allied fields related with the use of radioactive sources in various branches of science, engineering, and the national economy.

Nuclear Power Engineering

G. V. Tsiklauri, L. I. Seleznev, and V. S. Danilin, Adiabatic Two-Phase Flows. The monograph is devoted to problems of two-phase, high-velocity flows. The hydrodynamics of two-phase flows of various

structures (drop, bubble, chain), problems of their stability, problems of mechanical interaction, and heat and mass transfer are discussed in detail. Results of experimental and theoretical investigations of two-phase flows in nozzles, pipes, and jet apparatus in a wide range of concentrations of the liquid phase up to unity and discharge of a saturated and underheated fluid are presented. Data are given on the flow-rate and energy characteristics of nozzles and apparatuses, critical conditions in two-phase flows are analyzed, and methods are proposed for calculating two-phase flows; some problems of a two-phase boundary layer and separation and flow of films are considered.

The book is intended for a wide range of engineers and researchers engaged in investigations of two-phase flows and in the design of new types of stationary and transportable power plants, and can also be useful for senior students of power engineering and polytechnical institutes.

V. A. Tsykanov and B. V. Samsonov, Technique of Irradiating Materials in Reactors with a High Neutron Flux. Problems of the technique and procedure of irradiating materials in research nuclear reactors with a high neutron flux are presented. The main physical and technological characteristics of research reactors and their experimental channels are given, and the design, advantages, and shortcomings of loop and ampule devices for irradiating materials are examined, with reference, in particular, to the investigation of the properties of materials directly during irradiation. Some special features of measurements (of neutron fluxes, temperatures, etc.) during irradiation are indicated. Attention is given to experimental design and preparation, since the effectiveness of using a research reactor with a large number of experimental channels depends in many respects on this problem.

The book will be useful for researchers in the field of reactor techniques and reactor materials science, and also for senior students in this field.

Geology. Mineralogy. Raw Materials

N. Z. Bitkolov and V. S. Nikitin, Working Conditions and Ventilation of Quarries in the Mining of Radioactive Ores (A. I. Burnazyan, editor). The sanitary and hygienic working conditions in quarries in the mining of radioactive ores are considered. The processes determining air exchange in quarries under various meteorological conditions and different geometries of the quarry space are described. Methods of normalizing and maintaining the composition of the air are described. The design of devices is discussed and their effectiveness is determined. Considerable attention is given to the prognostication and design of methods and means of improving the air composition in quarries and the microclimatic parameters at the job sites.

The book takes into account the latest achievements in the field of quarry aerology, ventilation, dust trapping, gas scrubbing, and air conditioning. The book is intended for production workers and design and research institutes. It will also be useful to students of mining institutes and technical schools.

R. P. Rafal'skii, Hydrothermal Equilibria and Processes of Metallogenesis. The book generalizes the experimental and calculated literature data for elevated temperatures that is of geochemical value: data characterizing ionic equilibria in solutions, the solubility of gases in water and aqueous solutions, the solubility of the most important ore and vein minerals, and also the field of their stability. Considerable attention is given to equilibria of oxidation–reduction reactions in uranium-containing systems. The physicochemical conditions of hydrothermal metallogenesis are considered: the composition of hydrothermal solutions and the concentration of various components in them, the forms of transport of uranium and other heavy metals by hydrothermal solutions, the conditions of deposition of the most important ore minerals, etc.

The book is intended for geologists, geochemists, and mineralogists; it can be useful for hydrometallurgists, technologists, and chemists interested in processes occurring at elevated temperatures with the participation of aqueous solutions.

Atomic Materials Science

I. I. Papirov and G. F. Tikhinskii, Plastic Deformation of Beryllium. The physical bases of the plastic deformation and failure of beryllium are considered. The plastic deformation of beryllium single crystals and polycrystalline beryllium is described, and elementary forms of deformation and the character of failure of beryllium are described. The dependences of the plastic characteristics on the content of impurities, temperature, pressure, heat treatment, and crystal orientation are established. A theoretical analysis of the mechanisms of plastic flow, increase of strength, and failure of beryllium on the basis of dislocation concepts is given.

Cold shortness of beryllium is examined in detail and the possible methods of increasing the temperature of transition from the brittle to the plastic state are indicated. The types of pressure shaping and their effect on the structure, substructure, and mechanical properties are listed.

The book is designed for a wide range of specialists: researchers, technologists, and designers, and also for students and graduate students specializing in the field of plastic deformation, pressure shaping of metals, materials science, and atomic and aerospace engineering.

Solid-State Physics. Crystallography

I. S. Zheludev, Principles of Ferroelectricity. The essence of ferroelectricity is presented, and atomic and domain structures of ferroelectrics revealed by diffraction and spectral methods are described; the changes of these structures related with the appearance (disappearance) of spontaneous polarization and antipolarization are described. The characteristics of certain physical properties of ferroelectric crystals in the region of phase transitions are also considered. The fundamentals of theoretical concepts of the nature of ferroelectric phenomena, particularly concepts based on the crystal lattice theory, are presented.

The book is intended for engineers and researchers engaged in basic research, problems of physical materials science, and applied solid-state physics, and also for students.

E. S. Makarov, Isomorphism of Atoms in Crystals. Isomorphism as a phenomenon of mutual replaceability of atoms of different elements in crystals has an enormous effect on the chemical composition and properties of natural minerals and synthetic materials used in the most diverse areas of the national economy.

The book considers the theoretical and practical aspects of isomorphism. For each of 103 chemical elements a table of elements isomorphous with them is given, the type of their interaction in elementary systems and differences in electronegativity and values of atomic (ionic) radii are indicated, and examples of isomorphous mixtures for the investigated isomorphous pairs of elements with an evaluation of the limits of isomorphous replacements are presented. Isomorphous ratios of uranium, thorium, plutonium, and other actinides with other elements in primary and secondary uranium minerals and ores are examined in detail.

The book can serve as a handbook for geochemists, metal scientists, engineers, and technologists working in the indicated fields of science and engineering.

D. M. Skorov, A. I. Dashkovskii, V. N. Maskelets, and V. M. Khizhnyi, Surface Energy of Solid Metallic Phases. The book presents current concepts on the role of surface energy and surface diffusion in solids, mainly metals, alloys, and compounds, used in reactor engineering. The effect of surface energy and surface diffusion on certain processes and phenomena essential in the manufacture of materials or occurring during their operation in a reactor is investigated. The capabilities of experimental methods used for investigating surface diffusion and measurement of surface energy in the solid phase are discussed.

The book can be useful for researchers and engineers working in the field of reactor materials, technology of cermet articles, solid-state physics, and the effect of radiation on materials, and also for students and graduate students in these fields.

Radiology. Radiobiology. Radiation Hygiene

M. I. Amiragova, N. A. Duzhenkova, N. P. Krushinskaya, et al., Primary Radiobiological Processes *(N. V. Timofeeva-Resovskii, editor). The conversion of the energy of ionizing radiation in biological media and the effect of radiation on phospholipids and their components, amino acids and proteins, nucleic acids and their components, and porphyrin-containing compounds are considered. The role of the disturbance of these substances in radiation injury of the cell and organism is discussed. The molecular basis of radiation-induced pathology, repair, and radiation protection of the organism is presented.

The second edition of the book (the first edition was published in 1964) has been greatly revised. The experimental material has been supplemented by new sections on radiochemical conversions of carboxylic acids, phospholipids, and carbohydrates.

*Second edition.

The book is intended for specialists in the field of molecular and general radiobiology, radiation chemistry, radiation genetics, and also for physicists, chemists, biologists, and other specialists interested in the effect of ionizing radiations on living organisms.

E. N. Annenkov, I. K. Dibobes, and R. M. Aleksakhin (editors), Radiobiology and Radioecology of Livestock. The book elucidates problems of the migration of the most important artificial radionuclides in biological food chains – livestock. The metabolism of radionuclides in livestock and the effect of ionizing radiations on these animals are considered. The results of extensive experimental investigations in the USSR and abroad are generalized. In addition to their theoretical interest, the data generalized in the monograph have a practical value for developing measures aimed at reducing the passage of radioactive substances into livestock products.

The book is intended for radiobiologists, radioecologists, and hygienists.

NEW BOOKS FROM MIR (SECOND QUARTER OF 1973)

H. Pugh (editor), Mechanical Behavior of Materials under Pressure. The book is devoted to an investigation of the effect of high hydrostatic pressure on the mechanical properties of materials and to the use of the results of these investigations in modern technology. It is a group monograph written by prominent scientists and specialists working actively in pertinent fields, published under the editorship of the well-known metallophysicist H. Pugh. It is being published in two parts in the Russian translation.

Part 1 (General Problems of the Effect of High Pressures on the Mechanical Properties of Materials) describes the formal theory of the effect of pressure on the elastic constants of solids, examines the effect of pressure on the mechanical properties of plastic and brittle materials, including metal fatigue and the behavior of thin cylinders under repeated cyclic loads, the effect of pressure on defects in solids (dislocations, point defects) and the change of mechanical properties related with them. A separate chapter is devoted to a discussion of the methods of calculation and the basic principles of design of high-pressure vessels.

Part 2 (Use of High Pressures in Production Processes) examines the use of high pressure in the cold working of metals and indicates the design features of equipment used for hydraulic extrusion, technological parameters of hydraulic extrusion (speed, pressure-transmitting media, lubrication, etc.), and the effect of hydraulic extrusion on the properties of materials. Processes of hydrostatic pressing of powders are described. A separate chapter is devoted to the effect of shock waves on metals; it also presents some possible technological aspects of the use of shock-wave pressures.

The book is of interest for researchers and engineers working in the area of solid-state and high-pressure physics, the extrusion of metals, and the design of apparatus. It is quite useful for teachers, graduate students, and senior students of technical and engineering institutes interested in these problems.

T. Farrar and E. Becker, Pulse and Fourier Transform NMR. Introduction to Theory and Methods. The book is devoted to a new physical method of investigation—pulse and Fourier transform NMR. This is the world's first monograph in the given field, written, moreover, by prominent specialists with an outstanding pedagogical mastery. It presents concisely and clearly the basic principles of pulse NMR methods and gives an explicit concept of their information capabilities and development in the near future. A special chapter is devoted to apparatus and methods of measurement. Several examples of the use of the method for kinetic and other investigations are given.

The book is intended for organic chemists, chemical physicists, and physicists.

Translated from Atomnaya Énergiya, Vol. 35, No. 1, pp. 79-80, July, 1973.

breaking the language barrier

WITH COVER-TO-COVER ENGLISH TRANSLATIONS OF SOVIET JOURNALS

in mathematics and information science

Title	# of Issues	Subscription Price
Algebra and Logic *Algebra i logika*	6	$120.00
Automation and Remote Control *Avtomatika i telemekhanika*	24	$195.00
Cybernetics *Kibernetika*	6	$125.00
Differential Equations *Differentsial'nye uravneniya*	12	$150.00
Functional Analysis and Its Applications *Funktsional'nyi analiz i ego prilozheniya*	4	$110.00
Journal of Soviet Mathematics	6	$135.00
Mathematical Notes *Matematicheskie zametki*	12 (2 vols./yr. 6 issues ea.)	$185.00
Mathematical Transactions of the Academy of Sciences of the Lithuanian SSR *Litovskii Matematicheskii Sbornik*	4	$150.00
Problems of Information Transmission *Problemy peredachi informatsii*	4	$100.00
Siberian Mathematical Journal of the Academy of Sciences of the USSR Novosibirski *Sibirskii matematicheskii zhurnal*	6	$195.00
Theoretical and Mathematical Physics *Teoreticheskaya i matematicheskaya fizika*	12 (4 vols./yr. 3 issues ea.)	$145.00
Ukrainian Mathematical Journal *Ukrainskii matematicheskii zhurnal*	6	$155.00

Back volumes are available.
For further information, please contact the Publishers.

SEND FOR YOUR FREE EXAMINATION COPIES

PLENUM PUBLISHING CORPORATION
Plenum Press • Consultants Bureau
• IFI/Plenum Data Corporation
227 WEST 17th STREET
NEW YORK, N. Y. 10011

In United Kingdom
Plenur Publishing Co. Ltd., Davis House (4th Floor)
8 Scrubs Lane, Harlesden, NW10 6SE, England

breaking the language barrier

WITH COVER-TO-COVER ENGLISH TRANSLATIONS OF SOVIET JOURNALS

in physics

Title	# of Issues	Subscription Price
Astrophysics *Astrofizika*	4	$100.00
Fluid Dynamics *Izvestiya Akademii Nauk SSSR mekhanika zhidkosti i gaza*	6	$160.00
High-Energy Chemistry *Khimiya vysokikh énergii*	6	$155.00
High Temperature *Teplofizika vysokikh temperatur*	6	$125.00
Journal of Applied Mechanics and Technical Physics *Zhurnal prikladnoi mekhaniki i tekhnicheskoi fiziki*	6	$150.00
Journal of Engineering Physics *Inzhenerno-fizicheskii zhurnal*	12 (2 vols./yr. 6 issues ea.)	$150.00
Magnetohydrodynamics *Magnitnaya gidrodinamika*	4	$100.00
Mathematical Notes *Matematicheskie zametki*	12 (2 vols./yr. 6 issues ea.)	$185.00
Polymer Mechanics *Mekhanika polimerov*	6	$120.00
Radiophysics and Quantum Electronics (Formerly Soviet Radiophysics) *Izvestiya VUZ. radiofizika*	12	$160.00
Solar System Research *Astronomicheskii vestnik*	4	$ 95.00
Soviet Applied Mechanics *Prikladnaya mekhanika*	12	$160.00
Soviet Atomic Energy *Atomnaya énergiya*	12 (2 vols./yr. 6 issues ea.)	$160.00
Soviet Physics Journal *Izvestiya VUZ. fizika*	12	$160.00
Soviet Radiochemistry *Radiokhimiya*	6	$155.00
Theoretical and Mathematical Physics *Teoreticheskaya i matematicheskaya fizika*	12 (4 vols./yr. 3 issues ea.)	$145.00

Back volumes are available. For further information, please contact the Publishers.

SEND FOR YOUR FREE EXAMINATION COPIES

PLENUM PUBLISHING CORPORATION
227 WEST 17th STREET
NEW YORK, N. Y. 10011
Plenum Press • Consultants Bureau
• IFI/Plenum Data Corporation

In United Kingdom
Plenum Publishing Co. Ltd., Davis House (4th Floor)
8 Scrubs Lane, Harlesden, NW10 6SE, England